IEEE PES Task Force on Benchmark Systems for Stability Controls

Simplified 14-Generator Model of the South East Australian Power System:

(Including implementations in Mudpack for small-signal analysis and PSS®/E for transient-stability analysis)

14 June 2014

Mike Gibbard & David Vowles

Power Systems Dynamics Group
School of Electrical and Electronic Engineering
The University of Adelaide, South Australia

---

1 Introduction

The purpose of this document is to provide a test system which can be used as a test bed for the small-signal analysis and design of power system stabilisers (PSSs) and other controllers *in a multi-machine power system*.

Frequently papers are published in which the performance of PSSs designed using a new 'advanced' method is compared to that of PSSs designed using so-called 'conventional' techniques. Often the 'conventional' PSSs employed in such papers do not represent a properly-designed 'conventional' PSS. In the following a sound basis for a 'conventional' PSS design is outlined and its performance demonstrated. It is a tuning method used in practice by a number of organisations.

An important aspect of the design of PSSs for use on practical systems is that PSSs should contribute to the damping of inter-area, local-area and intra-station modes. This aspect is seldom tested adequately in most 'advanced' design methods because:

- a single-machine infinite-bus test system is typically employed by the proponent; it does not reveal the damping performance of the proposed PSS over the full range of modal frequencies likely to be encountered in practice, i.e. from the low frequency inter-area modes (~1.5 rad/s) to the higher local / intra-station frequencies (12+ rad/s);

- the contributions to modal damping by the proposed PSS are not validated over a wide range of operating conditions encountered in practice, light to peak load, for normal and contingency operation, etc.;

- the models of AVR/excitation systems employed in the proponent's system are often very simple. In practice such models may be third or higher order.

For designs of advanced PSSs to be credible for practical application, the proponents should demonstrate the above issues have been adequately addressed. An aim of the 14-generator test system is to provide researchers and developers with a system possessing the features highlighted above, i.e. a range of modal frequencies, a range of operating conditions, and higher-order avr/excitation system models.

Each generator in the 14-machine system is in fact an aggregated equivalent generator representing a power station (PS) of between 2 to 12 units. While the generators in each station could have been individually represented, this adds an additional level of complexity and increases system size, moreover, it is not warranted for the primary purpose of this document.

Included in Appendix I is a complete set of power flow and small-signal dynamics data that allows an interested party (i) to replicate the results provided using that party's loadflow and small-signal dynamics analysis packages, (ii) to cross-check results obtained by the party with those presented here, (iii) to insert in a Matlab environment the party's own controller, etc., into the power system for the analysis being conducted for research purposes.

A large-signal model of the system has been developed to allow transient stability analysis. As summarized in Section 9 the data for the large-signal model is presented in Appendix II in a format amenable to use with the PSS®/E [1] transient-stability program. Benchmarking studies in

Appendix III show that the small-disturbance performance of the PSS®/E implementation of the model is in close agreement with that of the original Mudpack implementation. A comprehensive set of transient stability studies are conducted in Appendix IV using the PSS®/E implementation of the model. It is found that the system is transiently stable for a comprehensive set of two-phase to ground faults across all six base case scenarios.

2 Caveats

The model of the power system used in this document is *loosely* based on the southern and eastern Australian networks. Therefore,

- it does not accurately represent any particular aspect of those networks;
- the model should not be used to draw any conclusions relating to the actual performance of the networks comprising the southern and eastern Australian grid, either for any normal or any hypothetical contingency condition;
- the model is suitable for educational purposes / research-oriented analysis only.

3 Information provided

The following data are provided. Refer to Appendix V for details of information provided in electronic format.

- The load flow data and results files in PSS®/E format together with the associated data tables for six normal operating conditions. These cover peak, medium and light load conditions with various inter-area power transfers and directions of flow.
- Tables of the parameters for the generators, SVCs, excitation systems and PSSs for use in both the small- and large-signal analysis of the dynamic performance of the system.
- The P-Vr frequency response characteristics of the generators over the range of operating conditions. These are presented in graphical form (on machine base).
- Tables of the rotor modes of oscillation for the six cases with PSSs in- and out-of-service.
- Matlab *.mat files of the state-space model matrices (i.e. ABCD matrices), eigenvalues, eigenvectors and participation factors for two of the six cases with the PSSs both in- and out-of-service.
- Small-disturbance step-response analysis results in comma-separated-value (*.csv) and Matlab (*.mat) formats for a selection of scenarios computed by both Mudpack and PSS®/E.
- Transient-stability time-domain analysis results in comma-separated-value (*.csv) and Matlab (*.mat) formats for a selection of faults computed by PSS®/E.
- A rudimentary Matlab function is also provided to allow the user to compare their own time-response results (small- or large-signal) with those provided.

4 The Simplified System

The simplified 14-generator, 50 Hz system is shown in Figure 1. It represents a long, linear system as opposed to the more tightly meshed networks found in Europe and the USA. For convenience, it has been divided into 5 areas in which areas 1 and 2 are more closely coupled electrically. There are in essence 4 main areas and hence 3 inter-area modes, as well as 10 local-area modes. Without PSSs many of these modes are unstable.

In order to tune generator PSSs in practice an encompassing range of normal operating conditions and contingencies are considered. In the data provided in the Appendices, however, only six normal conditions are used for illustrative purposes. The operating conditions, system loads and major inter-area flows are listed in Table 1.

Table 1 Six normal steady-state operating conditions

	Case 1	Case 2	Case 3	Case 4	Case 5	Case 6
Load Condition	Heavy	Medium-heavy	Peak	Light	Medium	Light
Total generation (MW)	23030	21590	25430	15050	19060	14840
Total load (MW)	22300	21000	24800	14810	18600	14630
Inter-area flows	(North to south)	(South to north)	(Hydro to N & S)	(Area 2 to N & S)	(N & S to pumping)	(~Zero transfers)
Area 4 to Area 2 (MW)	500	-500	-500	-200	300	0
Area 2 to Area 1 (MW)	1134	-1120	-1525	470	740	270
Area 1 to Area 3 (MW)	1000	-1000	1000	200	-200	0
Area 3 to Area 5 (MW)	500	-500	250	200	250	0

The schedules of generation for the six cases are listed in Appendix I, Table 8. Note that the number of generating units on-line in certain power stations (designated *PS_#, e.g. HPS_1) can vary considerably over the range of operating conditions.

5 Power flow analysis

Data for the power flow analysis of the six normal operating conditions given in Table 1 is supplied in Appendix I.1. Included in Appendix I.1 are relevant results of the analysis such as reactive outputs of generators and SVCs, together with tap positions on generator and network transformers. This information permits the power flows to be set up on any power flow platform and the results checked against those provided in this document.

The power flow data is also provided in Siemens-PTI PSS®/E version 29 format[1]. These files for the six operating conditions are accessible from the web site in Appendix V.1.

1. The specification of the Siemens-PTI PSS®/E version 29 power flow raw data format is available by application from Siemens-PTI at the following web-site http://w3.usa.siemens.com/smartgrid/us/en/transmission-grid/products/grid-analysis-tools/transmission-system-planning/Pages/PSSERawData-Format.aspx

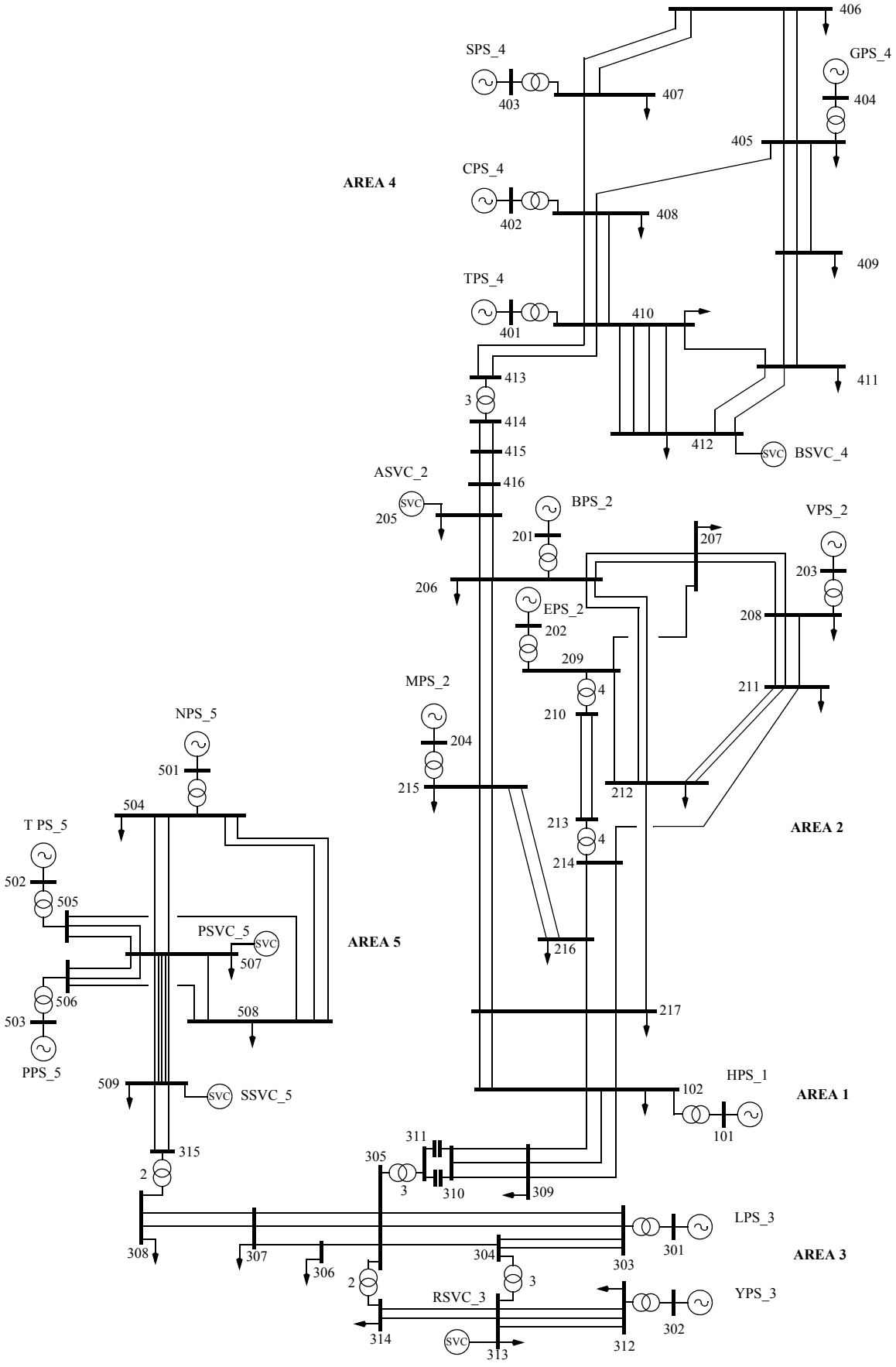

Figure 1 Simplified 14-generator, 50 Hz system.

6 Design of PSSs based on the P-Vr Method for multi-machine systems

6.1 Introduction

Comparisons between conventional PSS design methods such as the 'GEP', 'P-Vr' - and a method based on residues - for multi-machine power systems are discussed in [7] and [11]. A comparison of the P-Vr and GEP methods and their features are provided in Table 21 of Appendix I.4.

6.2 Concepts based on an ideal PSS

Consider the idealised shaft dynamics of the simplified generator model shown in Figure 2. Assume that a feedback loop can be added from the rotor speed signal $\Delta\omega$ to the torque signal ΔP_d - as shown in Figure 2 - such that $\Delta P_{ds} = k\,\Delta\omega$. It is clear that increasing the gain k has the same effect as increasing the *inherent damping torque coefficient* k_d [13], that is, enhancing the damping of rotor oscillations. The block with gain k represents an ideal PSS that induces on the rotor a torque of electro-magnetic origin proportional to speed perturbations. The gain k, like k_d, is a *damping torque coefficient* which we call the *damping gain* of the PSS. (The difference between the latter gain and the conventional 'PSS gain' is discussed shortly.) The goal in the design of a practical PSS is to achieve the same result, the damping gain being adjusted to meet the specifications on the damping for the rotor modes of oscillation. Framed in this context, the damping gain k of a practical PSS expressed in per unit on machine base becomes a meaningful quantity.

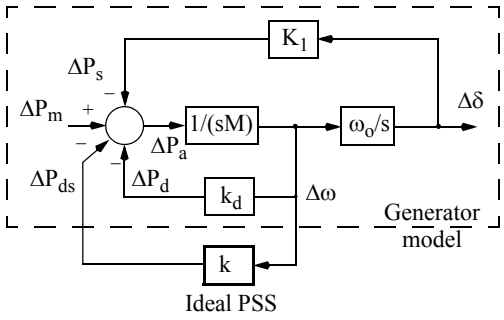

Figure 2 The ideal PSS, represented by a damping gain k, introduces a pure damping torque on the rotor of a simplified generator model.

6.3 Theoretical background

The design of the compensating transfer function (TF) for the PSS of generator i in a multi-machine power system is based on the so-called P-Vr TF of generator i. This is the TF from the AVR voltage reference input, 'Vr', on generator i to the torque of electromagnetic origin (or electrical power output, 'P') on that generator, calculated with the shaft dynamics of *all* machines disabled [2], [3]. In the following, $\Delta V_{ri}(s)$ and $\Delta P_{ei}(s)$ are perturbations in the reference voltage and the electrical torque, respectively. (For small disturbances the per-unit perturbations in electrical power and electrical torque are identical.)

The frequency response of the P-Vr TF, $H_{PVri}(s) = \Delta P_{ei}(s)/\Delta V_{ri}(s)$, is easily calculated. To disable the shaft dynamics of all machines the rows and/or columns of all generator speed states are eliminated in the ABCD matrices of the linearized state equations of the system. The

frequency response(s) $\Delta P_{ei}(j\omega_f)/\Delta V_{ri}(j\omega_f)$ are then calculated over the range of rotor modal frequencies (typically 1.5 to 12 rad/s).

The TF $H_{PSSi}(s)$ of a PSS is typically of the form $k_i G_i(s)$. When the transfer functions of the PSS compensation block $G_{ci}(s)$, and the wash-out and low-pass filters, $G_{Wi}(s)$ and $G_{LPi}(s)$ respectively, are added the PSS TF takes the form,

$$H_{PSSi}(s) = k_i G_i(s) = k_i G_{ci}(s) \cdot G_{Wi}(s) \cdot G_{LPi}(s). \quad (1)$$

Alternatively, considering the typical forms of the relevant TFs, the PSS TF is

$$H_{PSSi}(s) = k_i G_i(s) = k_i \cdot \left[\frac{sT_W}{1+sT_W} \cdot \frac{1}{k_c} \cdot \frac{(1+c_1 s + c_2 s^2)(1+sT_{a1})\ldots}{(1+sT_{b1})\ldots(1+sT_1)(1+sT_2)\ldots} \right] \quad (2)$$

where, for generator *i*, T_W is the time constant of the washout filter; k_c, c_1, c_2, T_{a1}, …, T_{b1}, … are the parameters of the compensation TF $G_{ci}(s)$ determined in the design procedure described below, and T_1, T_2, … are the time constants of the low-pass filter. The corner frequencies of the washout and low-pass filters are selected such that the phase shifts introduced at the frequencies of the rotor modes are negligible. The PSS TF must be proper.

Note that, in the context of (2), the gain k_i has been referred to as the '*damping gain*' of the PSS. If the washout filter is ignored the 'dc' gain of the PSS TF is k_i/k_c; *conventionally this is referred to as the 'PSS Gain'*. However, the PSS gain k_i/k_c has little meaning as k_c is machine and system dependent.

The compensation TF $G_{ci}(s)$ is designed to achieve the desired *left-shift* in the relevant modes of rotor oscillation. The damping gain k_i (on machine base) of the PSS determines the *extent* of the left-shift. The aim of the design procedure is to introduce on the generator shaft a damping torque (a torque proportional to machine speed); this causes the modes of rotor oscillation to be shifted to the left in the *s*-plane. Thus the ideal TF between speed $\Delta\omega_i$ and the electrical damping torque perturbations ΔP_{ei} due to the PSS over the range of complex frequencies of the rotor modes should be

$$D_{ei} = \Delta P_{ei}(s)/\Delta\omega_i(s)\big|_{PSSi}, \quad (3)$$

where D_{ei} is a damping torque coefficient (e.g. as is *k* in Figure 2) and - for design purposes - is a real number (p.u. on machine base). The TF $G_{ci}(s)$ compensates in *magnitude as well as phase* for the P-Vr TF $H_{PVri}(s)$ of machine *i*. With rotor speed being used as the input signal to the PSS, whose output is $\Delta V_{si}(s)$, the expression (3) for D_{ei} can be written:

$$D_{ei} = \frac{\Delta P_{ei}(s)}{\Delta V_{si}(s)} \cdot \frac{\Delta V_{si}(s)}{\Delta \omega_i(s)} = H_{PVri}(s)[k_i G_{ci}(s)]; \quad (4)$$

hence, rearranging (4), we find

$$[k_i G_{ci}(s)] = D_{ei} / (H_{PVri}(s)). \quad (5)$$

It follows from an examination of (5) that $k_i = D_{ei}$ and $G_{ci}(s) = 1/(H_{PVri}(s))$. As in the case of the simplified generator model of Figure 2, the gain k_i of the PSS can thus also be considered to be a damping torque coefficient. The practical, proper TF for the *i*-th PSS is that of (2), i.e.:

$$[k_i G_i(s)] = k_i \{1/(PVR_i(s))\} \{\text{washout \& low-pass filters}\}$$

where $PVR_i(s)$ is the *synthesized form* of P-Vr characteristic, $H_{PVri}(s)$. As most rotor modes are relatively lightly damped, s can be replaced by $\jmath\omega_f$ and conventional frequency response methods can be employed in the design procedure. In practice, the aim of a design is to ensure that, over the range of frequencies of rotor oscillations, the magnitude response of the RHS of (3) is flat with zero or slightly lagging phase shift. This means that the PSS introduces an almost pure damping torque over the frequency range of the rotor modes. Because of the more-or-less invariant nature of the TF $H_{PVri}(s)$ over a wide range of operating conditions, fixed-parameter PSSs tend to be robust [5].

Note that speed appears to be the ideal stabilizing signal because the damping torque induced on the shaft of the generator by the associated PSS is related to speed through a simple gain. Moreover, this gain being a damping torque coefficient has practical significance, e.g. a damping gain k_i of 20 pu on machine rating can typically be considered a moderate gain setting for a speed-PSS. A practical form of the "speed-PSS" is the "Integral-of-accelerating-power PSS" for which the design procedure outlined above is applicable.

The approach to the design of speed-PSSs can be adapted to the design of power-input PSSs. If the perturbations in mechanical power are negligible over the frequency range of interest the equation of motion of the unit's shaft can be written $\Delta\omega(s) = -\Delta P_{ei}(s)/(2Hs)$ [13]; $\Delta\omega$ is then the input to the speed-PSS.

7 The P-Vr characteristics of the 14 generators and the associated synthesized characteristics

For each of the generators the P-Vr characteristics are determined for the six power flow cases as shown in Figure 3 to Figure 16. These characteristics were calculated using Mudpack, a software package for the analysis of the small-signal dynamic performance and control of large power systems [14].

It should be noted in this analysis that the operating conditions on which the load flows, and therefore the P-Vr characteristics, are based are normal operating conditions. In practice, the P-Vr characteristics for a relevant set of contingency conditions are also considered when determining the synthesized characteristic.

The synthesized P-Vr characteristic for each generator is derived based on the following:

- The modal frequency range of interest is 1.5 to 12 rad/s.

- The synthesized characteristic is a best fit of the P-Vr characteristics for the range of cases examined over the modal frequency range 1.5 to 12 rad/s. The 'best fit' characteristic is considered to be that characteristic which lies in the middle of the magnitude and phase bands formed by the P-Vr characteristics. If particular P-Vr characteristics tend lie outside the bands formed by the majority of the characteristics, the synthesized P-Vr is offset towards the band formed by the majority (e.g. see Figure 12).

- Less phase lead at the inter-area model frequencies may be required than that provided by the synthesized TF based on P-Vr characteristic [11]. It can be accommodated by a gain-lag-lead transfer function block or by adjusting the synthesized transfer function at the inter-area frequencies. This feature has the effect of increasing the damping of the inter-area modes, however, it is not incorporated in following analysis.

The P-Vr characteristics for the 14 generators, shown in Figure 3 to Figure 16, are in per unit on the machine rating given in Table 8.

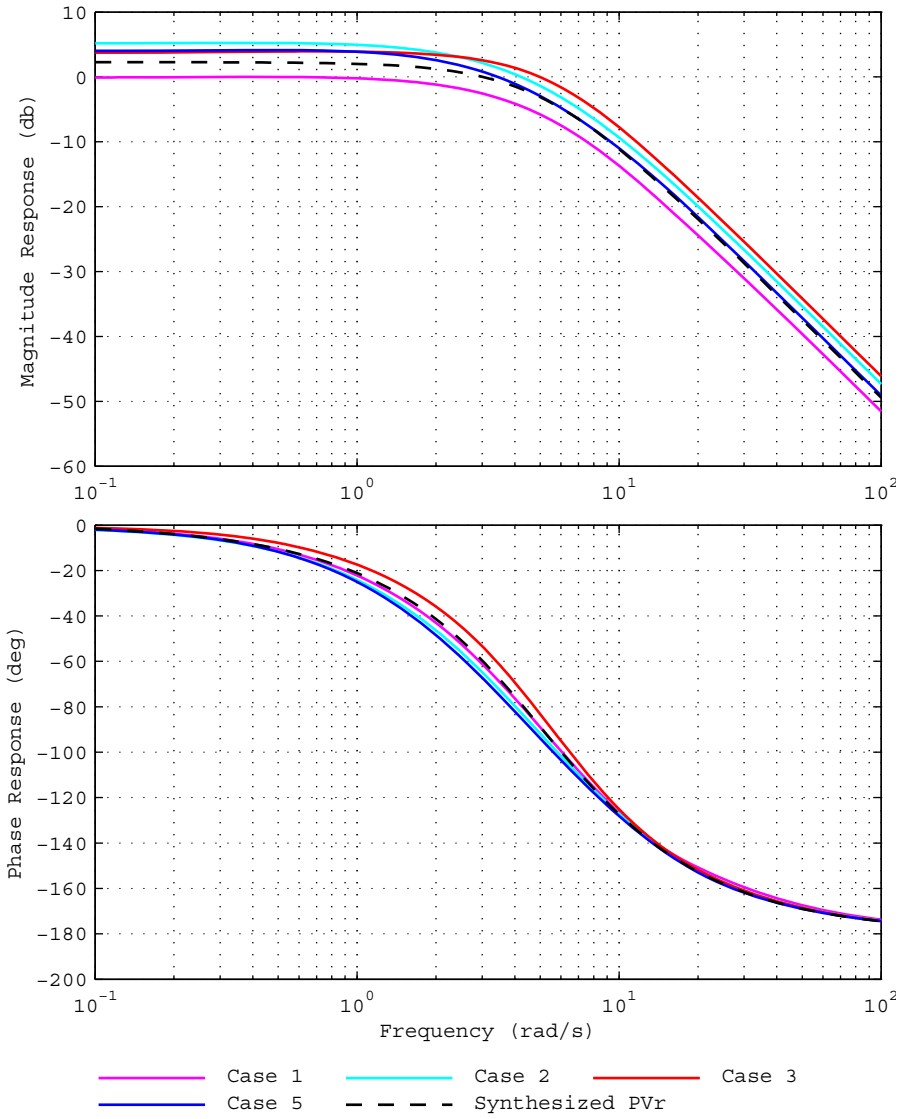

Figure 3 P-Vr characteristics, calculated and synthesized ($PVR(s)$), for generator HPS_1. (In cases 4 & 6 the PSS is switched off as it is operating as a synchronous compensator.)

$$PVR(s) = 1.3/(1 + s0.373 + s^2 0.0385)$$

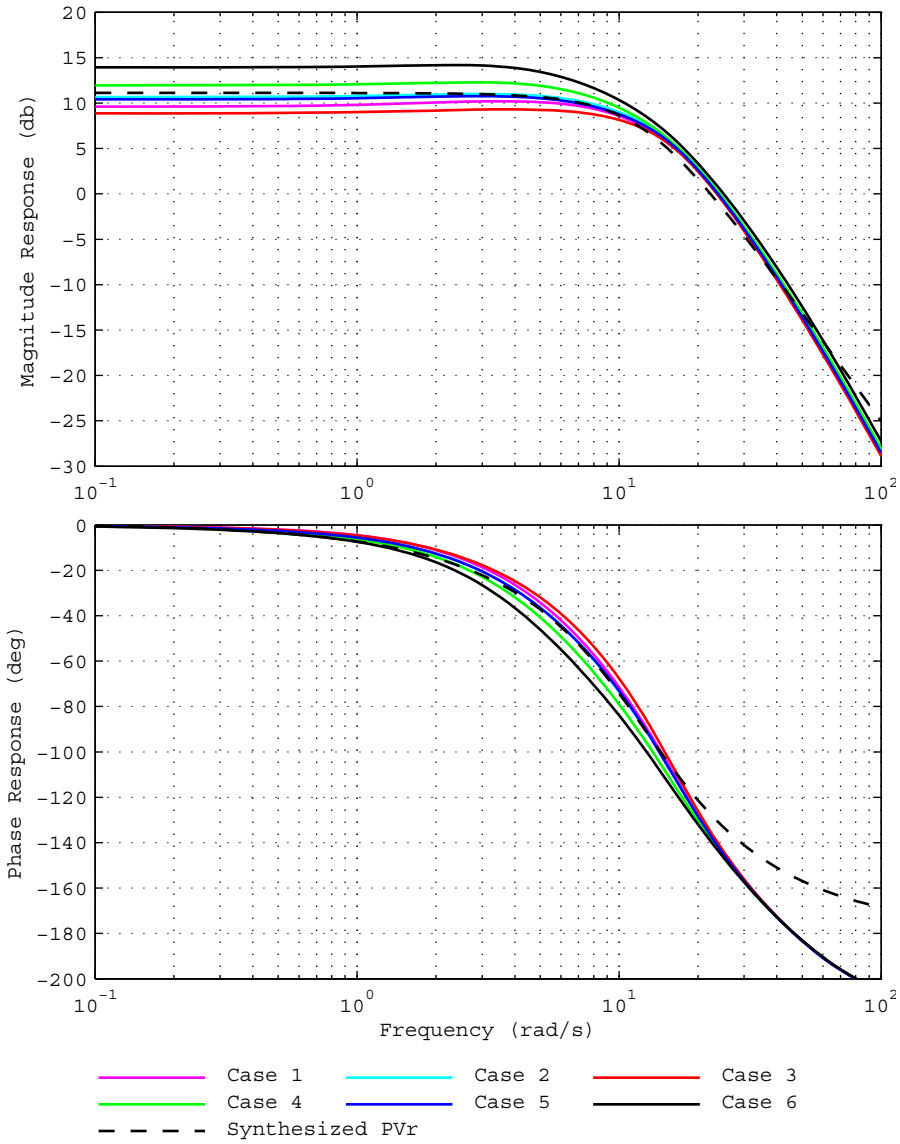

Figure 4 P-Vr characteristics, calculated and synthesized ($PVR(s)$), for generator BPS_2.

$$PVR(s) = 3.6/(1 + s0.128 + s^2 0.0064)$$

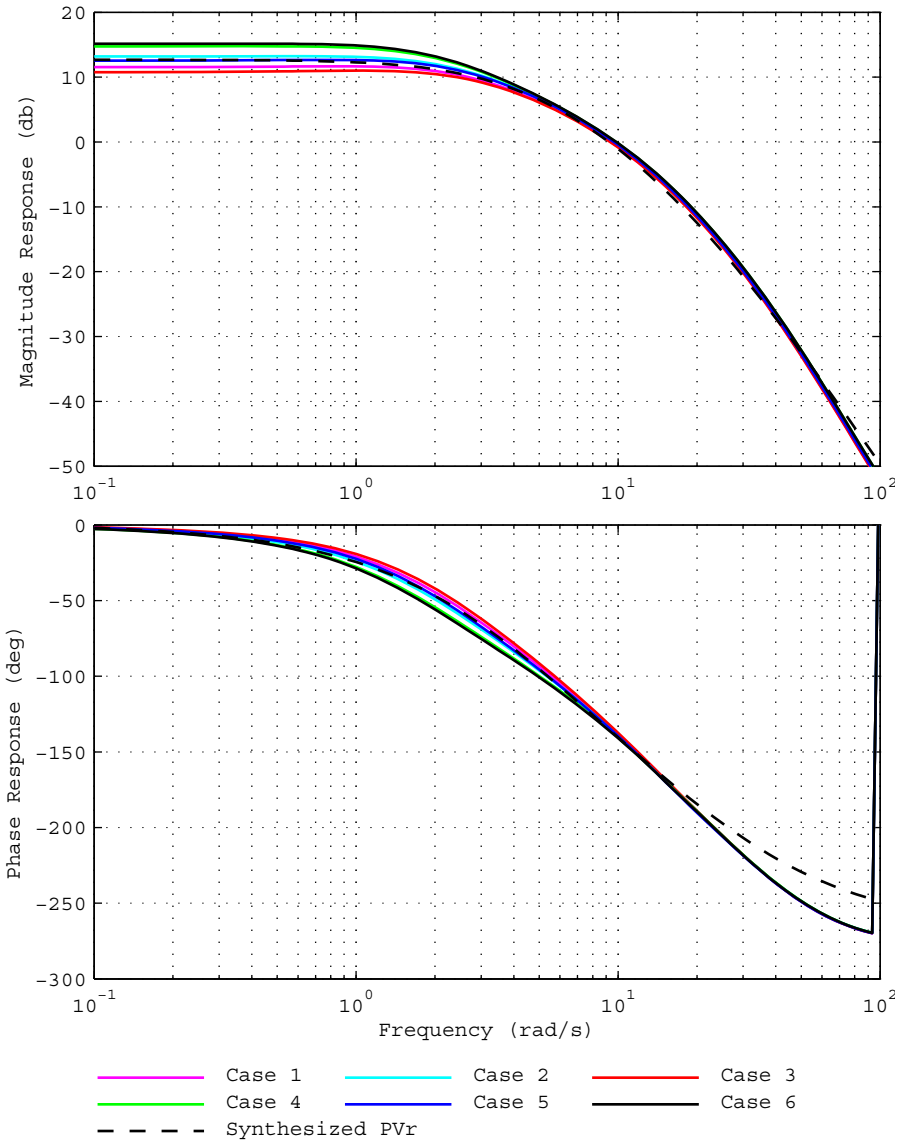

Figure 5 P-Vr characteristics, calculated and synthesized ($PVR(s)$), for generator EPS_2.

$$PVR(s) = 4.3/[(1+s0.286)(1+s\dot{0}.111)(1+s0.040)]$$

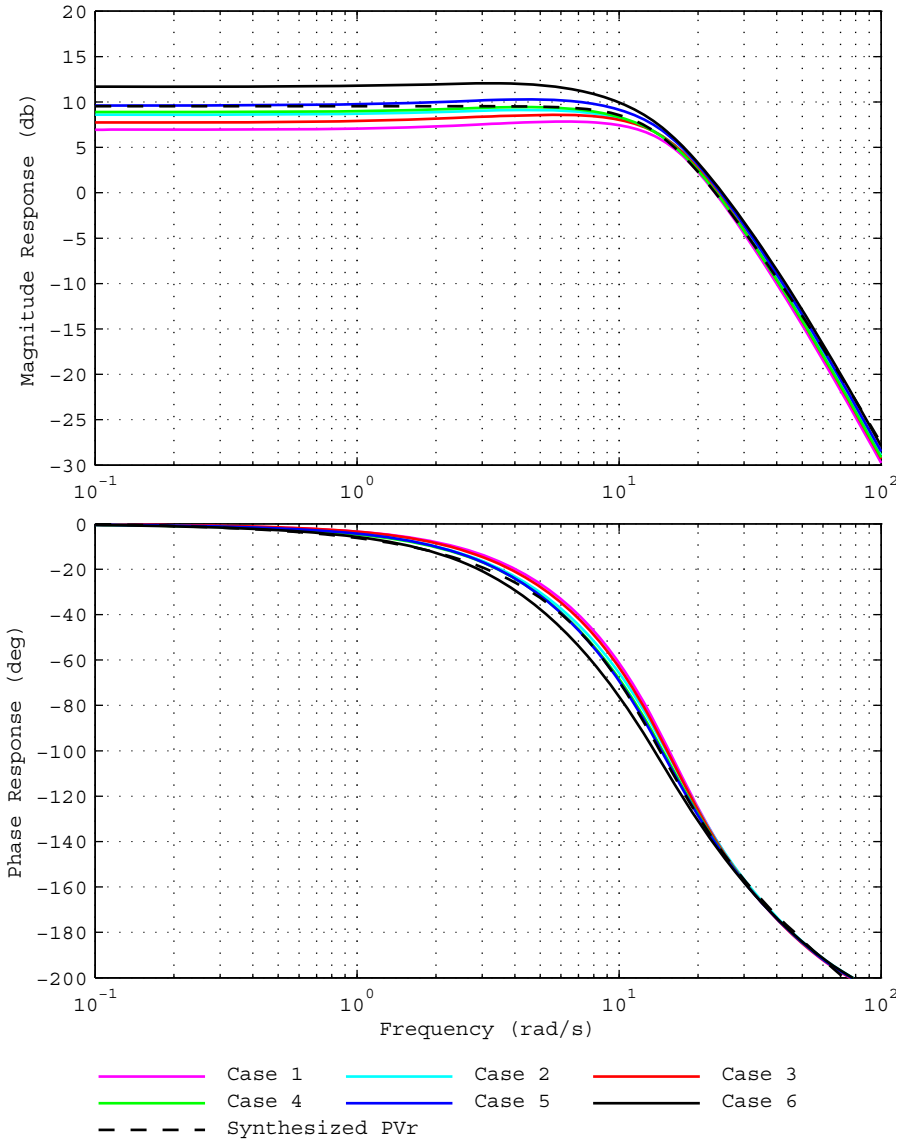

Figure 6 P-Vr characteristics, calculated and synthesized ($PVR(s)$), for generator MPS_2.

$$PVR(s) = 3.0/[(1+s0.01)(1+s\dot{0}.1+s^2 0.0051)]$$

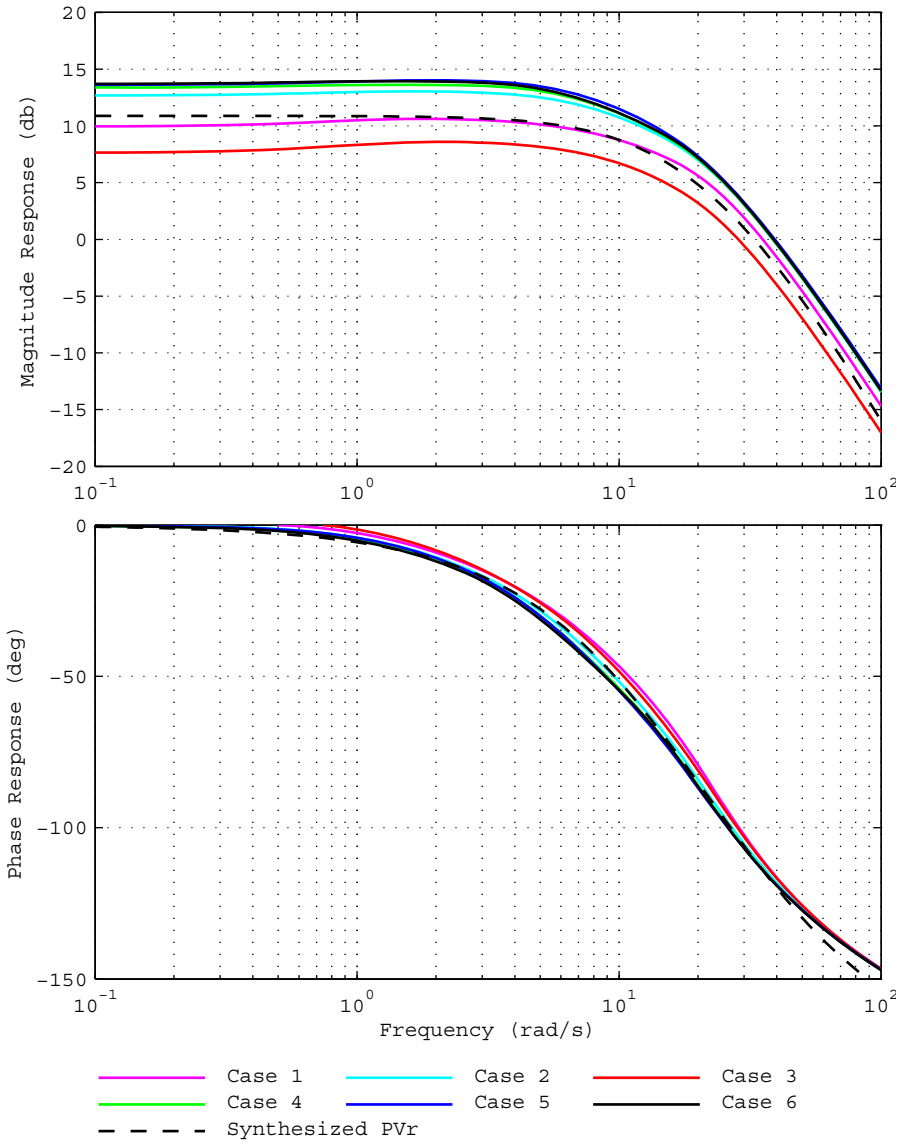

Figure 7 P-Vr characteristics, calculated and synthesized ($PVR(s)$), for generator VPS_2.
$PVR(s) = 3.5/[(1 + s0.0292)(1 + s0.0708)]$

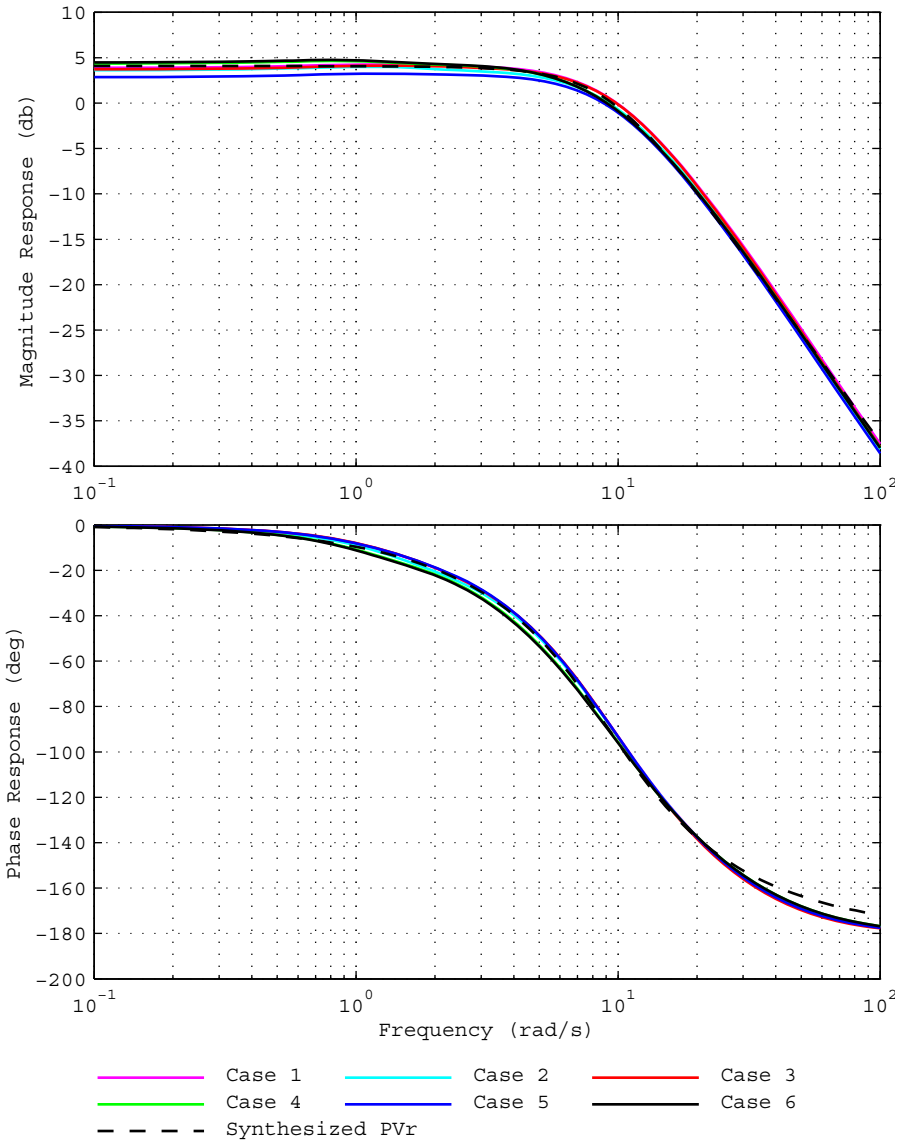

Figure 8 P-Vr characteristics, calculated and synthesized ($PVR(s)$), for generator LPS_3.

$$PVR(s) = 1.6/(1 + s0.168 + s^2 0.0118)$$

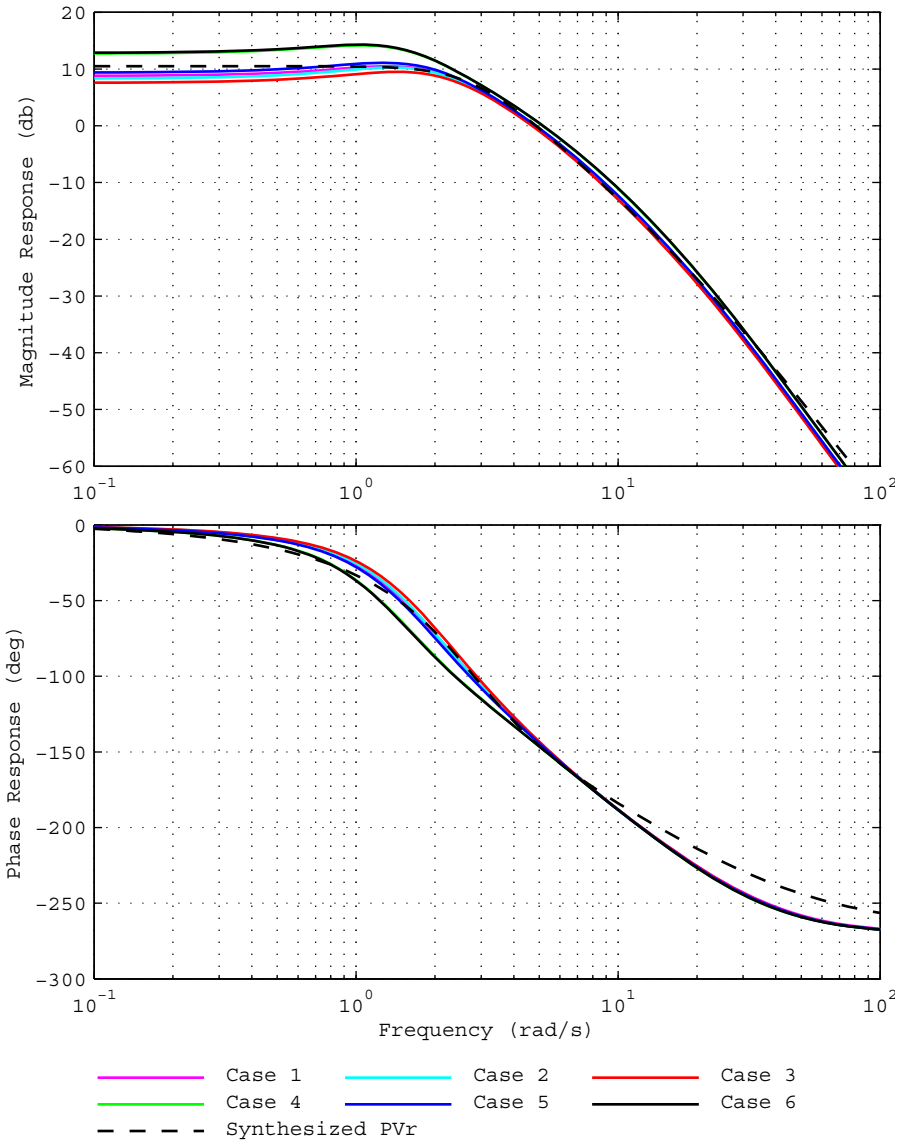

Figure 9 P-Vr characteristics, calculated and synthesized ($PVR(s)$), for generator YPS_3

$$PVR(s) = 3.35/[(1 + s0.05)(1 + s\dot{0}.509 + s^2 0.132)]$$

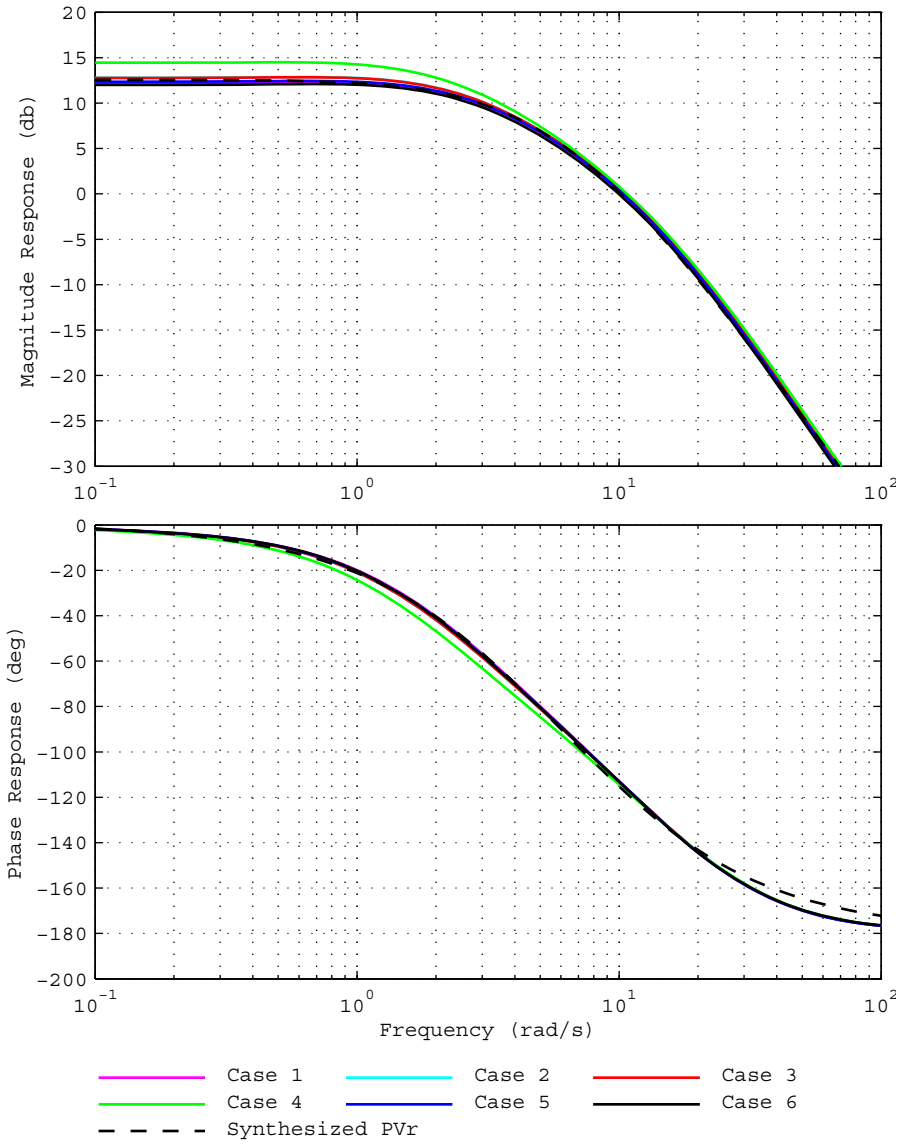

Figure 10 P-Vr characteristics, calculated and synthesized ($PVR(s)$), for generator CPS_4.
$PVR(s) = 4.25/[(1+s0.278)(1+s0.100)]$

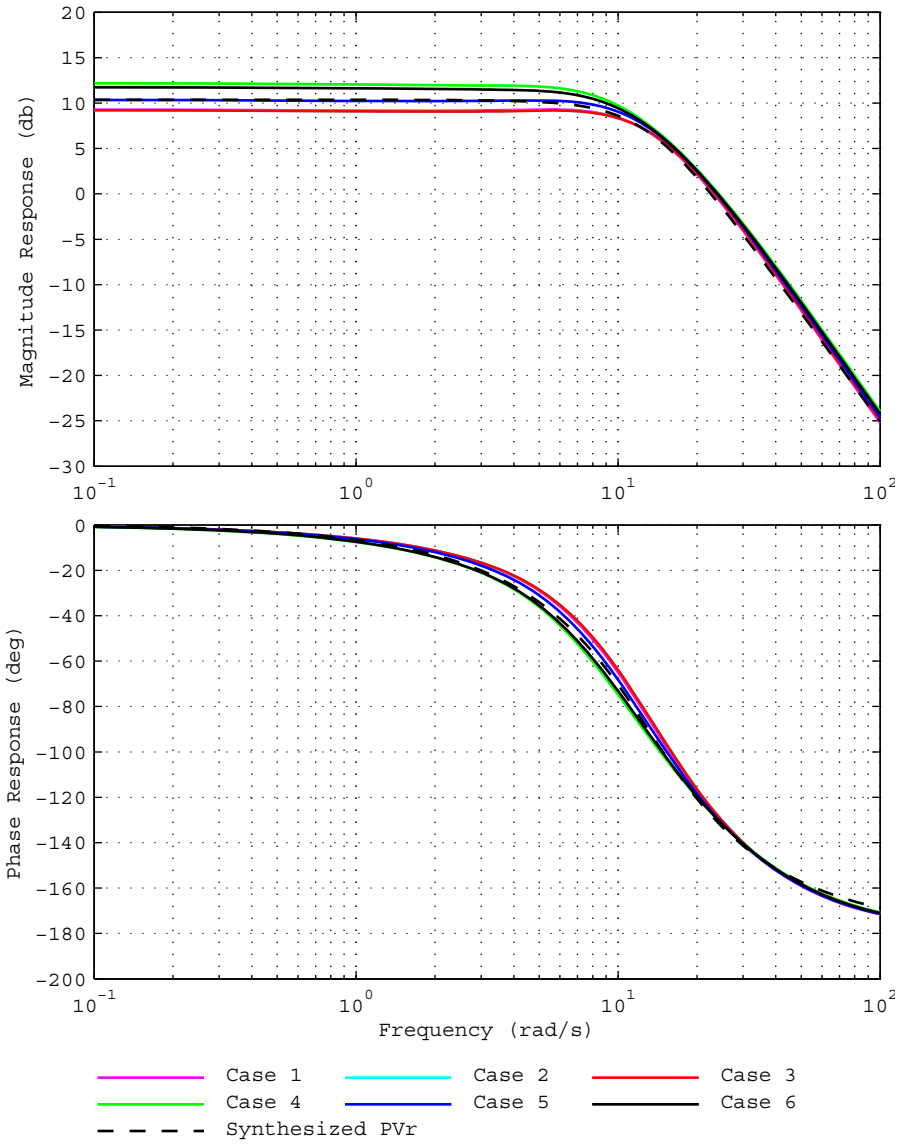

Figure 11 P-Vr characteristics, calculated and synthesized ($PVR(s)$), for generator GPS_4.

$$PVR(s) = 3.3/(1 + s0.115 + s^2 0.00592)$$

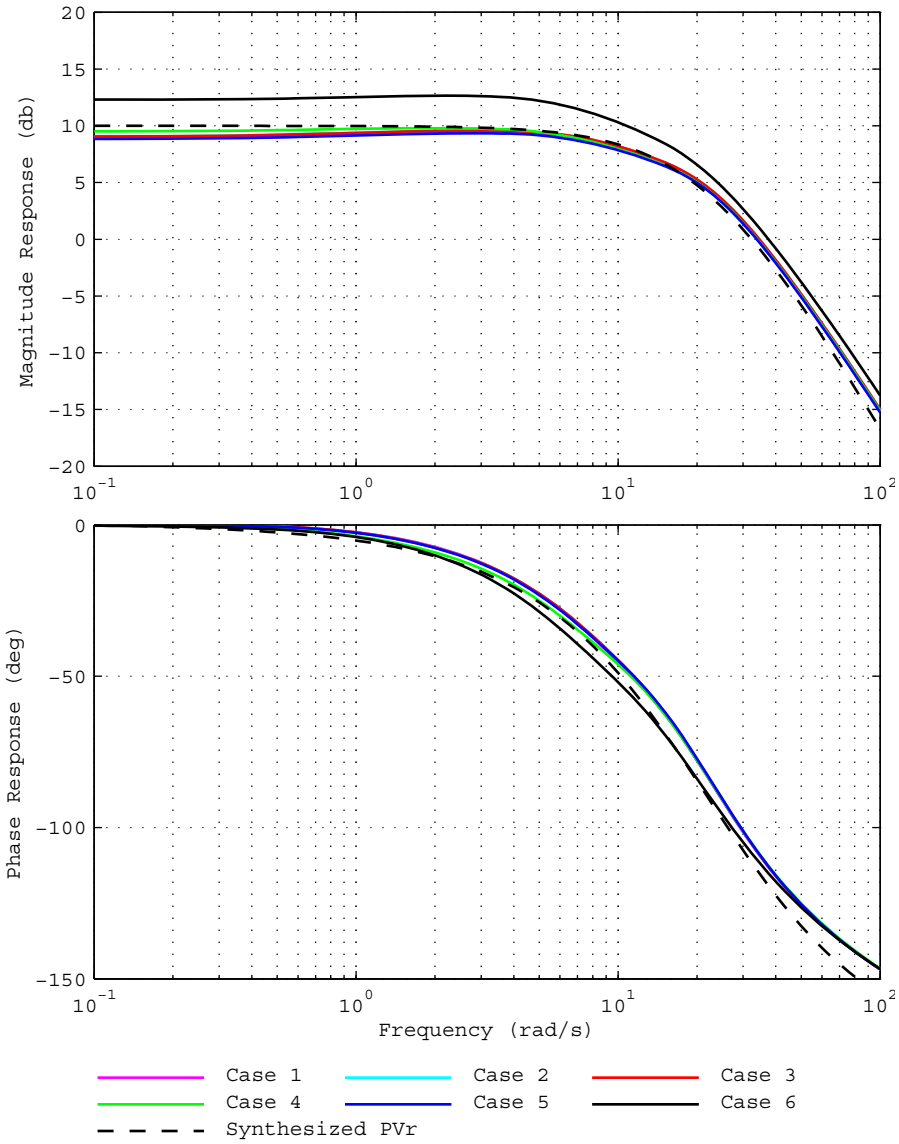

Figure 12 P-Vr characteristics, calculated and synthesized ($PVR(s)$), for generator SPS_4. The synthesized P-Vr characteristic is weighted towards those of Cases 1 to 5.

$$PVR(s) = 3.16/(1 + s0.0909 + s^2 0.00207)$$

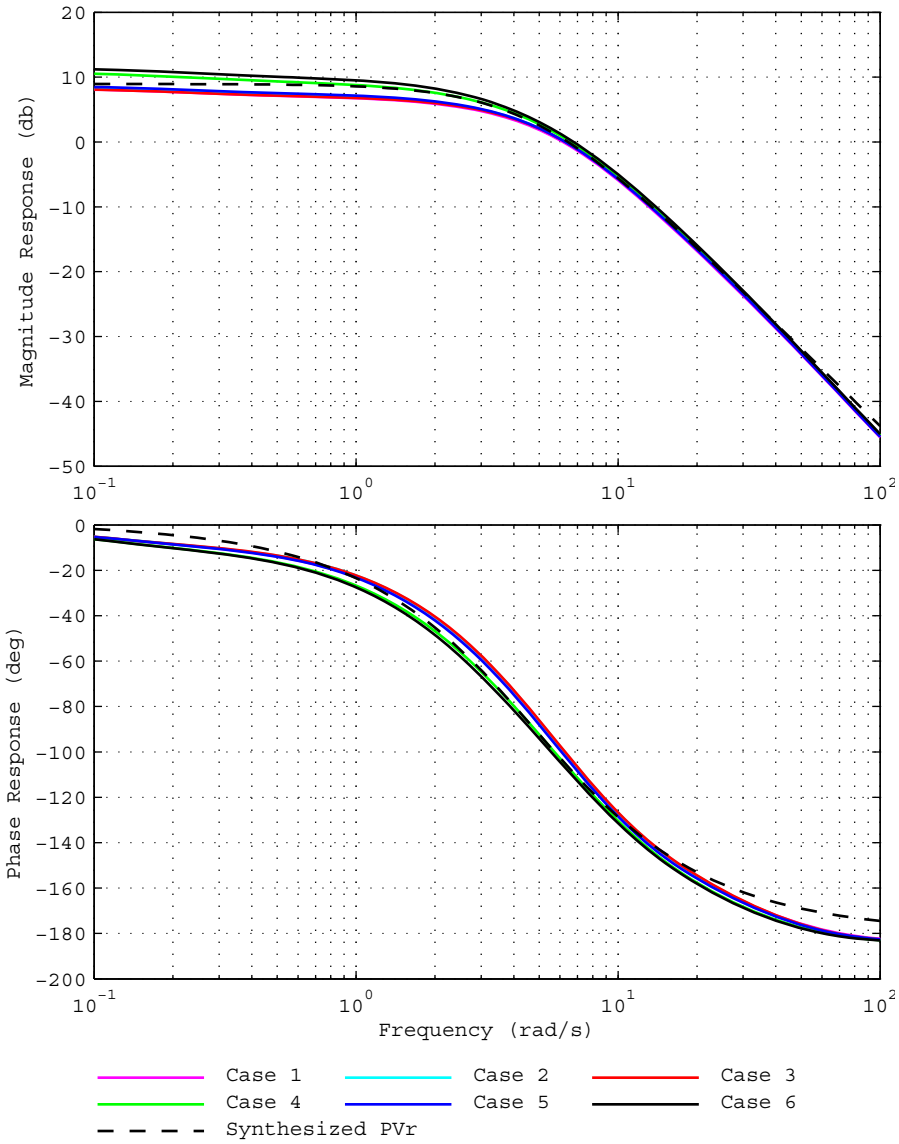

Figure 13 P-Vr characteristics, calculated and synthesized ($PVR(s)$), for generator TPS_4.

$$PVR(s) = 2.8/[(1 + s0.208)(1 + s0.208)]$$

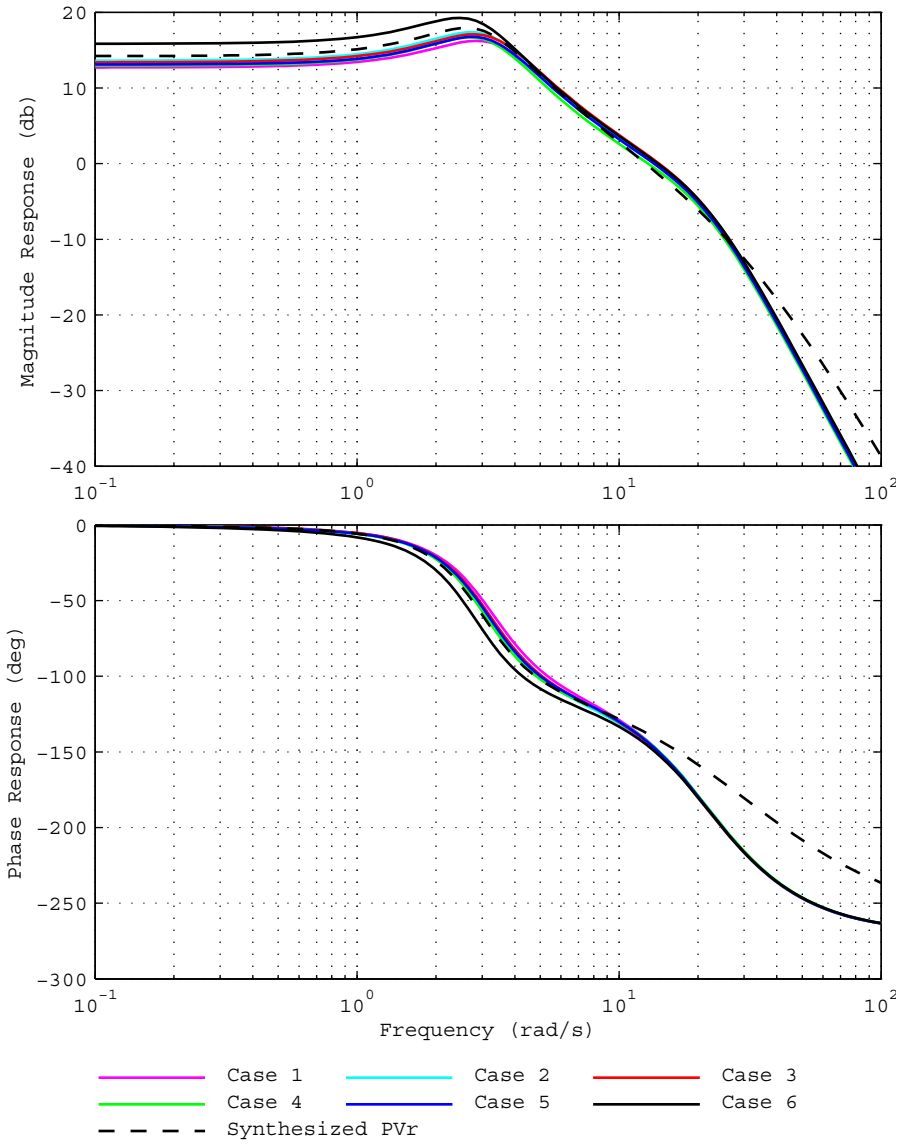

Figure 14 P-Vr characteristics, calculated and synthesized ($PVR(s)$), for generator NPS_5.

$$PVR(s) = 5.13(1 + s0.300)/[(1 + s0.033)^2(1 + s0.300 + s^2 0.111)]$$

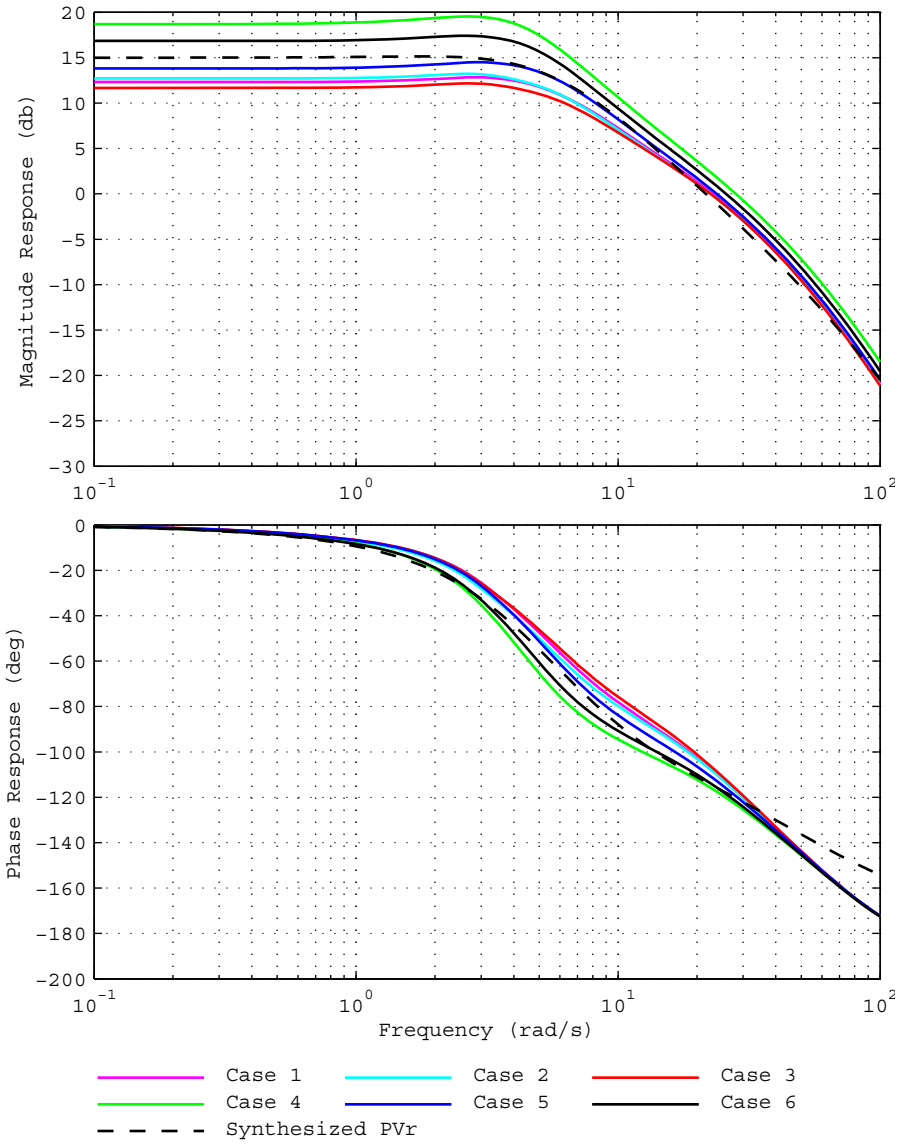

Figure 15 P-Vr characteristics, calculated and synthesized ($PVR(s)$), for generator PPS_5.

$$PVR(s) = \frac{5.62(1 + s0.350)(1 + s0.0667)}{(1 + s0.020)(1 + s0.167)(1 + s0.187)(1 + s0.200)}$$

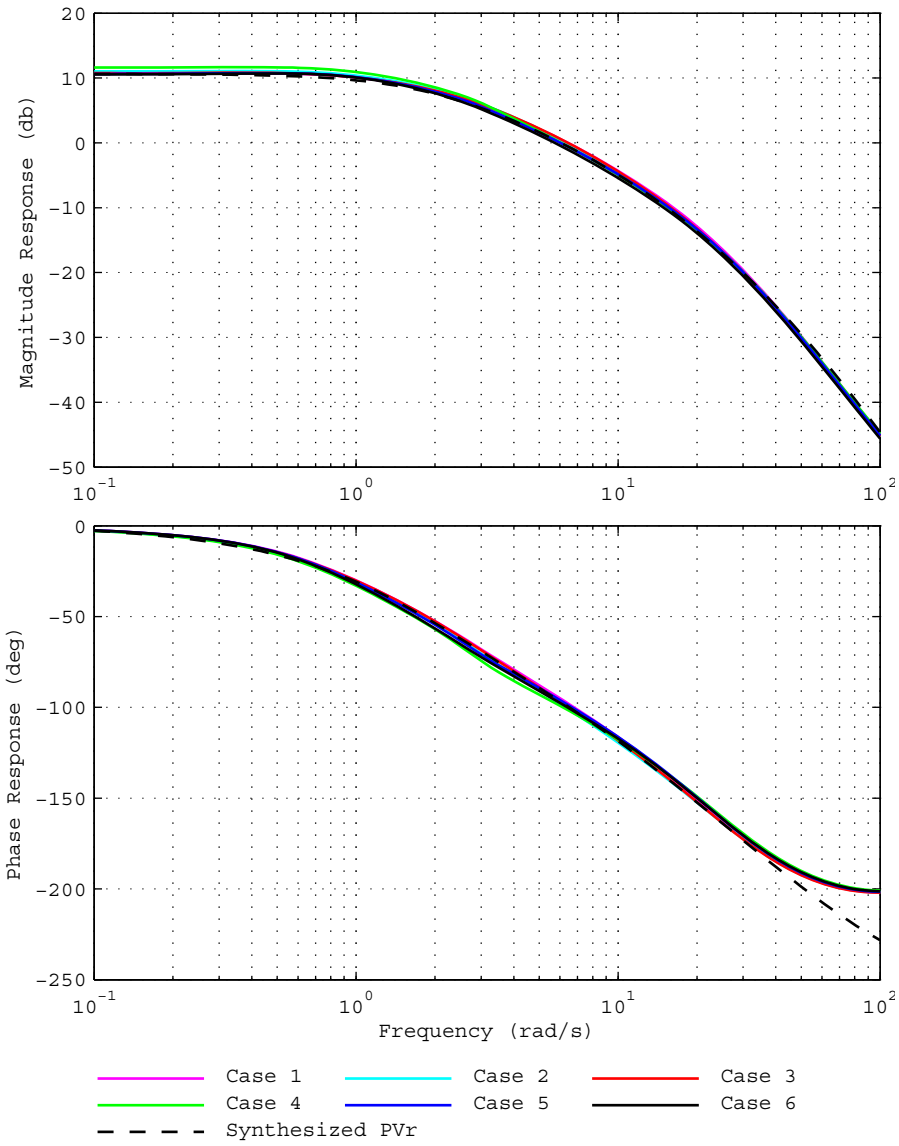

Figure 16 P-Vr characteristics, calculated and synthesized ($PVR(s)$), for generator TPS_5.
$PVR(s) = 3.4/[(1+s0.500)(1+s0.0588)(1+s0.0167)]$

8 Results of small-signal analysis for the six cases

Please note the Caveats listed in Section 2 before interpreting these results.

For each of the six cases the rotor modes of oscillation without and with all PSSs in service are listed in Table 2 to Table 7.

In Figure 17 is shown the plot of the electro-mechanical modes for Case 1 as the PSS damping gains on all generators are increased from zero (no PSSs in service) to 30 pu in 5 pu steps. Note that the modes shift more or less directly into the left-half of the *s*-plane. Without the special compensation referred to in Section 7 for the inter-area modes, the frequencies of the inter-area modes tend to decrease relatively more than the local-area modes due to the effects of interactions [6], [11]; the damping of the inter-area modes is also poorer.

Table 2 Rotor modes. Case 1: PSSs out and in service. (Damping gains 20pu on rating)

Case1: No PSSs			Case 1: All PSS in service		
Real	Imag	Damping Ratio	Real	Imag	Damping Ratio
-0.175	10.442	0.017	-2.193	10.386	0.207
0.109	9.583	-0.011	-1.978	9.742	0.199
0.041	8.959	-0.005	-1.926	9.293	0.203
-0.557	8.634	0.064	-2.505	8.858	0.272
-0.260	8.368	0.031	-1.953	8.261	0.230
-0.612	8.047	0.076	-1.971	8.490	0.226
-0.439	7.965	0.055	-1.875	7.756	0.235
0.014	7.812	-0.002	-1.777	7.643	0.226
-0.189	7.724	0.024	-2.061	7.872	0.253
-0.617	7.425	0.083	-1.878	7.588	0.240
0.115	3.970	-0.029	-1.044	3.640	0.276
0.088	2.601	-0.034	-0.385	2.402	0.158
-0.016	2.028	0.008	-0.522	1.798	0.279

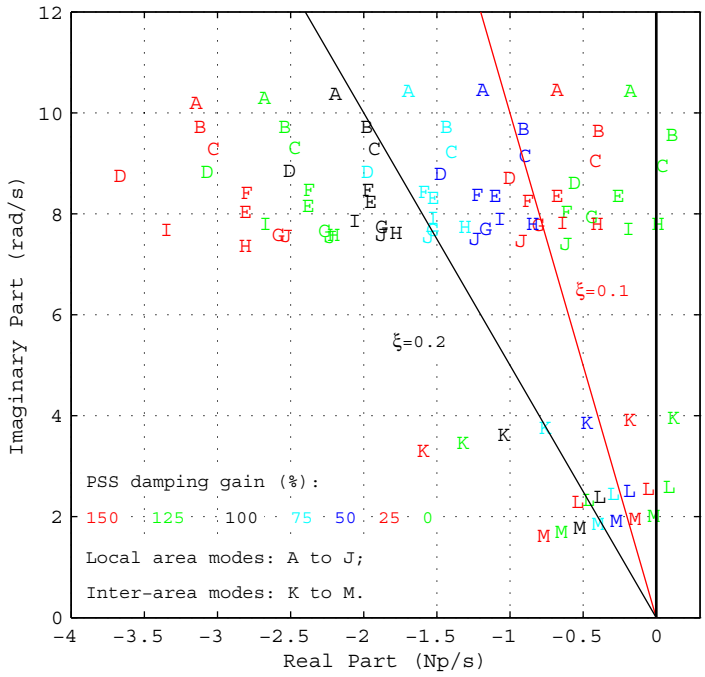

Figure 17 Rotor modes for Case 1 as the PSS damping gain on each generator is increased from zero (no PSSs in service) to 30 pu (150%) in 5 pu (25%) steps.
(100% gain is equivalent to PSS damping gain De=20 pu on machine base)

Table 3 Rotor modes. Case 2: PSSs out and in service. (Damping gains 20pu on rating)

Case 2: No PSSs			Case 2: All PSS in service		
Real	Imag	Damping Ratio	Real	Imag	Damping Ratio
0.066	10.743	-0.006	-2.403	10.964	0.214
0.101	9.563	-0.011	-2.038	9.725	0.205
-0.250	9.261	0.027	-2.370	9.644	0.239
-0.922	8.613	0.106	-2.805	8.962	0.299
-0.534	8.669	0.062	-2.494	8.936	0.269
-0.184	8.482	0.022	-2.039	8.379	0.236
-0.700	8.293	0.084	-2.442	8.370	0.280
-0.208	7.929	0.026	-2.029	7.739	0.254
-0.065	7.385	0.009	-2.021	7.490	0.261
-0.485	7.570	0.064	-1.814	7.772	0.227
0.193	3.772	-0.051	-0.769	3.537	0.212
0.054	2.863	-0.019	-0.447	2.542	0.173
0.081	1.915	-0.042	-0.431	1.759	0.238

Table 4 Rotor modes. Case 3: PSSs out and in service. (Damping gains 20pu on rating)

Case 3: No PSSs			Case 3: All PSS in service		
Real	Imag	Damping Ratio	Real	Imag	Damping Ratio
-0.377	11.109	0.034	-1.909	11.244	0.167
0.101	9.563	-0.011	-2.037	9.724	0.205
-0.301	9.019	0.033	-2.278	9.100	0.243
-0.583	8.660	0.067	-2.519	8.914	0.272
-0.182	8.476	0.021	-2.025	8.376	0.235
-0.140	8.256	0.017	-1.948	8.492	0.224
-0.191	7.909	0.024	-2.011	7.727	0.252
-0.076	7.381	0.010	-1.932	7.535	0.248
-0.576	7.625	0.075	-1.933	7.800	0.241
-0.131	6.314	0.021	-2.030	5.909	0.325
0.011	4.076	-0.003	-1.119	3.707	0.289
0.020	2.670	-0.007	-0.428	2.418	0.174
-0.032	2.050	0.015	-0.580	1.860	0.298

Table 5 Rotor modes. Case 4: PSSs out and in service. (Damping gains 20pu on rating)

Case 4: No PSSs			Case 4: All PSS in service .†		
Real	Imag	Damping Ratio	Real	Imag	Damping Ratio
0.197	10.484	-0.019	-2.374	10.774	0.215
0.030	9.665	-0.003	-2.163	9.951	0.212
-0.173	9.369	0.018	-2.269	9.813	0.225
-1.541	8.276	0.183	-1.695	8.169	0.203
-0.178	8.779	0.020	-2.272	8.793	0.250
-0.561	8.581	0.065	-2.496	9.064	0.266
-0.211	8.278	0.025	-2.554	8.445	0.289
-0.508	8.522	0.060	-2.492	8.826	0.272
-0.431	8.211	0.052	-2.280	8.279	0.265
-0.190	7.200	0.026	-1.319	7.494	0.173
0.165	4.743	-0.035	-1.080	4.581	0.229
0.023	3.573	-0.007	-0.563	3.322	0.167
-0.009	2.678	0.003	-0.589	2.513	0.228
..† PSS of HPS_1 is OFF as it operates as a synchronous compensator in this case					

Table 6 Rotor modes. Case 5: PSSs out and in service. (Damping gains 20pu on rating)

Case 5: No PSSs			Case 5: All PSS in service		
Real	Imag	Damping Ratio	Real	Imag	Damping Ratio
0.181	10.940	-0.017	-2.409	11.257	0.209
0.086	9.570	-0.009	-1.988	9.762	0.200
-0.163	9.171	0.018	-2.093	9.395	0.217
-0.182	8.696	0.021	-2.187	9.119	0.233
-0.496	8.554	0.058	-2.471	8.828	0.270
-0.263	8.452	0.031	-2.024	8.382	0.235
-0.524	7.975	0.066	-2.382	7.969	0.286
0.008	7.896	0.000	-1.853	7.809	0.231
-0.157	7.736	0.020	-2.116	7.865	0.260
-0.765	7.241	0.105	-1.858	7.449	0.242
0.191	4.152	-0.046	-0.884	3.902	0.221
0.006	3.122	-0.002	-0.457	2.889	0.156
0.059	2.154	-0.027	-0.497	1.957	0.246

Table 7 Rotor modes. Case 6: PSSs out and in service. (Damping gains 20pu on rating)

Case 6: No PSSs			Case 6: All PSS in service …†		
Real	Imag	Damping Ratio	Real	Imag	Damping Ratio
0.276	10.390	-0.027	-2.217	10.708	0.203
0.318	10.138	-0.031	-2.142	10.652	0.197
-0.129	9.423	0.014	-2.069	10.017	0.202
-0.233	8.920	0.026	-2.522	9.541	0.256
-0.455	8.738	0.052	-2.381	9.023	0.255
-0.136	8.578	0.016	-2.320	8.506	0.263
-0.213	8.285	0.026	-2.579	8.453	0.292
-1.507	8.237	0.180	-1.701	8.168	0.204
-0.301	8.128	0.037	-2.076	8.242	0.244
-0.359	7.250	0.049	-1.598	7.553	0.207
0.200	4.810	-0.041	-1.078	4.644	0.226
0.054	3.552	-0.015	-0.565	3.298	0.169
0.036	2.597	-0.014	-0.520	2.451	0.207
…† PSS of HPS_1 is OFF as it operates as a synchronous compensator in this case.					

9 Transient stability analysis

A large-signal model of the system has been developed to allow transient stability analysis. The data for the large-signal model is presented in Appendix II in a format amenable to use with the PSS®/E transient-stability program. Since, at this stage, the model does not include representation of the generator turbine / governing systems this large signal is unsuitable for analysing loss of generation / load events.

The small-disturbance performance of the PSS®/E implementation of the simplified 14-generator model has been thoroughly benchmarked with the original Mudpack implementation of the model in Appendix III. With appropriate setting of PSS®/E simulation parameters there is close agreement between the respective simulation packages.

A comprehensive set of transient stability studies are conducted in Appendix IV. It is found that the system is transiently stable for a comprehensive set of two-phase to ground faults across all six base case scenarios. (Note that in accord with the Australian National Electricity Rules [18] two-phase to ground faults are considered to be the most severe *credible* contingency for voltages at and above 220 kV; the risk of solid three-phase to ground faults is, except under extraordinary circumstances, considered to be so low to be non-credible.)

10 Acknowledgements

The authors are most grateful for advice and assistance of Dr. Leonardo Lima in their development of the PSS®/E dynamics data set for the model. Some of the ideas on data presentation contained in his draft report have been employed in this report.

During the development of this and earlier versions of the 14-generator model of the Australian system we have been grateful for the opportunity to collaborate with Prof. Rodrigo Ramos and some of his students, particularly Dr. Rodrigo Salim, in their benchmarking of our model with the PacDyn software package.

We thank researchers who have identified errors or unrealistic parameter values in the model. We endeavour to address such matters, at least by notifying users of the deficiencies in reports such as this and, hopefully, over time correcting the model data and associated results.

11 References

[1] *PSS®/E Version 32, Program Operation Manual:* Siemens, June 2009.
Siemens-PTI PSS®/E web address:
http://w3.usa.siemens.com/smartgrid/us/en/transmission-grid/products/grid-analysis-tools/transmission-system-planning/Pages/transmission-system-planning.aspx

[2] Gibbard, M.J. "Coordinated design of multi-machine power system stabilisers based on damping torque concepts". Proceedings IEE, Pt.C, Vol.135, July 1988, pp.276-284.

[3] Gibbard, M.J. "Robust design of fixed-parameter power system stabilisers over a wide range of operating conditions". IEEE Transactions on Power Systems, Vol. 6, No. 2, May 1991, pp 794-800.

[4] Pourbeik, P. and Gibbard, M.J., "Damping and synchronising torques induced on generators by FACTS stabilizers in multi-machine power systems", IEEE Transactions on Power Systems, Vol. 11, no. 4, Nov. 1996, pp. 1920-1925.

[5] Pourbeik, P. and Gibbard, M.J., "Simultaneous coordination of Power-System Stabilizers and FACTS device stabilizers in a multi-machine power system for enhancing dynamic performance", IEEE Transactions on Power Systems, Vol. 13, no. 2, May 1998, pp. 473-479.

[6] Gibbard, M.J., Vowles, D.J. and Pourbeik, P., "Interactions between, and effectiveness of, power system stabilizers and FACTS stabilizers in multi-machine systems", IEEE Transactions on Power Systems, Vol. 15, no. 2, May 2000, pp. 748-755. (In February 2001 this paper received the Prize Paper Award for 2000 from the Power System Dynamic Performance Committee of the IEEE PES.)

[7] CIGRE Technical Brochure no. 166 prepared by Task Force 38.02.16, "Impact of Interactions among Power System Controls", published by CIGRE in August 2000.

[8] Gibbard, M.J. and Vowles, D.J., "Discussion of 'The application of Power System Stabilizers to multi-generator plant", IEEE Transactions on Power Systems. Vol. 15, no. 4, Nov. 2000, pp. 1462-1464.

[9] Gibbard, M.J., Martins, N., Sanchez-Gasca, J.J., Uchida, N., Vittal, V. and Wang, L., "Recent Applications in Linear Analysis Techniques", IEEE Transactions on Power Systems. Vol. 16, no. 1, Feb. 2001, pp. 154-162.

[10] Pourbeik, P., Gibbard, M.J. and Vowles, D.J., "Proof of the equivalence of residues and induced torque coefficients for use in the calculation of eigenvalue shifts", IEEE Power Engineering Review, Power Engineering Letters, Vol. 22, no.1, Jan. 2002, pp. 58-60.

[11] Gibbard, M.J. and Vowles, D.J., "Reconciliation of methods of compensation for PSSs in multimachine systems", IEEE Transactions on Power Systems. Vol. 19, no. 1, Feb. 2004, pp. 463-472.

[12] E.V. Larsen and D.A. Swann, "Applying power system stabilizers: Part I - III", IEEE Transactions PAS, Vol. 100, pp. 3017-3046, 1981.

[13] P. Kundur, *Power System Stability and Control*, McGraw-Hill, Inc., 1994.

[14] Vowles, D.J. and Gibbard, M.J., "Mudpack - a software package for the analysis of the small-signal dynamic performance and control of large electric power systems", School of Electrical & Electronic Engineering, The University of Adelaide, South Australia.

[15] IEEE Committee Report, "Static VAr compensator models for power flow and dynamic performance simulation," *Power Systems, IEEE Transactions on,* vol. 9, pp. 229-240, 1994.

[16] IEEE Recommended Practice for Excitation System Models for Power System Stability Studies, IEEE Standard No:421.5-2005, ISBN:0-7381-4787-7.

[17] IEEE Committee Report, "Excitation System Models for Power System Stability Studies," *Power Apparatus and Systems, IEEE Transactions on,* vol. PAS-100, pp. 494-509, 1981.

[18] *[Australian] National Electricity Rules, Version 60*.
Available: http://www.aemc.gov.au/Electricity/National-Electricity-Rules/Current-Rules.html

Appendix I Data

Please note the Caveats listed in Section 2 before using this data.

I.1 Steady-state analysis

Table 1 (repeated) Six normal steady-state operating conditions

	Case 1 Load	Case 2 Load	Case 3 Load	Case 4 Load	Case 5 Load	Case 6 Load
Load Condition	Heavy	Medium-heavy	Peak	Light	Medium	Light
Total generation MW	23030	21590	25430	15050	19060	14840
Total load MW	22300	21000	24800	14810	18600	14630
Inter-area flows	(North to south)	(South to north)	(Hydro to N & S)	(Area 2 to N & S)	(N & S to pumping)	(~Zero transfers)
Area 4 to Area 2 MW	500	-500	-500	-200	300	0
Area 2 to Area 1 MW	1134	-1120	-1525	470	740	270
Area 1 to Area 3 MW	1000	-1000	1000	200	-200	0
Area 3 to Area 5 MW	500	-500	250	200	250	0

Table 8 Generation conditions for six loadflow cases. (Voltage at all generator buses is 1.0 pu in all cases.)

Power Station / Bus # Rating Rated power factor	Case 1 No. units MW Mvar	Case 2 No. units MW Mvar	Case 3 No. units MW Mvar	Case 4: No. units MW Mvar	Case 5: No. units MW Mvar	Case 6: No. units MW Mvar
HPS_1 / 101 12 x 333.3 MVA 0.9 power factor lag	4 75.2 77.9	3 159.6 54.4	12 248.3 21.8	2 0 -97.4 Syn.Cond	3 -200.0 -26.0 Pumping	2 0 -102.2 Syn. Cond
BPS_2 / 201 6 x 666.7 MVA 0.9 power factor lag	6 600.0 95.6	5 560.0 38.9	6 550.0 109.1	4 540.0 -30.8	5 560.0 38.7	3 560.0 -53.5
EPS_2 / 202 5 x 555.6 MVA 0.9 power factor lag	5 500.0 132.7	4 480.0 60.5	5 470.0 127.6	3 460.0 -2.5	4 480.0 67.2	3 490.0 -7.3
VPS_2 / 203 4 x 555.6 MVA 0.9 power factor lag	4 375.0 132.8	3 450.0 82.4	2 225.0 157.0	3 470.0 9.4	2 460.0 83.1	3 490.0 3.7

Power Station / Bus # Rating Rated power factor	Case 1 No. units MW Mvar	Case 2 No. units MW Mvar	Case 3 No. units MW Mvar	Case 4: No. units MW Mvar	Case 5: No. units MW Mvar	Case 6: No. units MW Mvar
MPS_2 / 204 6 x 666.7 MVA 0.9 power factor lag	6 491.7 122.4	4 396.0 17.8	6 536.0 96.5	4 399.3 -43.6	4 534.4 55.2	3 488.6 -61.2
LPS_3 / 301 8 x 666.7 MVA 0.9 power factor lag	7 600.0 142.3	8 585.0 141.1	8 580.0 157.6	6 555.0 16.6	8 550.0 88.1	6 550.0 9.4
YPS_3 / 302 4 x 444.4 MVA 0.9 power factor lag	3 313.3 51.5	4 383.0 63.3	4 318.0 49.6	2 380.0 -9.3	3 342.0 43.8	2 393.0 -6.9
TPS_4 / 401 4 x 444.4 MVA 0.9 power factor lag	4 350.0 128.7	4 350.0 116.5	4 350.0 123.2	3 320.0 -21.9	4 346.0 84.9	3 350.0 -32.6
CPS_4 / 402 3 x 333.3 MVA 0.9 power factor lag	3 279.0 59.3	3 290.0 31.4	3 290.0 32.0	2 290.0 -2.4	3 280.0 45.4	3 270.0 4.7
SPS_4 / 403 4 x 444.4 MVA 0.9 power factor lag	4 350.0 52.3	4 350.0 47.2	4 350.0 47.3	3 320.0 14.2	4 340.0 46.3	2 380.0 25.2
GPS_4 / 404 6 x 333.3 MVA 0.9 power factor lag	6 258.3 54.5	6 244.0 39.8	6 244.0 40.0	3 217.0 -3.5	5 272.0 50.4	3 245.0 3.9
NPS_5 / 501 2 x 333.3 MVA 0.9 power factor lag	2 300.0 25.3	2 300.0 -8.8	2 300.0 6.5	2 280.0 -52.5	2 280.0 -35.2	1 270.0 -42.2
TPS_5 / 502 4 x 250 MVA 0.8 pf lag	4 200.0 40.1	4 200.0 53.0	4 180.0 48.8	3 180.0 -1.8	4 190.0 0.1	4 200.0 -9.7
PPS_5 / 503 6 x 166.7 MVA 0.9 power factor lag	4 109.0 25.2	5 138.0 36.9	6 125.0 32.6	1 150.0 2.2	2 87.0 3.5	2 120.0 -11.2

As mentioned in the introduction, in this report, the online generators within each of the 14 power-plants are each replaced by an aggregated equivalent generator. While the generators in each station could have been individually represented, this adds an additional level of complexity and increases system size, moreover, it is not warranted for the primary purpose of this document. If the researcher intends to investigate intra-plant dynamic performance for a particular power plant they can readily modify the power flow and dynamics data to individually represent each on-line unit within the plant. In general, a power plant has n identical generating units of which $m \leq n$ are online. If $m = 0$ the entire power-plant is off-line. It is also assumed that each of the n generator step-up transformers is identical. The steady-state operating conditions of each of the m online units are assumed to be identical. For the purpose of analysing any disturbance external to the power plant; or any disturbance which is applied identically to all on-line units within the plant we can aggregate the m on-line units to form a single equivalent unit as illustrated in Figure 18. For such disturbances the dynamic performance of the system in which the

generating plant is replaced by a single equivalent unit is identical to that of the system with the original *m* identical on-line units. Of course, the *m-1* intra-plant modes of oscillation do not exist in the single composite representation, however, these modes are not excited by such disturbances.

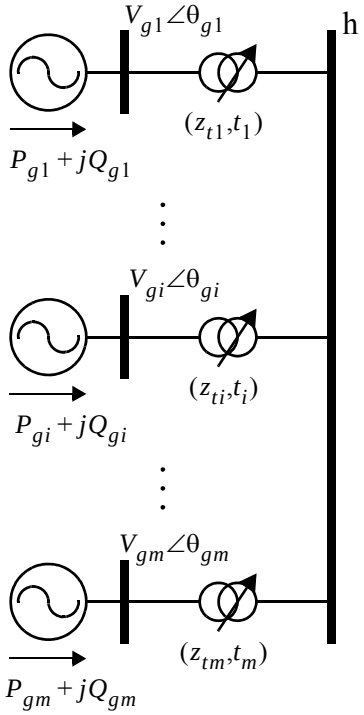

One line diagram of power-plant with *m* individual online generators.

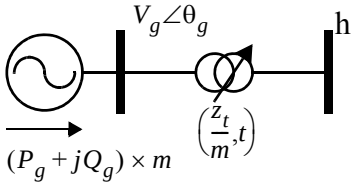

One line diagram of power-plant with single aggregated equivalent generator to represent the *m* online generators.

Notes:

(a) Generator terminal voltages, angles and power generation are identical: $V_{g1} = ... = V_{gi} = ... = V_{gm} = V_g$ pu; $\theta_{g1} = ... = \theta_{gi} = ... = \theta_{gm} = \theta_g$ deg; $P_{g1} = ... = P_{gi} = ... = P_{gm} = P_g$ MW; and $Q_{g1} = ... = Q_{gi} = ... = Q_{gm} = Q_g$ Mvar. The MVA base of each of the *m* generators is *MBASE*.

(b) For the aggregate equivalent generator the terminal voltage and angle is V_g pu and θ_g deg respectively. The real and reactive power output is $(m \times P_g)$ MW and $(m \times Q_g)$ Mvar respectively. The MVA base of the aggregate generator is (*m x MBASE)* MVA.

(c) The impedance and tap position of each generator transformer is identical: $z_{t1} = ... = z_{ti} = ... = z_{tm} = z_t = r_t + jx_t$ pu on system MVA base; and $t_1 = ... = t_i = ... = t_m = t$ pu;

(d) The impedance and tap position of the aggregate equivalent generator transformer is $(r_t + jx_t)/m$ pu on system MVA base; and t pu respectively.

(e) Usually, generator model parameters are specified on the generator MVA base. If so then it is unnecessary to modify the values of the generator parameters. Otherwise, the user must convert the parameters of the equivalent generator model from per-unit on (*m x MBASE)* to the base required by their simulation program.

Figure 18 Formulation of a single aggregated equivalent generator to represent *m* online generators in a power-plant.

Table 9 SVC ratings and operating conditions for loadflow Cases 1 to 6.

SVC name / BusNo.	Reactive Power Range (MBASE)	Qmax	Qmin	Case 1 Voltage Mvar	Case 2 Voltage Mvar	Case 3 Voltage Mvar	Case 4 Voltage Mvar	Case 5 Voltage Mvar	Case 6 Voltage Mvar
	Mvar @ 1.0 pu voltage								
ASVC_2 / 205	650.0	430.0	-220.0	1.055 -68.3	1.055 41.8	1.02 -5.2	1.045 -39.3	1.045 -118.3	1.045 -29.4
RSVC_3 / 313	800.0	600.0	-200.0	1.015 71.4	1.015 129.4	1.015 158.8	1.015 86.7	1.015 54.9	1.015 54.2
BSVC_4 / 412	1430.0	1100.0	-330.0	1.000 58.2	1.000 63.9	1.000 83.8	1.000 -52.2	1.000 22.8	1.000 -0.2
PSVC_5 / 507	500.0	320.0	-180.0	1.015 22.6	1.040 36.8	1.043 18.0	1.010 -4.0	1.015 13.8	1.000 -3.7
SSVC_5 / 509	550.0	400.0	-150.0	1.030 10.6	1.027 50.2	1.050 -63.4	1.030 -109.3	1.030 -123.8	1.030 -109.3

Table 10 Transmission Line Parameters: Values per circuit.

From bus / to bus	Line No.	Line r+jx; b (pu on 100MVA)
102 217	1,2	0.0084 0.0667 0.817
102 217	3,4	0.0078 0.0620 0.760
102 309	1,2	0.0045 0.0356 0.437
102 309	3	0.0109 0.0868 0.760
205 206	1,2	0.0096 0.0760 0.931
205 416	1,2	0.0037 0.0460 0.730
206 207	1,2	0.0045 0.0356 0.437
206 212	1,2	0.0066 0.0527 0.646
206 215	1,2	0.0066 0.0527 0.646
207 208	1,2	0.0018 0.0140 0.171
207 209	1	0.0008 0.0062 0.076
208 211	1,2,3	0.0031 0.0248 0.304
209 212	1	0.0045 0.0356 0.437
210 213	1,2	0.0010 0.0145 1.540
211 212	1,2	0.0014 0.0108 0.133
211 214	1	0.0019 0.0155 0.190
212 217	1	0.0070 0.0558 0.684
214 216	1	0.0010 0.0077 0.095
214 217	1	0.0049 0.0388 0.475
215 216	1,2	0.0051 0.0403 0.494
215 217	1,2	0.0072 0.0574 0.703
216 217	1	0.0051 0.0403 0.494

From bus / to bus	Line No.	Line r+jx; b (pu on 100MVA)
303 304	1,2	0.0020 0.0280 0.740
303 305	1,2	0.0011 0.0160 1.700
304 305	1	0.0003 0.0040 0.424
305 306	1	0.0002 0.0030 0.320
305 307	1,2	0.0003 0.0045 0.447
306 307	1	0.0001 0.0012 0.127
307 308	1,2	0.0023 0.0325 3.445
309 310	1,2,3	0.0135 0.1070 0.5827
310 311	1,2	0.0000 -0.0337 0.000
312 313	1,2,3	0.0060 0.0450 0.300
313 314	1,2	0.0010 0.0100 0.260
315 509	1,2	0.0070 0.0500 0.190
405 406	1,2	0.0039 0.0475 0.381
405 408	1	0.0054 0.0500 0.189
405 409	1,2,3	0.0180 0.1220 0.790
406 407	1,2	0.0006 0.0076 0.062
407 408	1	0.0042 0.0513 0.412
408 410	1,2,3	0.0165 0.1920 0.673
409 411	1,2	0.0103 0.0709 0.460
410 411	1	0.0043 0.0532 0.427
410 412	1 to 4	0.0043 0.0532 0.427
410 413	1,2	0.0040 0.0494 0.400
411 412	1,2	0.0012 0.0152 0.122
414 415	1,2	0.0020 0.0250 0.390
415 416	1,2	0.0037 0.0460 0.730
504 507	1,2	0.0230 0.1500 0.560
504 508	1,2	0.0260 0.0190 0.870
505 507	1,2	0.0016 0.0170 0.030
505 508	1	0.0025 0.0280 0.170
506 507	1,2	0.0016 0.0170 0.030
506 508	1	0.0030 0.0280 0.140
507 508	1	0.0020 0.0190 0.090
507 509	1-6	0.0900 0.6600 0.300

Notes:
(a) System frequency is 50 Hz.
(b) In Version 4 the number of parallel circuits between the following pairs of buses were increased:
303-304: 1 to 2 ckt
309-310: 2 to 3 ckt
312-313: 1 to 3 ckt.
313-314: 1 to 2 ckt
505-507: 1 to 2 ckt
506-507: 1 to 2 ckt
507-509: 2 to 6 ckt
If the number of parallel circuits between a pair of nodes is changed from *m* to *n* then the per-circuit impedance and susceptance *(r + jx, b)* is changed to *((r + jx)*n/m, b*m/n)*. Consequently, the aggregate impedance and susceptance between the pair of nodes is unchanged.

Table 11 Transformer Ratings and Reactance.

Buses		Number	Rating, each Unit (MVA)	Reactance per transformer	
From	To			% on Rating	per unit on 100MVA
101	102	ng	333.3	12.0	0.0360
201	206	ng	666.7	16.0	0.0240
202	209	ng	555.6	16.0	0.0288
203	208	ng	555.6	17.0	0.0306
204	215	ng	666.7	16.0	0.0240
209	210	4	625.0	17.0	0.0272
213	214	4	625.0	17.0	0.0272
301	303	ng	666.7	16.0	0.0240
302	312	ng	444.4	15.0	0.0338
304	313	2	500.0	16.0	0.0320
305	311	3	333.3	12.0	0.0360
305	314	2	700.0	17.0	0.0243
308	315	2	370.0	10.0	0.0270
401	410	ng	444.4	15.0	0.0338
402	408	ng	333.3	17.0	0.0510
403	407	ng	444.4	15.0	0.0338
404	405	ng	333.3	17.0	0.0510
413	414	3	750.0	6.0	0.0080
501	504	ng	333.3	17.0	0.0510
502	505	ng	250.0	16.0	0.0640
503	506	ng	166.7	16.7	0.1000

Notes:
(a) System frequency is 50 Hz.
(b) n_g - Generator/transformer unit; in-service if associated generator is on-line. (Thus, if n_g generator units are on-line then the impedance of the aggregated generator step-up transformer is x_t/n_g where x_t is the impedance of a single generator step-up transformer.)

Table 12 Switched Shunt Capacitor / Reactor banks (C/R) in service, Cases 1-6 (Mvar)

Bus Number	Case 1	Case 2	Case 3	Case 4	Case 5:	Case 6:
211	-	-	100 C	-	-	-
212	400 C	150 C	150 C	400 C	400 C	400 C
216	300 C	150 C	150 C	300 C	300 C	300 C
409	60 C	60 C	60 C	60 C	60 C	60 C
411	30 C	30 C	30 C	30 C	30 C	30 C
414	30 R	30 R	30 R	30 R	30 R	30 R
415	60 R	60 R	60 R	60 R	60 R	60 R
416	60 R	60 R	60 R	60 R	60 R	90 R
504	-	90 R	90 R	-	-	-

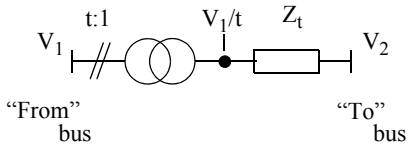

Taps-ratio convention employed

Figure 19 Transformer Taps Convention

The transformer tap ratios listed in Table 13 are based upon the convention shown in Figure 19.

Table 13 Transformer Tap Ratios for Loadflow Cases 1 to 6

Buses		Case 1	Case 2	Case 3	Case 4	Case 5	Case 6
From	To						
101	102	0.939	0.948	0.948	1.000	1.000	1.000
201	206	0.943	0.948	0.939	1.000	0.971	1.010
202	209	0.939	0.948	0.939	1.000	0.971	1.010
203	208	0.939	0.948	0.939	1.000	0.971	1.010
204	215	0.939	0.948	0.939	1.000	0.971	1.010
209	210	0.976	0.990	0.976	0.976	0.976	0.976
213	214	1.000	1.000	1.000	1.000	1.000	1.000
301	303	0.939	0.935	0.930	1.000	0.961	1.000
302	312	0.952	0.952	0.952	1.000	0.961	1.000
304	313	0.961	0.961	0.948	0.961	0.961	0.961
305	311	1.000	1.000	1.000	1.000	1.000	1.000
305	314	1.000	1.000	1.000	1.000	1.000	1.000
308	315	1.000	0.960	1.000	1.000	1.000	1.000
401	410	0.939	0.939	0.939	1.000	0.952	1.010
402	408	0.952	0.952	0.952	1.000	0.952	1.000
403	407	0.952	0.952	0.952	1.000	0.952	1.000
404	405	0.952	0.952	0.952	1.000	0.952	1.000
413	414	1.000	1.000	1.000	1.000	1.015	1.000
501	504	0.952	0.952	0.952	1.000	0.985	1.015
502	505	0.962	0.930	0.930	1.000	0.995	1.020
503	506	0.962	0.930	0.930	1.000	0.985	1.020

For simplicity, loads are assumed to behave as constant impedances in the small- and large-signal analysis.

Table 14 Busbar Loads (P MW, Q Mvar) for Cases 1 to 6

	Case 1		Case 2		Case 3		Case 4		Case 5		Case 6	
Bus No.	P	Q	P	Q	P	Q	P	Q	P	Q	P	Q
102	450	45	380	38	475	50	270	30	340	35	270	30
205	390	39	330	33	410	40	235	25	290	30	235	25
206	130	13	110	11	140	15	80	10	100	10	80	10
207	1880	188	1600	160	1975	200	1130	120	1410	145	1110	120
208	210	21	180	18	220	25	125	15	160	20	125	15
211	1700	170	1445	145	1785	180	1060	110	1275	130	1035	110
212	1660	166	1410	140	1740	180	1000	110	1245	125	1000	110
215	480	48	410	40	505	50	290	30	360	40	290	30
216	1840	184	1565	155	1930	200	1105	120	1380	140	1105	120
217	1260	126	1070	110	1320	140	750	80	940	95	750	80
306	1230	123	1230	123	1450	150	900	90	1085	110	900	90
307	650	65	650	65	770	80	470	50	580	60	470	50
308	655	66	655	66	770	80	620	100	580	60	620	100
309	195	20	195	20	230	25	140	15	170	20	140	15
312	115	12	115	12	140	15	92	10	105	15	92	10
313	2405	240	2405	240	2840	290	1625	165	2130	220	1625	165
314	250	25	250	25	300	30	180	20	222	25	180	20
405	990	99	1215	120	1215	120	730	75	990	100	730	75
406	740	74	905	90	905	90	540	55	740	75	540	55
407	0	0	0	0	0	0	0	0	0	0	0	0
408	150	15	185	20	185	20	110	10	150	15	110	10
409	260	26	310	30	310	30	190	20	260	30	190	20
410	530	53	650	65	650	65	390	40	530	55	390	40
411	575	58	700	70	700	70	420	45	575	60	420	45
412	1255	126	1535	155	1535	155	922	100	1255	130	922	100
504	300	60	200	40	300	60	180	20	225	25	170	20
507	1000	200	710	140	1100	220	640	65	750	75	565	65
508	800	160	520	105	800	160	490	50	600	60	450	50
509	200	40	70	15	100	20	122	15	150	15	117	15

Load Characteristics: Constant Impedance

I.2 Dynamic performance analysis

I.2.1 Generator model parameters (small- and large-signal)

The parameters of the fourteen generators are listed in Table 15. The generator model to which these parameters apply are given in Section I.5. It should be noted that various simulation packages may adopt the same set of generator model parameters but employ different model formulations. Differences in the representation of generator saturation between simulation packages are frequently observed. For that reason, and since generator saturation tends to have a small effect of damping performance, generator saturation has been neglected in this benchmark model.

Table 15 Generator Parameters

Generator	Bus	Order	Rating MVA per Unit	Max. No. of Units	H MWs/MVA	Xa pu	Xd pu	Xq pu	Xd' pu	Tdo's	Xd" pu	Tdo"s	Xq' pu	Tqo's	Xq" pu	Tqo"s
HPS_1	101	5	333.3	12	3.60	0.14	1.10	0.65	0.25	8.50	0.25	0.050	-	-	0.25	0.200
BPS_2	201	6	666.7	6	3.20	0.20	1.80	1.75	0.30	8.50	0.21	0.040	0.70	0.30	0.21	0.080
EPS_2	202	6	555.6	5	2.80	0.17	2.20	2.10	0.30	4.50	0.20	0.040	0.50	1.50	0.21	0.060
MPS_2	204	6	666.7	6	3.20	0.20	1.80	1.75	0.30	8.50	0.21	0.040	0.70	0.30	0.21	0.080
VPS_2	203	6	555.6	4	2.60	0.20	2.30	1.70	0.30	5.00	0.25	0.030	0.40	2.00	0.25	0.250
LPS_3	301	6	666.7	8	2.80	0.20	2.70	1.50	0.30	7.50	0.25	0.040	0.85	0.85	0.25	0.120
YPS_3	302	5	444.4	4	3.50	0.15	2.00	1.80	0.25	7.50	0.20	0.040	-	-	0.20	0.250
CPS_4	402	6	333.3	3	3.00	0.20	1.90	1.80	0.30	6.50	0.26	0.035	0.55	1.40	0.26	0.040
GPS_4	404	6	333.3	6	4.00	0.18	2.20	1.40	0.32	9.00	0.24	0.040	0.75	1.40	0.24	0.130
SPS_4	403	6	444.4	4	2.60	0.20	2.30	1.70	0.30	5.00	0.25	0.030	0.40	2.00	0.25	0.250
TPS_4	401	6	444.4	4	2.60	0.20	2.30	1.70	0.30	5.00	0.25	0.030	0.40	2.00	0.25	0.250
NPS_5	501	6	333.3	2	3.50	0.15	2.20	1.70	0.30	7.50	0.24	0.025	0.80	1.50	0.24	0.100
TPS_5	502	6	250.0	4	4.00	0.20	2.00	1.50	0.30	7.50	0.22	0.040	0.80	3.00	0.22	0.200
PPS_5	503	6	166.7	6	7.50	0.15	2.30	2.00	0.25	5.00	0.17	0.022	0.35	1.00	0.17	0.035

Generator reactances in per unit on machine rating as base.
For all generators the stator winding resistance (Ra) and damping torque coefficient (D) are both assumed to be zero.
System frequency is 50 Hz.

I.2.2 Small-signal Excitation System Models and Parameters

Two basic types of excitation systems are employed, ST1A and AC1A [16]. For simplicity exciter saturation, exciter armature reaction and voltage-drop due to rectifier regulation are neglected in the AC1A model. The parameters of the AVR have been tuned to ensure that the open-circuit generator under closed-loop voltage control is stable and satisfies the performance specifications. The small-signal models for the ST1A and AC1A excitation systems are shown in Figures 20 and 21, respectively.

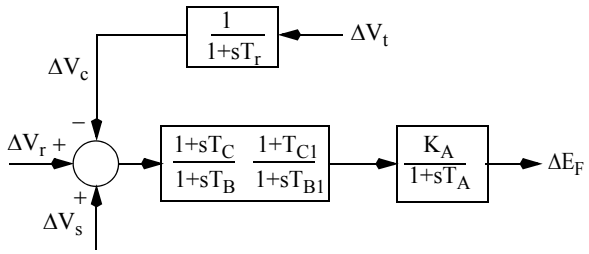

Figure 20 Small-signal model of a type ST1A excitation system.

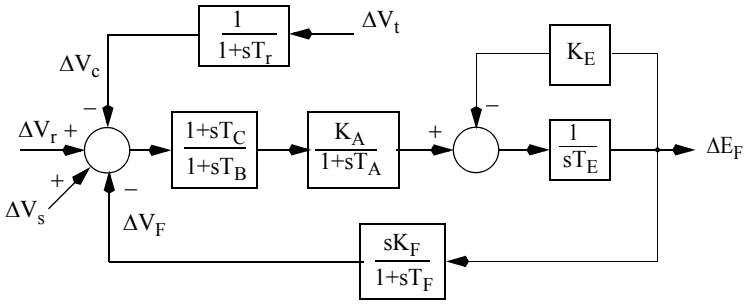

Figure 21 Small-signal model of a type AC1A Excitation System; exciter saturation, the demagnetizing effect of generator field current and the voltage drop due to rectifier regulation are neglected.

Table 16 Small-signal excitation System Model Parameters: 14-generator system

	HPS_1 / 101	BPS_2 / 201	EPS_2 / 202	VPS_2 / 203	MPS_2 / 204	LPS_3 / 301	YPS_3 / 302	TPS_4 / 401	CPS_4 / 402	SPS_4 / 403	GPS_4 / 404	NPS_5 / 501	TPS_5 / 502	PPS_5 / 503
Type	ST1A	ST1A	AC1A	ST1A	ST1A	ST1A	AC1A	ST1A	ST1A	ST1A	ST1A	AC1A	ST1A	ST1A
T_r (s)	0	0	0	0	0	0	0	0	0.02	0	0	0	0	0
K_A (s)	200	400	400	300	400	400	200	300	300	300	250	1000	400	300
T_A (s)	0.10	0.02	0.02	0.01	0.02	0.05	0.05	0.10	0.05	0.01	0.20	0.04	0.50	0.01
T_B (s)	13.25	1.12	0	0.70	1.12	6.42	0	40.0	9.80	0.70	0.0232	0	16.0	0.8
T_C (s)	2.50	0.50	0	0.35	0.50	1.14	0	4.00	1.52	0.35	0.1360	0	1.40	0.2
K_E	-	-	1.0	-	-	-	1.0	0	0	0	0	0	0.05	0
T_E (s)	-	-	1.0	-	-	-	1.333	0	0	0	0	0	0.60	0
K_F	-	-	0.029	-	-	-	0.020	-	-	-	-	1.00	-	-
T_F (s)	-	-	1.0	-	-	-	0.8	-	-	-	-	0.87	-	-

I.2.3 SVC small-signal model and parameters

From a small-signal perspective the SVC is represented as a perturbation in the shunt susceptance ΔB connected to the bus. The susceptance is controlled by a voltage-regulator with SVC current droop as depicted in Figure 22. (Note: In Version 3 and earlier ΔB and $\Delta[Q/V_t]$ were in per-unit on the system MVA base of 100 MVA, whereas now they are in per-unit on the SVC Mvar base. Consequently the base conversion factor K_s is now included in the model. It is emphasized that this change in base has no effect on the dynamic performance of the model.)

An alternative formulation of the SVC model in which the current droop signal is represented implicitly, under the assumption that the perturbation in voltage is "small" compared to the associated perturbation in susceptance, is developed in Appendix II.2.2. The alternative formulation is developed to allow the SVC to be represented in the PSS®/E program using one of its built-in SVC models. It is shown in the later appendix that the damping performance of the system with the alternative SVC model formulation is practically identical to that obtained with the SVC model in Figure 22.

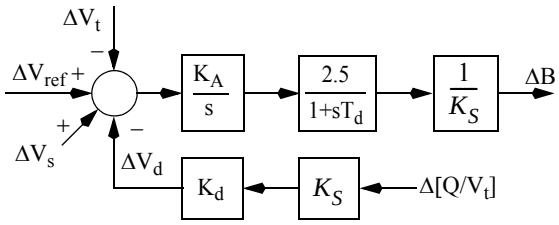

SVC name / bus number	MBASE (Mvar)	K_A	K_S
ASVC_2/205	650.0	500.0	6.5
RSVC_3/313	800.0	500.0	8.0
BSVC_4/412	1430.0	500.0	14.3
PSVC_5/507	500.0	250.0	5.0
SSVC_5/509	550.0	250.0	5.5

ΔB and $\Delta[Q/V_t]$ are in per-unit on MBASE.

K_d = 0.01 pu on SBASE and T_d = 0.005 s

Figure 22 Small-signal model of the SVCs.

I.3 Power System Stabiliser (PSS) Parameters

The structure of the PSS employing a speed-stabilising signal is shown in Figure 23. The design based on the P-Vr method of the block labelled 'Compensation TF and LP Filter' has been outlined in Section 6.3.

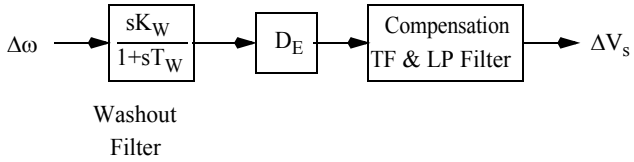

Figure 23 Structure of the PSS for analysis and design purposes

Assuming a single washout filter block is employed, the general form of the PSS TF is given in (2), i.e.

$$H_{PSS}(s) = kG_c(s) = k \cdot \left[\frac{sT_W}{1+sT_W} \cdot \frac{1}{k_c} \cdot \frac{(1+c_1 s + c_2 s^2)(1+sT_a)\ldots}{(1+sT_{b1})\ldots(1+sT_1)(1+sT_2)\ldots} \right].$$

The 'Compensation TF & LP Filter' (which excludes the Washout Filter) in Figure 23 represents a general form of that component in the above PSS TF given by:

$$H_c(s) = K_c \cdot \frac{(1+c_1 s + c_2 s^2)(1+sT_{a1})\ldots}{(1+sT_{b1})\ldots(1+sT_1)(1+sT_2)\ldots} \quad \text{where} \quad K_c = 1/k_c \tag{6}$$

In the PSS transfer function of Figure 23, (i) the damping gain of the PSS is $k = D_e = 20$ pu on generator MVA rating, and (ii) the washout time constant T_W is 7.5 s.

I.3.1 PSS compensating transfer functions and parameters

Form of the fourth-order TF having real zeros:

$$H_c(s) = K_c \cdot \frac{1+sT_a}{1+sT_e} \cdot \frac{1+sT_b}{1+sT_f} \cdot \frac{1+sT_c}{1+sT_g} \cdot \frac{1+sT_d}{1+sT_h} \tag{7}$$

Table 17 Compensation and LP Filter Parameters for PSS based on (7).

Generator Name / Number	K_c	T_a	T_b	T_c	T_d	T_e	T_f	T_g	T_h
EPS_2 / 202	0.233	0.286	0.111	0.040	0	0.00667	0.00667	0.00667	0
TPS_5 / 502	0.294	0.500	0.0588	0.0167	0	0.00667	0.00667	0.00667	0
PPS_5 / 503	0.178	0.200	0.187	0.167	0.020	0.350	0.0667	0.00667	0.00667

Form of the fourth-order TF having real and complex zeros:

$$H_c(s) = K_c \cdot \frac{1+sT_a}{1+sT_d} \cdot \frac{1+sT_b}{1+sT_e} \cdot \frac{1+as+bs^2}{(1+sT_f)(1+sT_g)} \tag{8}$$

Table 18 Compensation and LP Filter Parameters for PSS based on (8)

Generator Name / Number	K_c	T_a	T_b	a	b	T_d	T_e	T_f	T_g
MPS_2 / 204	0.333	0.010	0	0.10	0.0051	0.00667	0	0.00667	0.00667
YPS_3 / 302	0.298	0.050	0	0.5091	0.1322	0.00667	0	0.00667	0.00667
NPS_5 / 501	0.195	0.033	0.033	0.30	0.1111	0.300	0.00667	0.00667	0.00667

Form of the second-order TF having real zeros:

$$H_c(s) = K_c \cdot \frac{1+sT_a}{1+sT_e} \cdot \frac{1+sT_b}{1+sT_f} \tag{9}$$

Table 19 Compensation and LP Filter Parameters for PSS based on (9)

Generator Name / Number	K_c	T_a	T_b	T_e	T_f
VPS_2 / 203	0.286	0.0708	0.0292	0.00667	0.00667
TPS_4 / 401	0.357	0.2083	0.2083	0.00667	0.00667
CPS_4 / 402	0.235	0.2777	0.1000	0.00667	0.00667

Form of the second-order TF having a pair of complex zeros:

$$H_c(s) = K_c \cdot \frac{1+as+bs^2}{(1+sT_e)(1+sT_f)} \tag{10}$$

Table 20 Compensation and LP Filter Parameters for PSS based on (10)

Generator Name / Number	K_c	a	b	T_e	T_f
HPS_1 / 101 *	0.769	0.3725	0.03845	0.00667	0.00667
BPS_2 / 201	0.278	0.1280	0.00640	0.00667	0.00667
LPS_3 / 301	0.625	0.1684	0.01180	0.00667	0.00667
SPS_4 / 403	0.316	0.0909	0.002067	0.00667	0.00667
GPS_4 / 404	0.303	0.1154	0.005917	0.00667	0.00667
* Note for HPS_1: PSSs are OFF in Cases 4 and 6. When motoring in Case5 the sign of the PSS output ΔV_S at the summing junction is negated - or equivalently the PSS gain setting is negated..					

I.4 Comparison of P-Vr and GEP methods

Table 21 P-Vr and GEP methods for the design of PSS compensation TFs

Comparison of two methods for the design of the PSS compensation transfer functions		
Feature	P-Vr	GEP [12]
1	Essentially an analytical frequency response approach using small-signal analysis software or Matlab. A wide range of normal and contingency operating conditions occurring on the power system is examined.	Originally a field-based frequency response method for tuning the PSS on a particular generator in a station for the particular operating condition(s) existing at the time.

Comparison of two methods for the design of the PSS compensation transfer functions		
Feature	P-Vr	GEP [12]
2	Calculates magnitude and phase of the P-Vr over the complete range of rotor modes.	Field measurements provide the phase response $\Delta V_{term}/\Delta V_{ref}$ over a frequency range. Higher frequency measurements may be limited by resonances at lightly-damped local-area or intra-station modal frequencies.
3	The shaft dynamics are disabled.	The phase response of the TF $\Delta V_{term}/\Delta V_{ref}$ is close to that of the P-Vr TF because the speed perturbations associated with measurements are small (i.e. the shaft dynamics are virtually disabled).
4	PSS TF synthesized in *both* magnitude and phase from P-Vr characteristic.	PSS TF is synthesized from phase response.
5	Using magnitude information from P-Vr TF, damping gain k_i is set to provide the left-shift required to satisfy relevant system stability criteria.	The gain setting of the PSS (on site) is determined by increasing the gain until the onset of instability is detected; the gain is set to 1/3rd the latter value.

I.5 Machine Equations

In Table 15 both fifth- and sixth-order generator models are represented; in the fifth-order model the q-axis representation is simplified.

I.5.1 Sixth-order generator model

The following is a sixth-order model of a synchronous generator employed in PSS®/E. In this model the "classically" defined, unsaturated operational-impedance parameters are used [13], section 4.1-2. A linearized form of these equations are provided in small-signal analysis packages such as [14].

Equations of motion:

$$\frac{d\delta}{dt} = \omega_0(\omega - 1), \tag{11}$$

$$2H\omega\frac{d\omega}{dt} = -D\omega(\omega - 1) + P_m - (v_D i_D + v_Q i_Q + r_a i_D^2 + r_a i_Q^2). \tag{12}$$

$$\omega_0 = 2\pi f_0, \; f_0 \text{ is 50 Hz},$$

where δ is the rotor angle (rad), and ω is the shaft speed in per-unit.

The rates of change of voltage behind transient reactance (E'_q and E'_d) and damper winding flux linkages (ψ_{kd} and ψ_{kq}) are given by:

$$\frac{dE'_q}{dt} = \frac{1}{T'_{d0}}(E_{fd} - X_{ad} i_{fd}); \tag{13}$$

$$\frac{d\psi_{kd}}{dt} = \frac{1}{T''_{d0}}(E'_q - \psi_{kd} - (X'_d - x_a)i_d); \tag{14}$$

$$\frac{dE'_d}{dt} = \frac{1}{T'_{q0}}X_{aq}i_{kq}; \tag{15}$$

$$\frac{d\psi_{kq}}{dt} = \frac{1}{T''_{q0}}(E'_d - \psi_{kq} - (X'_q - x_a)i_q). \tag{16}$$

The d- and q-axis components of the generator terminal voltage are:

$$v_d = -r_a i_d + X''_q i_q + \psi''_q, \tag{17}$$

$$v_q = -r_a i_q - X''_d i_d + \psi''_d. \tag{18}$$

The transformer voltages and the speed dependency of the rotational voltages in the stator equations are neglected.

The d- and q-axis components of the stator subtransient flux linkages, ψ''_d and ψ''_q, are:

$$\psi''_d = \left(\frac{X''_d - x_a}{X'_d - x_a}\right)E'_q + \left(\frac{X'_d - X''_d}{X'_d - x_a}\right)\psi_{kd}, \tag{19}$$

$$\psi''_q = \left(\frac{X''_q - x_a}{X'_q - x_a}\right)E'_d + \left(\frac{X'_q - X''_q}{X'_q - x_a}\right)\psi_{kq}. \tag{20}$$

The field current ($I_{fd} = X_{ad}i_{fd}$) is given by:

$$X_{ad}i_{fd} = K_{1d}E'_q + K_{2d}\psi_{kd} + K_{3d}i_d, \tag{21}$$

where

$$K_{1d} = 1 + \frac{(X_d - X'_d)(X'_d - X''_d)}{(X'_d - x_a)^2}, \quad K_{2d} = 1 - K_{1d}, \quad K_{3d} = \frac{(X_d - X'_d)(X''_d - x_a)}{(X'_d - x_a)}. \tag{22}$$

The q-axis excitation is:

$$X_{aq}i_{kq} = K_{1q}E'_d + K_{2q}\psi_{kq} + K_{3q}i_q, \tag{23}$$

where

$$K_{1q} = -\left[1 + \frac{(X_q - X'_q)(X'_q - X''_q)}{(X'_q - x_a)^2}\right], \qquad K_{2q} = -(1 + K_{1q}),$$

$$K_{3q} = \frac{(X_q - X'_q)(X''_q - x_a)}{(X'_q - x_a)}. \quad (24)$$

I.5.2 Fifth-order generator model

In the fifth-order model, only one damper winding is represented on the quadrature axis. The equations of motion and those for the direct-axis of the generator are therefore the same as for the sixth-order generator model. However, (15) and (16) for the quadrature axis are replaced by:

$$\frac{d\psi''_q}{dt} = \frac{1}{T''_{q0}}[\psi''_q - (X_q - X''_q)i_q]; \quad (25)$$

furthermore, the following equation replaces (20), (23) and (24):

$$\psi_q = \psi''_q - X''_q i_q. \quad (26)$$

Appendix II Transient stability modelling data

The small-signal model of the simplified 14-generator model of the southern and eastern Australian power system is augmented to allow large-signal (i.e. transient-stability) analysis.The study results in this report are prepared using the Siemens-PTI PSS®/E program [1]. Consequently, the large-signal dynamics model data is presented in a format consistent with PSS®/E. However, it is expected the data can be readily adapted to other transient-stability programs as well.

II.1 Steady-state analysis data

The power flow data in Appendix I.1 is used as a basis for transient stability analysis.

II.2 Dynamic analysis data

II.2.1 Generator model and parameters

The generator model and parameters in Appendix I.2.1 are used in the transient stability analysis, with the exception of a difference in the formulation of the rotor equations of motion which is described below. In addition, since generator saturation is neglected, the parameters S(1.0) and S(1.2) are both set to zero in the PSS®/E data for each generator.

II.2.1.1 Formulation of the generator rotor-equations of motion

When using PSS®/E it is necessary that the frequency dependence of network parameters is represented by setting the simulation parameter NETFRQ = 1. This ensures a consistent formulation of the generator rotor-equations of motion.

II.2.2 Large-signal SVC model and parameters

To our knowledge there is no standard or built-in model in PSS®/E of a SVC with the structure used in the small-signal formulation described in Appendix I.2.3. In the following it is shown that, subject to certain assumptions, the PSS®/E 'CSVGN1' SVC model has similar small-signal dynamic performance to the model in Appendix I.2.3.

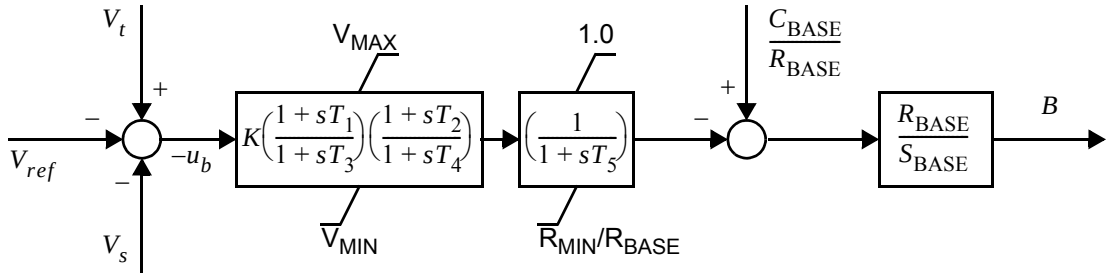

Notes:
(a) Vref is the external SVC AVR voltage reference input; Vt is the SVC terminal voltage in pu; Vs is the output from an optional power oscillation damper and is not used in the 14 generator system model; B is the SVC susceptance in pu on system MVA base (S_{BASE}).
(b) R_{BASE} is the maximum value of the SVC inductance (in Mvar @ 1.0 pu voltage) and in the 14 generator system model is equal to the SVC reactive power range $M_{BASE} = Q_{MAX} - Q_{MIN}$ (Mvar) as specified in Table 9, The SVC inductance is assumed to be continuously controllable between R_{MIN} and R_{BASE} (Mvar @ 1.0 pu voltage).
(c) C_{BASE} is the total SVC capacitance (in Mvar @ 1.0 pu voltage) and in the 14 generator model is equal to the maximum SVC reactive power output Q_{MAX} (Mvar @ 1.0 pu voltage) as specified in Table 9.
(d) R_{MIN} is the minimum value of the controllable inductance (in Mvar @ 1.0 pu voltage) and is zero for all five SVCs in the 14 generator system model.
(e) V_{MAX} = 1.0 pu and V_{MIN} = 0.0 pu and for the 14 generator system model corresponds to the inductance range of the SVC in pu of R_{BASE}.

Figure 24 PSS®/E 'CSVGN1' SVC model structure used to represent the five SVCs in transient stability simulations.

Linearizing the PSS®/E 'CSVGN1' model we have the following transfer-function from Δu_b to ΔB:

$$\frac{\Delta B(s)}{\Delta u_b(s)} = K\left(\frac{R_{\text{BASE}}}{S_{\text{BASE}}}\right)\left(\frac{1+sT_1}{1+sT_3}\right)\left(\frac{1+sT_2}{1+sT_4}\right)\left(\frac{1}{1+sT_5}\right) \text{ pu on SBASE} \tag{27}$$

Referring to Figure 22 we seek to develop the transfer-function from the perturbation in the voltage-error signal $\Delta u_b = \Delta V_{ref} - \Delta V_t + \Delta V_s$ to the perturbation in the SVC susceptance ΔB.

$$\Delta B(s) = \left(\frac{2.5K_A}{sK_S}\right)\left(\frac{1}{1+sT_d}\right)\left(\Delta u_b(s) - (K_d K_S)\Delta\left(\frac{Q(s)}{V_t(s)}\right)\right) \text{ pu on MBASE} \tag{28}$$

Now, consider the expression for the SVC current, Q/V_t. Recall that $Q = BV_t^2$ and therefore, $Q/V_t = BV_t$. Linearizing the latter expression and transforming to the Laplace domain yields:

$$\Delta\left(\frac{Q(s)}{V_t(s)}\right) = B_0\Delta V_t(s) + V_{t0}\Delta B(s) \tag{29}$$

Assuming that the perturbation in susceptance is large when compared to the associated change in voltage we can simplify (29) to:

$$\Delta\left(\frac{Q(s)}{V_t(s)}\right) \approx V_{t0}\Delta B(s) \tag{30}$$

Substituting for $\Delta\left(\frac{Q(s)}{V_t(s)}\right)$ in (28) from the approximation in (30) yields:

$$\Delta B(s) = \left(\frac{2.5K_A}{sK_S}\right)\left(\frac{1}{1+sT_d}\right)(\Delta u_b(s) - (K_d K_S V_{t0})\Delta B(s)) \tag{31}$$

which, upon rearrangement yields the following transfer-function:

$$\frac{\Delta B(s)}{\Delta u_b(s)} = \frac{1/(K_d K_S V_{t0})}{\left(1 + \left(\frac{1}{2.5K_d K_A V_{t0}}\right)s + \left(\frac{T_d}{2.5K_d K_A V_{t0}}\right)s^2\right)} \tag{32}$$

Let us now factorize the characteristic equation $1 + \left(\frac{1}{2.5K_d K_A V_{t0}}\right)s + \left(\frac{T_d}{2.5K_d K_A V_{t0}}\right)s^2 = 0$ into the form $(1+sT_a)(1+sT_b) = 0$.

$$\text{After defining } a = \frac{1}{2.5K_d K_A V_{t0}} \tag{33}$$

we have $T_a + T_b = a$ and $T_a T_b = aT_d$. Eliminating T_b from the preceding two equations we have the following quadratic equation for T_a: $T_a^2 - aT_a + aT_d = 0$. Taking the largest root we have

$$\begin{aligned} T_a &= \frac{a + \sqrt{a(a-4T_d)}}{2} \\ T_b &= a - T_a = \frac{a - \sqrt{a(a-4T_d)}}{2} \end{aligned} \tag{34}$$

Thus, subject to the assumption that $\Delta V_t \ll \Delta B$, the small-signal transfer-function representation of the SVC in Figure 22 is:

$$\frac{\Delta B(s)}{\Delta u_b(s)} = \left(\frac{1}{K_d K_S V_{t0}}\right)\left(\frac{1}{1+sT_a}\right)\left(\frac{1}{1+sT_b}\right) \text{ pu on MBASE.} \tag{35}$$

With minimal loss of accuracy we can set $V_{t0} = 1.0$ pu, thereby avoiding the need to adjust the SVC model parameters with changes in the SVC bus voltage.

Comparing the transfer-function of the small-signal model of the SVC in (35) with that of the PSS®/E 'CSVGN1' model in (27) we can see that the 'CSVGN1' model can be used to represent the SVC according to the following relationships between the small-signal model parameters and 'CSVGN1' model parameters:

Table 22 Transformation from the small-signal SVC model parameters in (35) to the PSS®/E 'CSVGN1' model parameters in (27).

PSS®/E 'CSVGN1' Parameter	**in terms of small-signal model parameters**
K	$\left(\frac{1}{K_d K_S V_{t0}}\right)$
T_1	0.0
T_2	0.0
T_3	$T_a = \frac{a + \sqrt{a(a-4T_d)}}{2}$
T_4	0.0
T_5	$T_b = \frac{a - \sqrt{a(a-4T_d)}}{2}$
Notes: (a) from (), $a = \frac{1}{2.5 K_d K_A V_{t0}}$ (b) set $V_{t0} = 1.0$ for fixed model parameters.	

Table 23 Parameter values of the PSS®/E 'CSVGN1' SVC model [1] used in the transient stability studies. (Note that K, T_3 and T_5 are calculated assuming V_{t0} = 1.0 pu)

Parameter	Parameter values for five SVCs in the 14-generator system				
	ASVC_2	RSVC_3	BSVC_4	PSVC_5	SSVC_5
IBUS	205	313	412	507	509
Model Code	'CSVGN1'	'CSVGN1'	'CSVGN1'	'CSVGN1'	'CSVGN1'
I	'1'	'1'	'1'	'1'	'1'
K	15.384615	12.5	6.993	20.0	18.181818
T_1	0.0	0.0	0.0	0.0	0.0
T_2	0.0	0.0	0.0	0.0	0.0
T_3	0.074641	0.074641	0.074641	0.154833	0.154833
T_4	0.0	0.0	0.0	0.0	0.0
T_5	0.005359	0.005359	0.005359	0.005167	0.005167
R_{MIN}	0.0	0.0	0.0	0.0	0.0
V_{MAX}	1.0	1.0	1.0	1.0	1.0
V_{MIN}	0.0	0.0	0.0	0.0	0.0
C_{BASE}	430.0	600.0	1100.0	320.0	400.0

II.2.2.1 Assessment of the effect of the modified SVC model on damping performance

The 13 electromechanical modes for Case 2 with all PSSs in-service with their design damping-gains are listed in Table 24 for two alternative SVC representations. The first is the small-signal representation with SVC-current droop explicitly represented as shown in Figure 22 and the second is the transfer-function in (35) which is derived from the first on the assumption that perturbation in SVC susceptance is large when compared to the associated change in voltage. It is thus clear from this comparison that employing the PSS®/E 'CSVGN1' model of the SVC in which current droop is implicitly represented will have negligible effect on the damping performance of the system.

Table 24 Comparison of electromechanical modes for Case 2 with two alternative SVC representations.

SVC model with explicit current droop (i.e. Figure 22)		SVC model with implicit current droop (i.e. transfer-function (35))		Difference	
				(3)-(1)	(4)-(2)
Real	Imag	Real	Imag	Real	Imag
Np/s	rad/s	Np/s	rad/s	Np/s	rad/s
(1)	(2)	(3)	(4)	(5)	(6)
-2.403	10.964	-2.403	10.964	0.000	0.000
-2.038	9.725	-2.038	9.725	0.000	0.000
-2.370	9.644	-2.370	9.644	0.000	0.000
-2.805	8.962	-2.805	8.962	0.000	0.000
-2.494	8.936	-2.494	8.936	0.000	0.000
-2.442	8.370	-2.443	8.370	-0.001	0.000
-2.039	8.379	-2.039	8.379	0.000	0.000
-1.814	7.772	-1.813	7.770	0.001	-0.002
-2.021	7.490	-2.021	7.490	0.000	0.000
-2.029	7.739	-2.030	7.738	-0.001	-0.001
-0.769	3.537	-0.769	3.538	0.000	0.001
-0.447	2.542	-0.446	2.545	0.001	0.003

SVC model with explicit current droop (i.e. Figure 22)		SVC model with implicit current droop (i.e. transfer-function (35))		Difference	
				(3)-(1)	(4)-(2)
Real	Imag	Real	Imag	Real	Imag
Np/s	rad/s	Np/s	rad/s	Np/s	rad/s
(1)	(2)	(3)	(4)	(5)	(6)
-0.431	1.759	-0.431	1.760	0.000	0.001

II.2.3 Large-signal excitation system models and data

II.2.3.1 IEEE Std. 421.5-2005 ST1A Model [16]

The PSS®/E 'ESST1A' implementation [1] of the IEEE Std 421.5-2005 ST1A excitation system model [16] is employed in the studies conducted in this report. The model data for the control-system block diagram of the PSS®/E 'ESST1A' implementation of the model in Figure 25 is presented in Table 25.

The source of power for generator excitation is the generator stator – consequently the limit on the generator field voltage is proportional to the generator stator voltage. The limit V_{RMAX} is specified such that when a three-phase short-circuit is applied to the high-voltage side of the generator step-up transformer the excitation system is able to produce a factor *k* times the field voltage which is required to produce rated power output at rated (lagging) power factor and a stator voltage of 1.05 pu. The factor *k* is, with the following exceptions, *1.5*. For the LPS_3 generator *k = 4.5* and for the TPS_5 and PPS_5 generators *k = 3.0*. These latter values of *k* are considered to be somewhat (probably unrealistically) high. They are set to these values to ensure that the six base cases in this version of the model are transiently stable. V_{RMIN} is set to $-V_{RMAX}$, V_{AMAX} to V_{RMAX} and V_{AMIN} to V_{RMIN}.

II.2.3.2 IEEE Std. 421.5-2005 AC1A Model [16]

The PSS®/E 'ESAC1A' implementation [1] of the IEEE Std 421.5-2005 AC1A excitation system model [16] is employed in the studies conducted in this report. The model data for the control-system block diagram of the PSS®/E 'ESAC1A' implementation of the model in Figure 26 is presented in Table 26.

The upper limit on the voltage regulator output (V_{AMAX}) is specified as a factor *k* times the generator field voltage which is required to produce rated power output at rated (lagging) power factor and a stator voltage of 1.05 pu. For generators EPS_2 and NPS_5 *k* is *2* and for YPS_3 k is *2.75*. The lower limit V_{AMIN} is set to $-V_{AMAX}$. The limits V_{RMAX} and V_{RMIN} are disabled by setting them to large positive and negative values respectively.

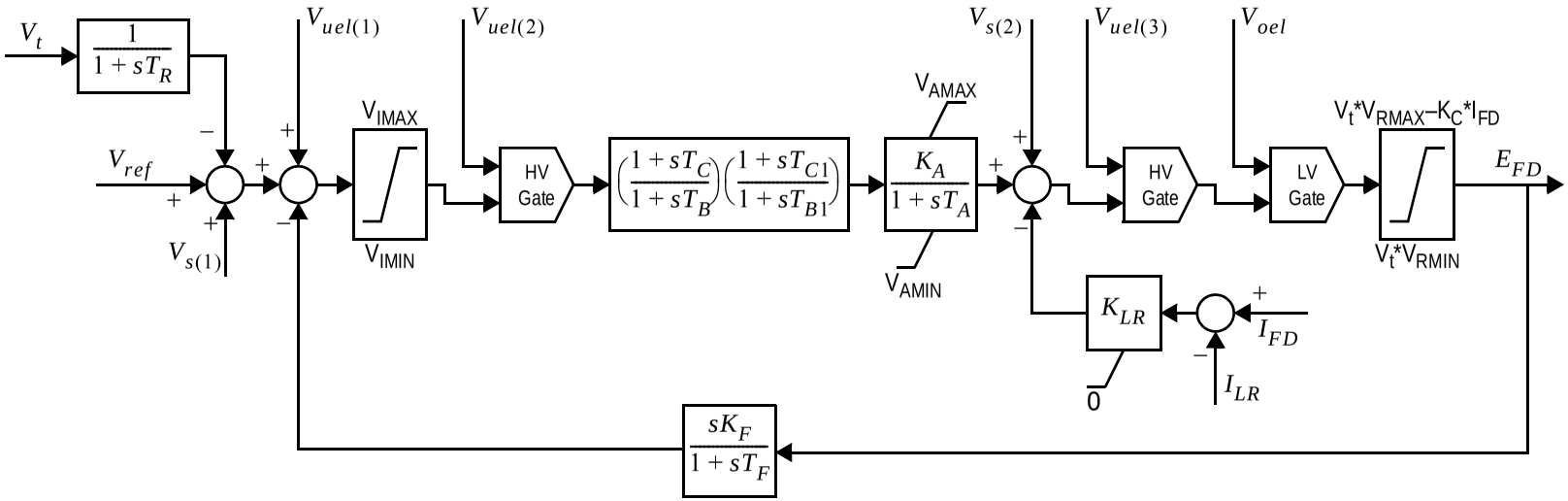

Figure 25 Control-system block diagram of the PSS®/E 'ESST1A' implementation [1] of the IEEE Std. 421.5-2005 ST1A model [16] used in the transient-stability studies conducted in this report. (Note: Vs(1) and Vs(2) are alternative inputs from the PSS; Vuel(1), Vuel(2) and Vuel(3) are alternative inputs from the under-excitation-limiter (UEL); and Voel is the input from the over-excitation-limiter. Vt is the generator stator voltage in pu; E_{FD} and I_{FD} are the generator field voltage and current respectively in per-unit as defined in Annex B of [16]) Note that under- and over-excitation limiters are not modelled in this report.

Table 25 Parameter values for the PSS®/E 'ESST1A' implementation [1] of the IEEE Std. 421.5-2005 ST1A model [16] used in the transient-stability studies conducted in this report.

Parameter Name	Parameter values for generators fitted with ESST1A AVR/exciter models										
	HPS_1	**BPS_2**	**VPS_2**	**MPS_2**	**LPS_3**	**TPS_4**	**CPS_4**	**SPS_4**	**GPS_4**	**TPS_5**	**PPS_5**
IBUS	101	201	203	204	301	401	402	403	404	502	503
Model Code	'ESST1A'	'ESST1A'	'ESST1A'	'ESST1A'	'ESST1A'	'ESST1A'	'ESST1A'	'ESST1A'	'ESST1A'	'ESST1A'	'ESST1A'
I	'1'	'1'	'1'	'1'	'1'	'1'	'1'	'1'	'1'	'1'	'1'
UEL [(a)]	1	1	1	1	1	1	1	1	1	1	1
VOS [(b)]	1	1	1	1	1	1	1	1	1	1	1
T_R (s)	0.0	0.0	0.0	0.0	0.0	0.0	0.02	0.0	0.0	0.0	0.0
V_{IMAX}	99.0	99.0	99.0	99.0	99.0	99.0	99.0	99.0	99.0	99.0	99.0
V_{IMIN}	-99.0	-99.0	-99.0	-99.0	-99.0	-99.0	-99.0	-99.0	-99.0	-99.0	-99.0
T_C (s)	2.500	0.500	0.350	0.500	1.140	4.000	1.520	0.350	0.136	1.400	0.200
T_B (s)	13.25	1.12	0.70	1.12	6.42	40.00	9.80	0.70	0.0232	16.0	0.80
T_{C1} (s)	0.0	0.0	0.0	0.0	0.0	0.0	0.0	0.0	0.0	0.60	0.0
T_{B1} (s)	0.0	0.0	0.0	0.0	0.0	0.0	0.0	0.0	0.0	0.05	0.0
K_A	200.0	400.0	300.0	400.0	400.0	300.0	300.0	300.0	250.0	400.0	300.0
T_A (s)	0.10	0.02	0.01	0.02	0.05	0.10	0.05	0.01	0.20	0.50	0.01
V_{AMAX}	9.5	9.5	10.5	9.5	42.0	13.0	11.0	13.0	11.0	22.0	18.5
V_{AMIN}	-9.5	-9.5	-10.5	-9.5	-42.0	-13.0	-11.0	-13.0	-11.0	-22.0	-18.5
V_{RMAX}	9.5	9.5	10.5	9.5	42.0	13.0	11.0	13.0	11.0	22.0	18.5
V_{RMIN}	-9.5	-9.5	-10.5	-9.5	-42.0	-13.0	-11.0	-13.0	-11.0	-22.0	-18.5
K_C	0.0	0.0	0.0	0.0	0.0	0.0	0.0	0.0	0.0	0.0	0.0
K_F	0.0	0.0	0.0	0.0	0.0	0.0	0.0	0.0	0.0	0.0	0.0
T_F (s)	1.0	1.0	1.0	1.0	1.0	1.0	1.0	1.0	1.0	1.0	1.0
K_{LR}	0.0	0.0	0.0	0.0	0.0	0.0	0.0	0.0	0.0	0.0	0.0
I_{LR}	999.0	999.0	999.0	999.0	999.0	999.0	999.0	999.0	999.0	999.0	999.0

Notes:
(a) UEL is ignored unless the under-excitation limiter is modelled. UEL = 1 means the output signal from the UEL is connected to Vuel(1); and similarly for UEL = 2 and UEL = 3.
(b) VOS is ignored unless the PSS is modelled. VOS = 1 means the output signal from the PSS is connected to Vs(1) and similarly for VOS = 2.

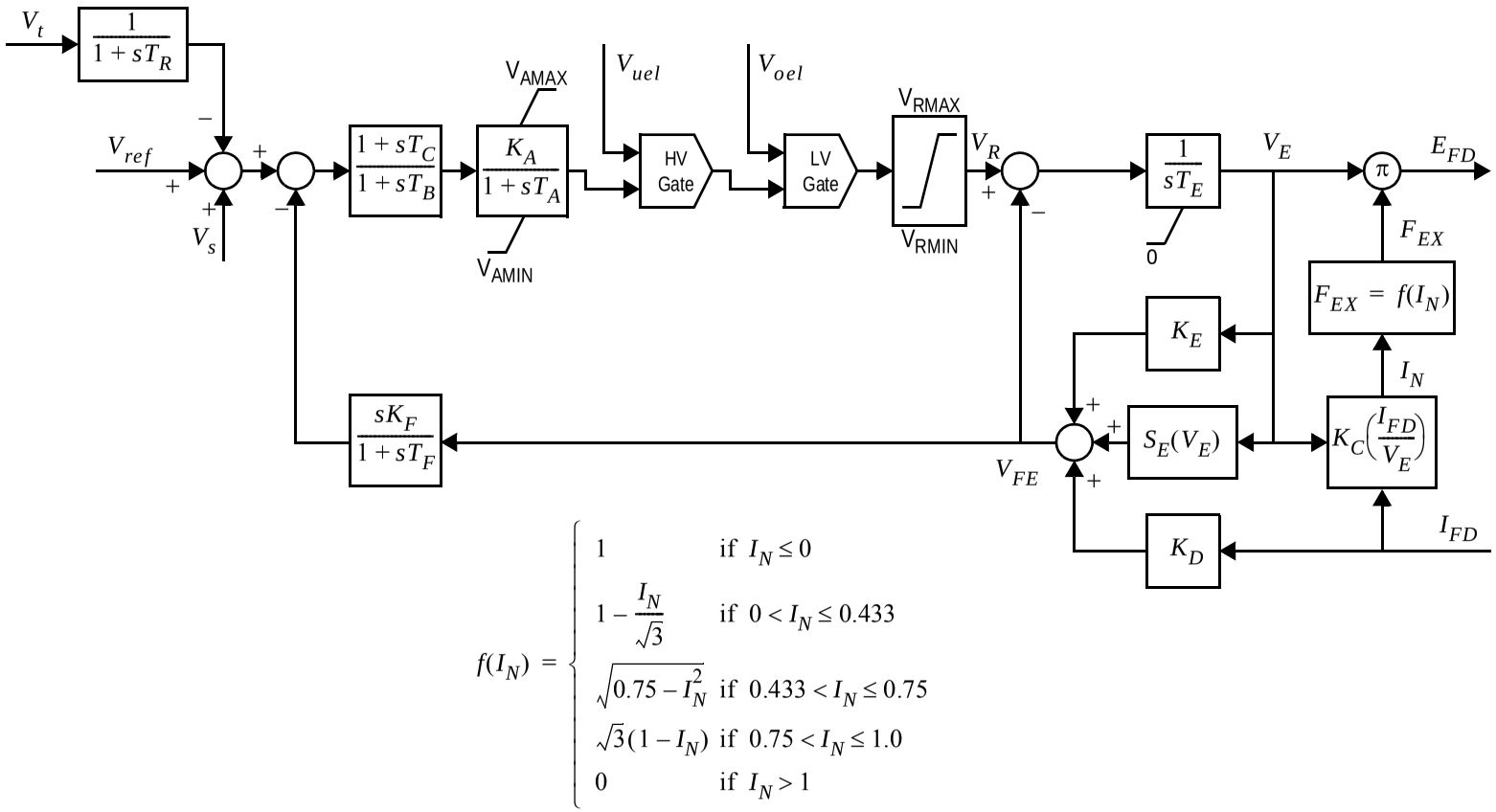

Figure 26 Control-system block diagram of the PSS®/E 'ESAC1A' implementation [1] of the IEEE Std. 421.5-2005 AC1A model [16] used in the transient-stability studies conducted in this report. (Note: Vs is the input from the PSS; Vuel is the input from the under-excitation-limiter; and Voel is the input from the over-excitation-limiter. Vt is the generator stator voltage in pu; E_{FD} and I_{FD} are the generator field voltage and current respectively in per-unit as defined in Annex B of [16]. Note that under- and over-excitation limiters are not modelled in this report.)

Table 26 Parameter values for the PSS®/E 'ESAC1A' implementation [1] of the IEEE Std. 421.5-2005 AC1A model [16] used in the transient-stability studies conducted in this report.

Parameter Name	Parameter values for generators fitted with ESAC1A AVR/exciter models		
	EPS_2	**YPS_3**	**NPS_5**
IBUS	202	302	501
Model Code	'ESAC1A'	'ESAC1A'	'ESAC1A'
I	'1'	'1'	'1'
T_R (s)	0.0	0.0	0.0
T_B (s)	0.0	0.0	0.0
T_C (s)	0.0	0.0	0.0
K_A	400.0	200.0	1000.0
T_A (s)	0.02	0.05	0.04
V_{AMAX}	5.5	7.0	5.5
V_{AMIN}	-5.5	-7.0	-5.5
T_E (s)	1.0	1.333	0.87
K_F	0.029	0.02	0.004
T_F (s)	1.0	0.8	0.27
K_C	0.0	0.0	0.0
K_D	0.0	0.0	0.0
K_E	1.0	1.0	1.0
E_1 (a)	0.0	0.0	0.0
$S_E(E_1)$	0.0	0.0	0.0
E_2	0.0	0.0	0.0
$S_E(E_2)$	0.0	0.0	0.0
V_{RMAX}	99.0	99.0	99.0
V_{RMIN}	-99.0	-99.0	-99.0

Notes:
(a) The exciter saturation function is defined by two points, (E_1, $S_E(E_1)$) and (E_2, $S_E(E_2)$). In the case of PSS®/E exciter saturation is neglected if (E_1, $S_E(E_1)$) = (0,0) and (E_2, $S_E(E_2)$). = (0,0). Other programs may have different ways to indicate that exciter saturation is to be neglected.

II.2.4 Large-signal PSS models and data

II.2.4.1 IEEE 1981 general purpose single-input PSS model [17]

The 1981 report of the IEEE Working Group on Computer Modelling for Excitation Systems [17] recommended a general purpose single-input PSS. This PSS model is implemented in PSS®/E as the 'IEEEST' model [1] as shown in the block diagram in Figure 27.

The parameters of the phase-compensation transfer-functions in equations (7) to (10) are transformed to the parameters A_1 to A_6, T_1 to T_6 and K_S of the PSS®/E formulation of the PSS transfer-function according to the mappings in Table 27. The parameters for the PSSs contained in Tables 17 to 20 are converted according to the transformations defined in Table 27 to the parameters required by the PSS®/E 'IEEEST' model. The resulting PSS®/E parameters are listed

in Table 28. Recall from Appendix I.3.1 that for all of the PSSs T_W = 7.5 s and D_e = 20.0 pu on the machine MVA rating.

Not shown in Figure 27 are the voltage-dependent limits on the output from the PSS®/E 'IEEEST' model. These latter limits are disabled by setting the parameters V_{CU} and V_{CL} to zero.

All PSS output limits have been set to +/- 0.1 pu. In this version no attempt has been made to optimize the setting of these limits.

Table 27 Transformation from the PSS parameters in equations (7) to (10) to the PSS parameters in the PSS®/E 'IEEEST' PSS model in Figure 27.

PSS®/E model Parameter	Eqn. (7)	Eqn. (8)	Eqn. (9)	Eqn. (10)
A_1	$T_g + T_h$	$T_f + T_g$	0.0	$T_e + T_f$
A_2	$T_g \times T_h$	$T_f \times T_g$	0.0	$T_e \times T_f$
A_3	0.0	0.0	0.0	0.0
A_4	0.0	0.0	0.0	0.0
A_5	$T_c + T_d$	a	0.0	a
A_6	$T_c \times T_d$	b	0.0	b
T_1	T_a	T_a	T_a	0.0
T_2	T_e	T_d	T_e	0.0
T_3	T_b	T_b	T_b	0.0
T_4	T_f	T_e	T_f	0.0
T_5	T_W			
T_6	T_W			
K_S	D_e / k_c			

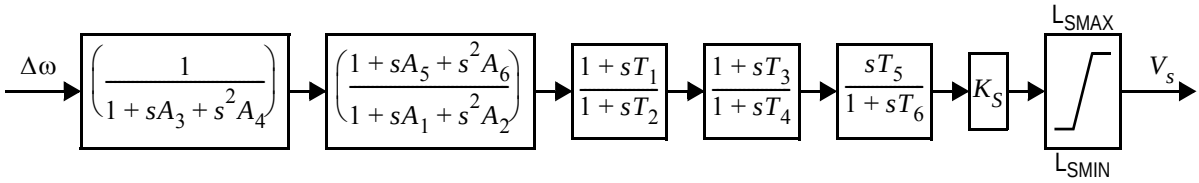

Figure 27 Control-system block diagram of the PSS®/E 'IEEEST' implementation [1] of the general-purpose PSS model developed in 1981 by the IEEE Working Group on Computer Modelling for Excitation Systems [17]. This model is used in the transient-stability studies conducted in this report. (Note: Δω is the rotor-speed perturbation (in pu of synchronous speed) and Vs is the output from the stabilizer which is connected to the AVR reference-input summing junction. The voltage-dependent output limits are not shown and are disabled.)

Table 28 Parameter values for the PSS®/E 'IEEEST' implementation [1] of the IEEE 1981 general-purpose PSS model [17] used in the transient-stability studies conducted in this report.

Parameter Name	Parameter Values													
	HPS_1 [(b)]	**BPS_2**	**EPS_2**	**VPS_2**	**MPS_2**	**LPS_3**	**YPS_3**	**TPS_4**	**CPS_4**	**SPS_4**	**GPS_4**	**NPS_5**	**TPS_5**	**PPS_5**
Eqn / Tab [(a)]	10 / 20	10 / 20	7 / 17	9 / 19	8 / 18	10 / 20	8 / 18	9 / 19	9 / 19	10 / 20	10 / 20	8 / 18	7 / 17	7 / 17
IBUS	101	201	202	203	204	301	302	401	402	403	404	501	502	503
Model Code	'IEEEST'	'IEEEST'	'IEEEST'	'IEEEST'	'IEEEST'	'IEEEST'	'IEEEST'	'IEEEST'	'IEEEST'	'IEEEST'	'IEEEST'	'IEEEST'	'IEEEST'	'IEEEST'
I	'1'	'1'	'1'	'1'	'1'	'1'	'1'	'1'	'1'	'1'	'1'	'1'	'1'	'1'
ICS	1	1	1	1	1	1	1	1	1	1	1	1	1	1
IB	0	0	0	0	0	0	0	0	0	0	0	0	0	0
A_1	0.01333	0.01333	0.006667	0	0.01333	0.01333	0.01333	0	0	0.01333	0.01333	0.01333	0.006667	0.01333
A_2	4.444e-5	4.444e-5	0	0	4.444e-5	4.444e-5	4.444e-5	0	0	4.444e-5	4.444e-5	4.444e-5	0	4.444e-5
A_3	0	0	0	0	0	0	0	0	0	0	0	0	0	0
A_4	0	0	0	0	0	0	0	0	0	0	0	0	0	0
A_5	0.3725	0.128	0.04	0	0.1	0.1684	0.5091	0	0	0.0909	0.1154	0.3	0.0167	0.187
A_6	0.03845	0.0064	0	0	0.0051	0.0118	0.1322	0	0	0.002067	0.005917	0.1111	0	0.00334
T_1	0	0	0.286	0.0708	0.01	0	0.05	0.2083	0.2777	0	0	0.033	0.5	0.2
T_2	0	0	0.006667	0.006667	0.006667	0	0.006667	0.006667	0.006667	0	0	0.3	0.006667	0.35
T_3	0	0	0.111	0.0292	0	0	0	0.2083	0.1	0	0	0.033	0.0588	0.187
T_4	0	0	0.006667	0.006667	0	0	0	0.006667	0.006667	0	0	0.006667	0.006667	0.0667
T_5	7.5	7.5	7.5	7.5	7.5	7.5	7.5	7.5	7.5	7.5	7.5	7.5	7.5	7.5
T_6	7.5	7.5	7.5	7.5	7.5	7.5	7.5	7.5	7.5	7.5	7.5	7.5	7.5	7.5
K_S	15.38	5.556	4.651	5.714	6.667	12.5	5.97	7.143	4.706	6.329	6.061	3.899	5.882	3.559
L_{SMAX}	0.1	0.1	0.1	0.1	0.1	0.1	0.1	0.1	0.1	0.1	0.1	0.1	0.1	0.1
L_{SMIN}	-0.1	-0.1	-0.1	-0.1	-0.1	-0.1	-0.1	-0.1	-0.1	-0.1	-0.1	-0.1	-0.1	-0.1
V_{CU}	0	0	0	0	0	0	0	0	0	0	0	0	0	0
V_{CL}	0	0	0	0	0	0	0	0	0	0	0	0	0	0

Notes:
(a) Eqn / Tab refers respectively to the equation describing the form of the PSS compensation transfer-function and the associated table of parameter values from which the 'IEEEST' model parameters are derived according to the parameter mappings in Table 27.
(b) The PSS fitted to machine HPS_1 is removed from service in cases 4 & 6 because it is operating as a synchronous condensor; in case 5 the PSS gain KS is negated because it is pumping.

II.3 Network sequence impedance data

In the South East Australian power system three-phase faults on the transmission network are *not* considered to be credible contingencies (except under exceptional circumstances) under the Australian National Electricity Rules [18]. Rather, for planning purposes solid two-phase to ground faults are generally treated as the most severe form of credible contingency. In order to reflect this practice on the simplified 14-generator model of the South East Australian system it is necessary to provide negative and zero sequence impedance data for the network so that the equivalent fault impedances required to represent two-phase to ground faults can be computed.

II.3.1 Transmission lines

It is assumed that the three-phase system is balanced and consequently the negative-sequence impedance of transmission lines are identical to the positive-sequence impedances listed in Table 10. The zero-sequence impedances are deemed to be 2.5 times the corresponding positive-sequence impedance. This multiplying factor is based on "rules-of-thumb" on the relationships between positive- and zero-sequence impedances on page 884 of [13].

Mutual coupling between transmission circuits is neglected.

II.3.2 Transformers

Since it is assumed that the three-phase system is balanced the negative-sequence impedances of the transformers are identical to the positive sequence impedances listed in Table 11.

All generator step-up transformers are assumed to have a delta/grounded-star connection with the delta on the generator side. The neutral of the high-voltage windings is solidly grounded. Consequently, there is no path for the flow of zero-sequence currents from the generator to the network. For the generator step-up transformers the zero-sequence impedances are identical to the corresponding positive-sequence impedances listed in Table 11.

All other network transformers, such as those between buses 315 and 308, are assumed to have a delta/delta connection. The implication is that there is no path for the flow of zero-sequence currents from the delta windings into the lines and thus viewed from either terminal the zero-sequence impedance is infinite. Although three-winding transformers are often employed in practice, it is considered an unnecessary complication for the purpose of this benchmark study system.

II.3.3 Generators

As discussed in Section 13.4.2 (pg. 877) of [13], if only the fundamental frequency component of the negative-sequence current produced by impressing a balanced set of fundamental frequency negative-phase sequence voltages on the stator terminals of a generator is considered the effective negative-sequence reactance of the generator is found to be:

$$X_2 = 2\frac{X_d'' X_q''}{X_d'' + X_q''} \tag{36}$$

Since we are neglecting saliency of sub-transient reactances (i.e. $X_q'' = X_d''$) it follows that $X_2 = X_d''$. Thus, for the generators, the negative-sequence impedances are identical to the d-axis sub-transient reactances listed in Table 15.

Since we are concerned only with faults on the high-voltage side of the generator step-up transformers; and since the generator step-up transformers have a delta/grounded-star connection the generator zero-sequence impedances of the generators are irrelevant and so we do not propose values for them.

II.3.4 Loads

All loads are represented as an equivalent impedance in the negative-sequence network; and as an infinite impedance in the zero-sequence network.

II.4 Effective negative and zero sequence admittances at network buses

For the purpose of representing an unbalanced fault in a transient stability study it is usual practice to represent the effect of the negative- and zero-sequence networks by their equivalent admittances (Y_2 and Y_0) as seen at the fault location [13]. These admittances (or impedances) are combined depending on the type of fault and the resulting effective fault admittance (Y_{fe}) is connected at the fault location in the detailed positive-phase sequence representation of the network for the duration of the fault. The fault is cleared by removing the effective fault admittance and (possibly) disconnecting the faulted network element (e.g. transmission line or transformer). It should be noted that this study system does not include models of generator turbines and governors and therefore, events involving the loss of generation or load should not be simulated.

The effective fault admittance for a two-phase to ground fault is given by $Y_{fe} = Y_2 + Y_0$; and for a single-phase to ground fault it is: $Y_{fe} = \frac{Y_2 Y_0}{Y_2 + Y_0}$.

The negative- and zero-sequence admittances seen from all of the high-voltage buses in the system are listed in Tables 29 & 30 respectively for each of the six study cases. These admittances are computed with the PSS®/E program based on the sequence impedance data in Appendix II.3.

The effective fault admittances for a solid two-phase to ground fault at each of the high-voltage buses in the system are listed in Table 31 for the six study cases.This data is intended to assist researchers to benchmark the system model in other simulation tools and, for users who do not have access to software capable of analysing sequence networks.

Table 29 Equivalent negative-sequence admittances at transmission network nodes.

BusID	Equivalent negative sequence admittance (pu on 100 MVA)											
	Case											
	1		2		3		4		5		6	
	G	B	G	B	G	B	G	B	G	B	G	B
102	16.965	-79.65	15.725	-70.544	17.434	-147.54	13.45	-61.791	15.18	-71.942	13.668	-60.986
205	7.5511	-30.363	7.0619	-29.959	8.0742	-30.446	6.1675	-29.198	6.694	-29.981	6.1846	-28.981
206	24.099	-183.25	23.19	-159.72	25.85	-181.32	20.106	-143.08	23.059	-159.26	20.448	-123.56
207	41.504	-142.34	36.879	-126.18	43.826	-132.26	30.163	-116.81	35.604	-119.87	30.585	-112.45
208	34.256	-137.15	30.856	-118.7	34.781	-114.42	25.995	-113.29	29.298	-106.07	26.661	-110.38
209	29.666	-157.06	27.436	-135.23	32.072	-152.39	22.98	-119.83	27.404	-132.2	23.825	-116.75
210	14.971	-97.353	15.009	-90.226	16.055	-96.267	13.195	-82.264	14.963	-87.135	13.87	-80.334
211	46.608	-113.61	40.68	-103.87	48.316	-106.81	32.791	-97.045	38.245	-97.061	33.088	-93.523
212	42.098	-102.93	37.239	-96.459	44.531	-101.26	29.857	-89.012	35.136	-90.763	30.116	-85.464
213	17.17	-88.871	16.681	-82.937	17.937	-88.755	14.461	-76.967	16.492	-80.303	15.135	-74.793
214	31.477	-103.74	28.791	-95.659	32.733	-104.77	23.933	-88.89	27.783	-92.089	24.468	-85.2
215	23.874	-165.72	21.818	-129.41	23.79	-168.37	18.927	-128.56	21.298	-129.85	19.221	-109.27
216	34.128	-88.128	29.99	-82.114	35.596	-90.964	24.227	-77.37	28.404	-79.461	24.432	-73.45
217	30.531	-90.366	27.086	-82.905	31.634	-103.49	22.385	-77.517	26.058	-82.235	22.666	-74.428
303	32.186	-140.23	30.726	-155.54	33.606	-159.96	27.299	-124.57	29.528	-156.35	27.154	-124.47
304	36.54	-95.185	35.02	-101.49	39.644	-106.24	29.553	-84.939	32.84	-98.98	29.4	-84.866
305	47.209	-101.19	45.86	-108.42	52.707	-113.74	37.169	-90.083	42.598	-105.97	36.934	-90.01
306	41.236	-87.168	39.81	-92.449	45.62	-96.344	32.836	-78.679	36.932	-90.556	32.612	-78.633
307	41.977	-88.051	40.513	-93.493	46.427	-97.458	33.454	-79.374	37.61	-91.509	33.218	-79.333
308	15.482	-39.026	14.359	-39.981	15.854	-40.595	13.868	-36.921	13.618	-39.039	13.686	-36.981
309	12.572	-54.639	12.233	-52.388	12.757	-67.072	11.101	-48.394	11.699	-52.625	11.175	-48.111
310	118.16	-119.98	129.85	-138.51	148.58	-130.97	84.199	-113.25	117.86	-138.8	83.684	-113.51
311	14.278	-62.688	13.185	-63.049	14.415	-68.943	12.74	-57.435	12.663	-62.445	12.715	-57.291
312	13.345	-65.999	12.989	-78.329	14.323	-79.422	10.957	-53.35	11.983	-66.325	10.94	-53.328
313	37.023	-73.143	36.782	-79.3	42.284	-80.882	27.167	-64.75	32.76	-74.848	27.091	-64.704
314	30.037	-70.831	29.026	-75.344	32.999	-77.563	23.24	-63.312	26.523	-72.124	23.161	-63.262
315	8.6531	-29.653	7.2494	-28.361	8.1737	-30.406	7.7893	-28.183	7.5665	-29.268	7.6386	-28.268
405	17.405	-84.43	20.214	-85.113	20.217	-85.121	14.456	-58.198	17.273	-76.781	14.648	-56.69
406	11.907	-68.179	13.877	-68.548	13.879	-68.551	10.69	-55.563	12.117	-66.736	10.471	-48.429

BusID	Equivalent negative sequence admittance (pu on 100 MVA)											
	Case											
	1		2		3		4		5		6	
	G	B	G	B	G	B	G	B	G	B	G	B
407	10.191	-75.287	11.857	-75.728	11.858	-75.731	9.5471	-60.53	10.449	-74.009	9.3717	-50.97
408	7.1565	-59.856	7.9054	-60.244	7.9093	-60.253	7.1093	-48.895	7.2825	-59.171	7.4645	-54.811
409	10.429	-30.954	11.448	-31.442	11.453	-31.453	8.9743	-27.567	10.336	-30.498	9.0026	-27.508
410	23.738	-67.921	27.597	-69.561	27.736	-69.667	18.896	-56.085	23.68	-68.186	18.973	-56.849
411	20.345	-40.669	23.853	-41.424	23.889	-41.461	16.097	-35.897	20.253	-40.591	16.126	-36.129
412	23.206	-43.332	27.478	-43.914	27.529	-43.957	18.035	-38.11	23.145	-43.338	18.079	-38.419
413	6.2368	-32.806	6.5949	-33.126	6.7649	-33.269	5.8232	-30.242	6.0359	-32.502	5.766	-30.205
414	5.7672	-31.562	6.0586	-31.834	6.2372	-31.981	5.5587	-30.097	5.7097	-32.139	5.6606	-30.921
415	4.8186	-27.582	4.9204	-27.677	5.1492	-27.856	4.5562	-26.537	4.6627	-27.839	4.6067	-27.056
416	4.8979	-25.878	4.7868	-25.761	5.2026	-26.039	4.3628	-25.008	4.5562	-25.819	4.4041	-25.306
504	16.449	-38.182	13.317	-39.793	16.765	-40.769	11.374	-32.061	13.39	-35.633	11.757	-28.447
505	14.636	-54.83	10.25	-54.506	13.952	-58.094	11.397	-38.827	12.539	-48.738	10.26	-44.869
506	14.181	-51.57	10.225	-53.859	14.216	-59.972	10.343	-32.934	11.414	-41.06	9.3366	-37.604
507	19.541	-54.41	13.684	-55.491	19.571	-60.109	13.52	-37.109	15.44	-45.916	12.254	-41.514
508	19.041	-47.291	13.762	-48.271	18.908	-51.387	13.679	-34.55	15.43	-41.156	11.565	-36.036
509	6.372	-21.723	4.8856	-21.055	5.4178	-21.97	5.5383	-20.582	5.5896	-21.22	5.3747	-20.726

Table 30 Equivalent zero-sequence admittances at transmission network nodes.

BusID	Equivalent zero sequence admittance (pu on 100 MVA)											
	Case											
	1		2		3		4		5		6	
	G	B	G	B	G	B	G	B	G	B	G	B
102	1.6634	-124.68	1.6301	-96.752	1.6558	-346.86	1.6275	-68.967	1.6249	-96.727	1.6	-68.845
205	1.2262	-10.016	1.2136	-9.9582	1.2258	-10.015	1.1972	-9.8786	1.2132	-9.9572	1.1741	-9.7606
206	4.8793	-291.8	4.6429	-249.09	4.7078	-290.91	4.5569	-207.07	4.5258	-248.49	4.4645	-164.99
207	10.666	-107.71	9.5677	-101.44	9.5527	-100.16	8.7957	-96.979	8.9301	-96.886	8.6251	-96.22
208	5.5817	-179.14	5.3427	-145.37	5.5978	-113.84	5.0306	-143.86	5.3427	-112.69	4.9157	-143.39
209	4.3886	-212.28	4.1447	-176.31	3.9155	-209.51	4.093	-141.38	3.8607	-174.59	4.0155	-141.07
210	0	0	0	-0	0	0	0	0	0	0	0	0
211	7.458	-68.53	6.9751	-65.831	6.748	-63.469	6.8158	-65.223	6.5425	-62.679	6.7023	-64.775
212	6.7248	-58.269	6.4218	-56.842	6.3896	-56.246	6.2525	-56.149	6.196	-55.491	6.132	-55.65
213	0	0	0	-0	0	0	0	0	0	0	0	0
214	4.7418	-40.019	4.5585	-39.192	4.7095	-39.705	4.4867	-38.902	4.4964	-38.824	4.3831	-38.451
215	3.6439	-280.78	3.5428	-197.01	3.7125	-281.04	3.407	-196.4	3.5187	-196.9	3.3288	-154.36
216	4.7708	-40.306	4.5459	-39.285	4.7831	-40.269	4.4814	-39.024	4.5111	-39.093	4.3287	-38.305
217	5.6728	-50.5	5.2859	-48.647	6.2433	-53.034	4.9161	-46.68	5.2618	-48.521	4.7906	-46.092
303	0	-291.55	0	-333.33	0	-333.33	0	-250	0	-333.33	0	-250
304	2.9847	-50.887	3.1198	-52.022	3.1198	-52.022	2.8188	-49.458	3.1198	-52.022	2.8188	-49.458
305	3.2288	-57.702	3.3952	-59.166	3.3952	-59.166	3.0265	-55.87	3.3952	-59.166	3.0265	-55.87
306	2.7379	-46.815	2.8515	-47.773	2.8515	-47.773	2.5974	-45.602	2.8515	-47.773	2.5974	-45.602
307	2.7664	-47.597	2.8832	-48.588	2.8832	-48.588	2.6221	-46.344	2.8832	-48.588	2.6221	-46.344
308	1.0749	-16.172	1.09	-16.285	1.09	-16.285	1.0553	-16.025	1.09	-16.285	1.0553	-16.025
309	2.3346	-22.001	2.1431	-20.94	2.9105	-24.777	1.8751	-19.266	2.1426	-20.939	1.8715	-19.256
310	0.87866	-7.3537	0.85297	-7.2316	0.94362	-7.6393	0.81204	-7.0213	0.85291	-7.2314	0.81153	-7.0201
311	0	0	0	-0	0	0	0	0	0	0	0	0
312	0	-88.739	0	-118.35	0	-118.35	0	-59.18	0	-88.739	0	-59.18
313	2.0803	-20.299	2.3404	-21.516	2.3404	-21.516	1.6754	-18.236	2.0803	-20.299	1.6754	-18.236
314	1.6477	-16.158	1.8087	-16.92	1.8087	-16.92	1.3844	-14.824	1.6477	-16.158	1.3844	-14.824
315	0.37366	-2.7786	0.37449	-2.784	0.37519	-2.7882	0.36865	-2.7317	0.37146	-2.7608	0.36668	-2.7548
405	2.1525	-141.69	2.1525	-141.69	2.1525	-141.69	2.0122	-82.022	2.1525	-122.08	1.9682	-81.597
406	3.6302	-71.835	3.6302	-71.835	3.6302	-71.835	2.8993	-63.28	3.5894	-71.524	2.3291	-53.908

BusID	Equivalent zero sequence admittance (pu on 100 MVA)											
	Case											
	1		2		3		4		5		6	
	G	B	G	B	G	B	G	B	G	B	G	B
407	1.4574	-138.16	1.4574	-138.16	1.4574	-138.16	1.2668	-107.08	1.4227	-137.91	1.3133	-77.866
408	1.7902	-79.409	1.7902	-79.409	1.7902	-79.409	1.6737	-59.147	1.773	-79.321	1.6289	-78.468
409	2.1169	-16.351	2.1169	-16.351	2.1169	-16.351	1.978	-15.784	2.0923	-16.255	1.9777	-15.783
410	1.0002	-128.22	1.0002	-128.22	1.0002	-128.22	0.94342	-98.297	0.99322	-128.19	0.96659	-98.473
411	2.1582	-26.807	2.1582	-26.807	2.1582	-26.807	1.9781	-25.513	2.1502	-26.776	1.9809	-25.523
412	2.3017	-31.925	2.3017	-31.925	2.3017	-31.925	2.0653	-29.987	2.296	-31.903	2.0693	-30.003
413	1.0408	-14.303	1.0408	-14.303	1.0408	-14.303	0.98054	-13.834	1.0406	-14.302	0.98142	-13.838
414	0.39389	-4.0498	0.39231	-4.0402	0.39383	-4.0496	0.39025	-4.027	0.39225	-4.04	0.38733	-4.0072
415	0.46309	-4.6406	0.46095	-4.6281	0.46301	-4.6404	0.45816	-4.6108	0.46088	-4.6279	0.45421	-4.5848
416	0.6783	-6.3433	0.67397	-6.3199	0.67815	-6.3429	0.66832	-6.2877	0.67383	-6.3196	0.66033	-6.2396
504	7.7156	-55.425	7.9791	-55.638	8.1862	-55.798	5.6668	-53.464	6.8971	-54.7	6.8971	-35.092
505	3.4127	-86.355	3.434	-87.54	3.4618	-88.472	3.5962	-63.953	3.448	-82.667	2.1968	-80.843
506	3.5219	-66.144	3.5219	-76.144	3.5219	-86.132	3.4771	-34.672	3.5219	-46.144	2.5902	-44.851
507	5.1748	-60.311	5.3215	-62.982	5.4662	-65.197	4.6854	-43.938	4.9269	-52.906	3.4863	-50.65
508	11.301	-45.26	11.478	-46.281	11.628	-47.094	10.233	-37.871	10.835	-42.178	6.7953	-39.143
509	0.45004	-3.3764	0.45126	-3.3844	0.45227	-3.3906	0.44283	-3.3074	0.44687	-3.3502	0.43986	-3.3413

Table 31 Equivalent two-phase to ground fault admittances at transmission network nodes.

BusID	Equivalent two phase to ground fault admittance (pu on 100 MVA)											
	Case											
	1		2		3		4		5		6	
	G	B	G	B	G	B	G	B	G	B	G	B
102	18.628	-204.33	17.355	-167.3	19.09	-494.4	15.078	-130.76	16.805	-168.67	15.268	-129.83
205	8.7773	-40.379	8.2755	-39.917	9.3	-40.461	7.3647	-39.076	7.9072	-39.938	7.3586	-38.742
206	28.979	-475.05	27.833	-408.81	30.558	-472.23	24.663	-350.15	27.585	-407.76	24.913	-288.55
207	52.17	-250.05	46.447	-227.62	53.378	-232.42	38.959	-213.79	44.535	-216.75	39.21	-208.67
208	39.838	-316.29	36.199	-264.07	40.379	-228.26	31.026	-257.15	34.64	-218.76	31.577	-253.77
209	34.054	-369.34	31.581	-311.54	35.988	-361.9	27.073	-261.22	31.264	-306.79	27.84	-257.83
210	14.971	-97.353	15.009	-90.226	16.055	-96.267	13.195	-82.264	14.963	-87.135	13.87	-80.334
211	54.066	-182.14	47.655	-169.71	55.064	-170.28	39.607	-162.27	44.788	-159.74	39.79	-158.3
212	48.822	-161.19	43.66	-153.3	50.92	-157.51	36.109	-145.16	41.332	-146.25	36.248	-141.11
213	17.17	-88.871	16.681	-82.937	17.937	-88.755	14.461	-76.967	16.492	-80.303	15.135	-74.793
214	36.219	-143.76	33.349	-134.85	37.442	-144.47	28.42	-127.79	32.279	-130.91	28.851	-123.65
215	27.517	-446.5	25.361	-326.42	27.503	-449.42	22.334	-324.96	24.817	-326.75	22.55	-263.63
216	38.898	-128.43	34.536	-121.4	40.379	-131.23	28.708	-116.39	32.915	-118.55	28.761	-111.76
217	36.204	-140.87	32.371	-131.55	37.877	-156.52	27.301	-124.2	31.32	-130.76	27.457	-120.52
303	32.186	-431.77	30.726	-488.87	33.606	-493.29	27.299	-374.57	29.528	-489.68	27.154	-374.47
304	39.525	-146.07	38.14	-153.51	42.764	-158.27	32.372	-134.4	35.96	-151	32.218	-134.32
305	50.438	-158.89	49.255	-167.59	56.102	-172.9	40.196	-145.95	45.994	-165.14	39.96	-145.88
306	43.974	-133.98	42.662	-140.22	48.471	-144.12	35.433	-124.28	39.784	-138.33	35.21	-124.24
307	44.744	-135.65	43.397	-142.08	49.31	-146.05	36.076	-125.72	40.494	-140.1	35.84	-125.68
308	16.557	-55.198	15.449	-56.265	16.944	-56.88	14.923	-52.946	14.708	-55.324	14.742	-53.005
309	14.907	-76.64	14.376	-73.329	15.667	-91.849	12.976	-67.66	13.842	-73.564	13.047	-67.367
310	119.04	-127.33	130.71	-145.74	149.53	-138.61	85.011	-120.27	118.72	-146.03	84.496	-120.53
311	14.278	-62.688	13.185	-63.049	14.415	-68.943	12.74	-57.435	12.663	-62.445	12.715	-57.291
312	13.345	-154.74	12.989	-196.68	14.323	-197.77	10.957	-112.53	11.983	-155.06	10.94	-112.51
313	39.104	-93.442	39.122	-100.82	44.625	-102.4	28.843	-82.987	34.84	-95.147	28.767	-82.941
314	31.685	-86.989	30.834	-92.264	34.808	-94.483	24.625	-78.136	28.171	-88.282	24.546	-78.086
315	9.0268	-32.431	7.6239	-31.145	8.5488	-33.194	8.158	-30.915	7.938	-32.029	8.0053	-31.023
405	19.558	-226.12	22.366	-226.8	22.37	-226.81	16.468	-140.22	19.426	-198.86	16.616	-138.29
406	15.537	-140.01	17.507	-140.38	17.509	-140.39	13.589	-118.84	15.706	-138.26	12.8	-102.34

BusID	Equivalent two phase to ground fault admittance (pu on 100 MVA)											
	Case											
	1		2		3		4		5		6	
	G	B	G	B	G	B	G	B	G	B	G	B
407	11.648	-213.45	13.314	-213.89	13.316	-213.89	10.814	-167.61	11.871	-211.92	10.685	-128.84
408	8.9466	-139.26	9.6955	-139.65	9.6994	-139.66	8.7831	-108.04	9.0556	-138.49	9.0933	-133.28
409	12.546	-47.305	13.565	-47.793	13.57	-47.804	10.952	-43.351	12.429	-46.752	10.98	-43.291
410	24.738	-196.14	28.597	-197.78	28.736	-197.89	19.84	-154.38	24.673	-196.38	19.939	-155.32
411	22.504	-67.475	26.011	-68.231	26.048	-68.268	18.075	-61.409	22.403	-67.367	18.107	-61.653
412	25.507	-75.257	29.78	-75.839	29.831	-75.882	20.1	-68.097	25.441	-75.242	20.148	-68.423
413	7.2776	-47.109	7.6357	-47.429	7.8056	-47.571	6.8038	-44.077	7.0765	-46.804	6.7474	-44.043
414	6.1611	-35.611	6.4509	-35.874	6.631	-36.031	5.9489	-34.124	6.1019	-36.179	6.048	-34.928
415	5.2817	-32.222	5.3813	-32.305	5.6122	-32.496	5.0143	-31.148	5.1236	-32.467	5.0609	-31.641
416	5.5762	-32.221	5.4607	-32.08	5.8808	-32.382	5.0312	-31.296	5.23	-32.138	5.0644	-31.546
504	24.165	-93.608	21.296	-95.43	24.952	-96.567	17.041	-85.525	20.287	-90.332	18.654	-63.539
505	18.049	-141.19	13.684	-142.05	17.414	-146.57	14.993	-102.78	15.987	-131.4	12.457	-125.71
506	17.703	-117.71	13.746	-130	17.738	-146.1	13.82	-67.606	14.936	-87.204	11.927	-82.455
507	24.716	-114.72	19.005	-118.47	25.038	-125.31	18.206	-81.047	20.367	-98.821	15.74	-92.163
508	30.342	-92.551	25.24	-94.552	30.535	-98.481	23.912	-72.421	26.265	-83.334	18.36	-75.178
509	6.822	-25.099	5.3368	-24.439	5.8701	-25.36	5.9811	-23.889	6.0365	-24.57	5.8146	-24.067

Appendix III Benchmark comparison between Mudpack and PSS®/E models of the 14-generator system

The small-signal stability analysis in this report is conducted with Mudpack [14]. Mudpack is an interactive software package for investigating the small-signal dynamic performance of large multi-machine power systems. It forms the linearized differential and algebraic equations of the power system based on an exact analytical evaluation of the partial derivatives of the non-linear system equations, rather than on the numerical estimation methods used in some other tools. Based on the linearized system model Mudpack computes and graphically displays the eigenvalues, mode-shapes, participation factors; computes and graphically displays time- and frequency-responses; computes and graphically displays transfer-function residues and performs a number of other specialized tasks associated with the tuning of stabilizers and investigation of the interactions between stabilizers and generators.

We employ the widely used PSS®/E software package [1] for power flow and transient stability analysis.

As a precursor to performing transient stability studies on the simplified 14-generator model of South East Australian power system we establish through a number of benchmark tests that the small-signal performance of the PSS®/E model of the system agrees closely with that of the Mudpack model.

As stated in Appendix II.2.1.1 in PSS®/E the frequency dependence of network parameters is represented by setting the simulation parameter NETFRQ = 1. This ensures that a consistent formulation of the generator rotor equations of motion in PSS®/E.

All benchmark studies are conducted with the PSSs in-service with their design damping gain of De = 20 pu on the machine MVA rating. (Comparison of PSS®/E and Mudpack responses with the PSSs out-of-service is ill-advised because the system is unstable without PSSs. Consequently, non-linear behaviour of the system will play a significant role in the PSS®/E step responses as the oscillations grow in amplitude.)

III.1 Generator voltage-reference step-responses

For study case 1, with all PSSs in service at their design damping gain of 20.0 pu, a 0.5% step increase in the voltage reference is applied to the AVR of generator HPS_1 and the *perturbations* in the power output (P), rotor-speed (W), stator-voltage (Vt), reactive-power output (Q), generator field voltage (Ef) and generator field current (If) are monitored. This test is conducted in both PSS®/E and Mudpack. As shown in Figure 28 the responses obtained with the two packages are practically identical. Such voltage-reference step-response tests are useful in verifying that the local mode behaviour obtained with the respective simulation packages are consistent.

Similar tests have been performed for all 14 generators in all six study cases and there is similarly very close agreement between the PSS®/E and Mudpack responses. A selection of these results is presented in Figures 29 to 41. A complete set of the 14 x 6 = 84 plots is provided in the form of a PDF file as part of the DataPackage. Furthermore, to aid the reader in benchmarking their own implementation of the model, the step-response time-series data is also provided in the DataPackage for a selection of the voltage-reference step-response tests.

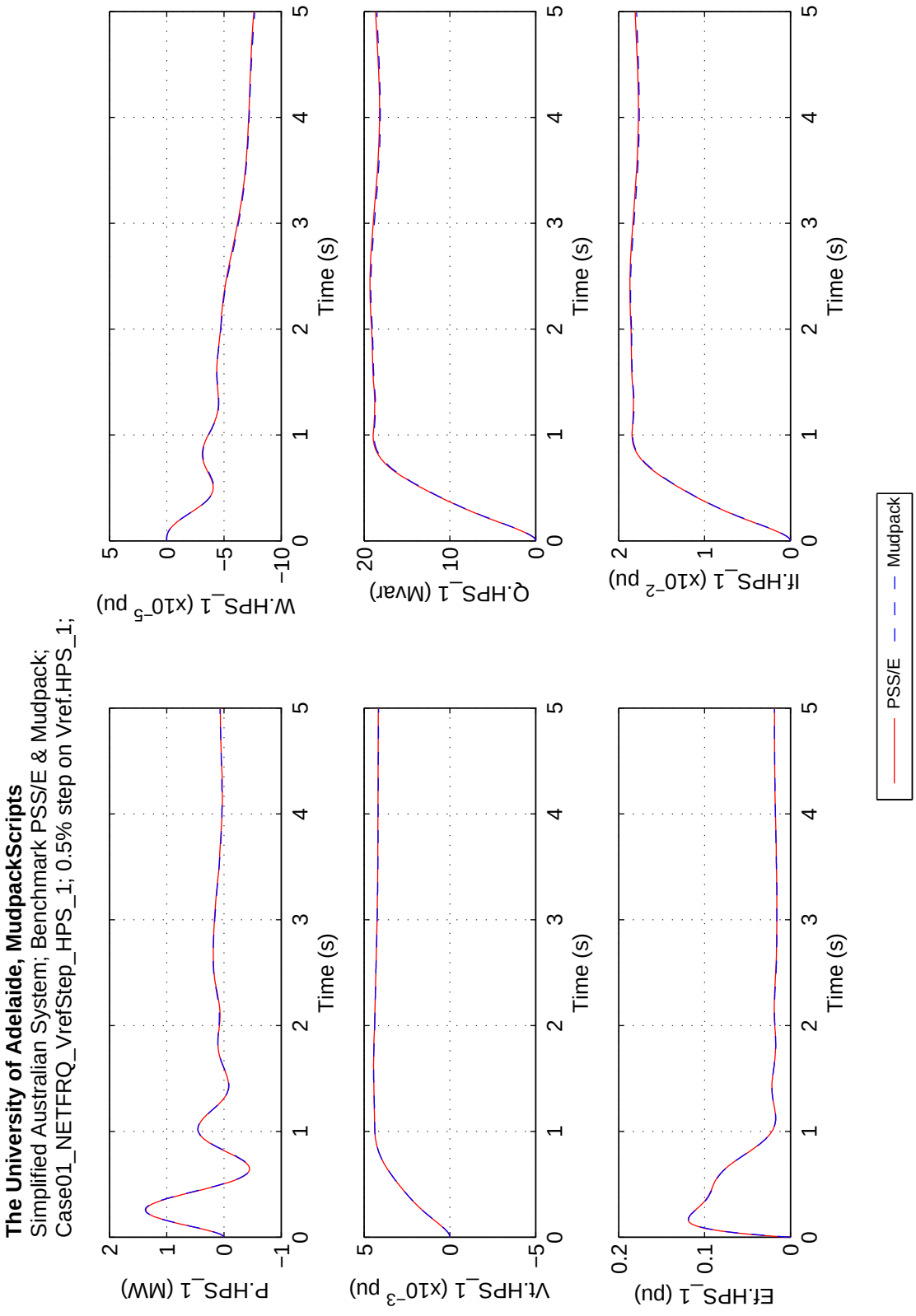

Figure 28 Case 1, Vref.HPS_1 step-response benchmark comparison between PSS®/E (with NETFRQ = 1) and Mudpack. A 0.5% step increase in the voltage-reference of the AVR of generator HPS_1 is applied and the perturbations in the electrical power output (P), rotor-speed (W), stator-voltage (Vt), reactive-power output (Q), generator field-voltage (Ef) and field-current (If) of HPS_1 are compared.

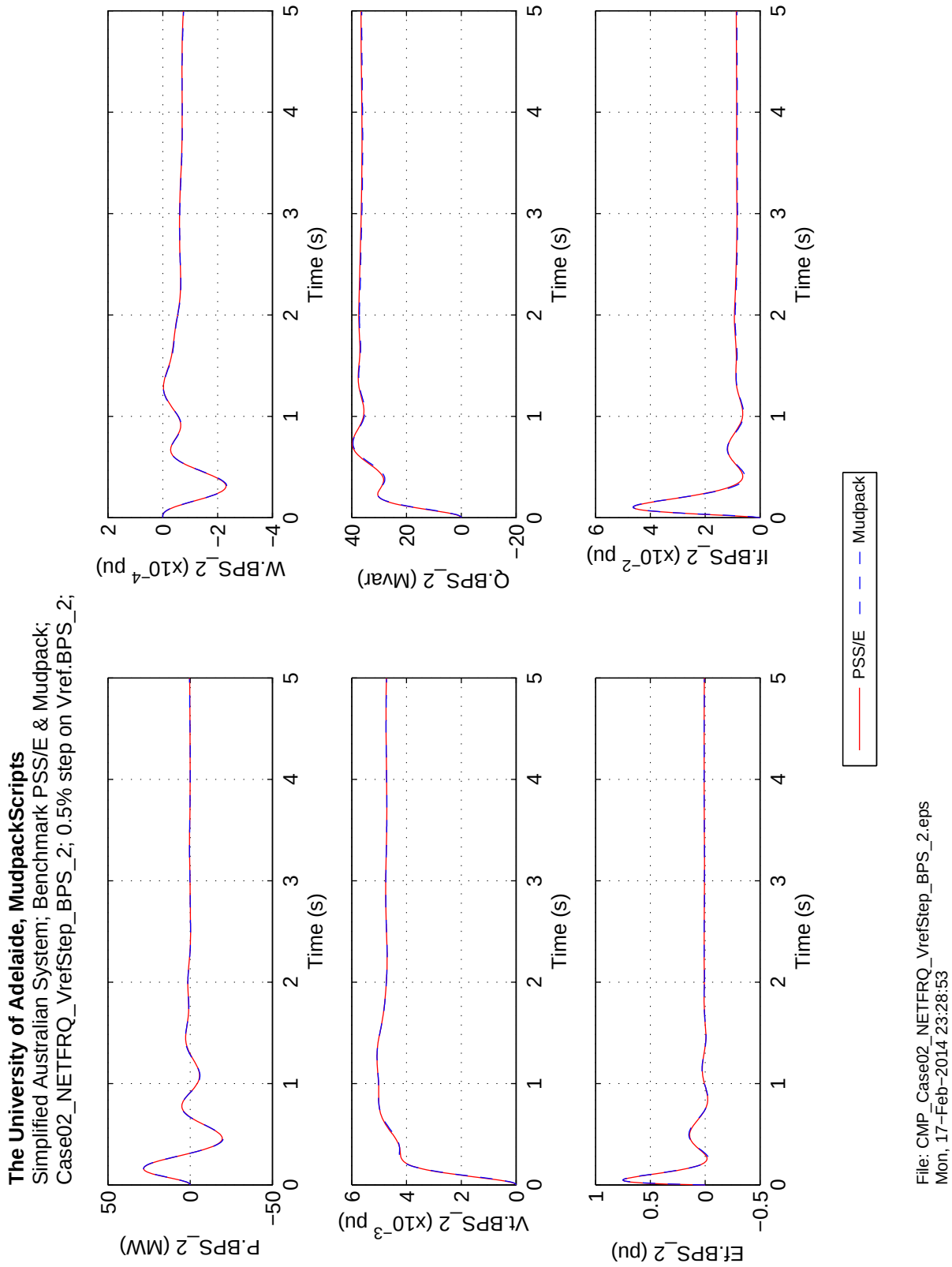

Figure 29 As for Figure 28 but for Case 2 and generator BPS_2.

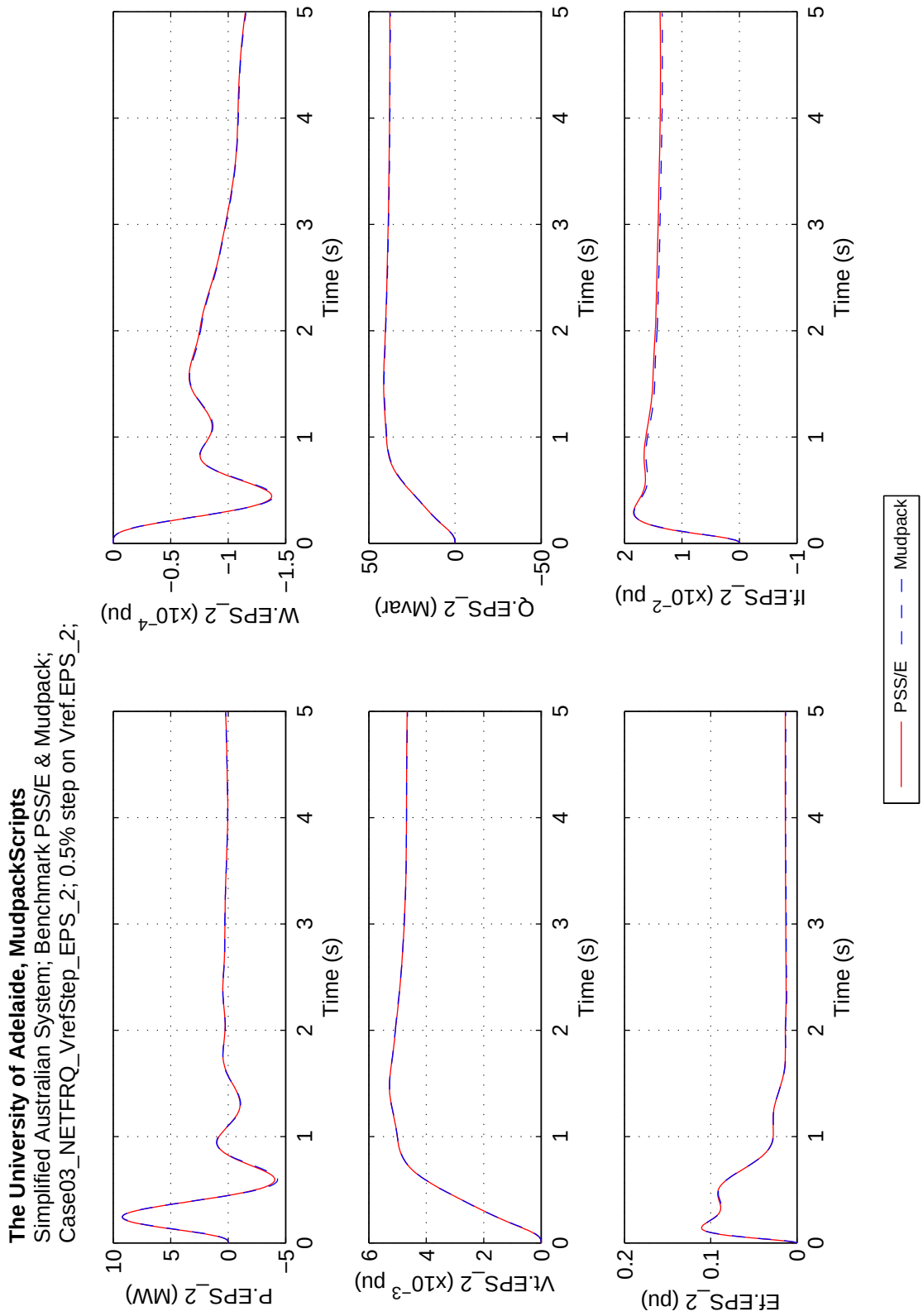

Figure 30 As for Figure 28 but for Case 3 and generator EPS_2.

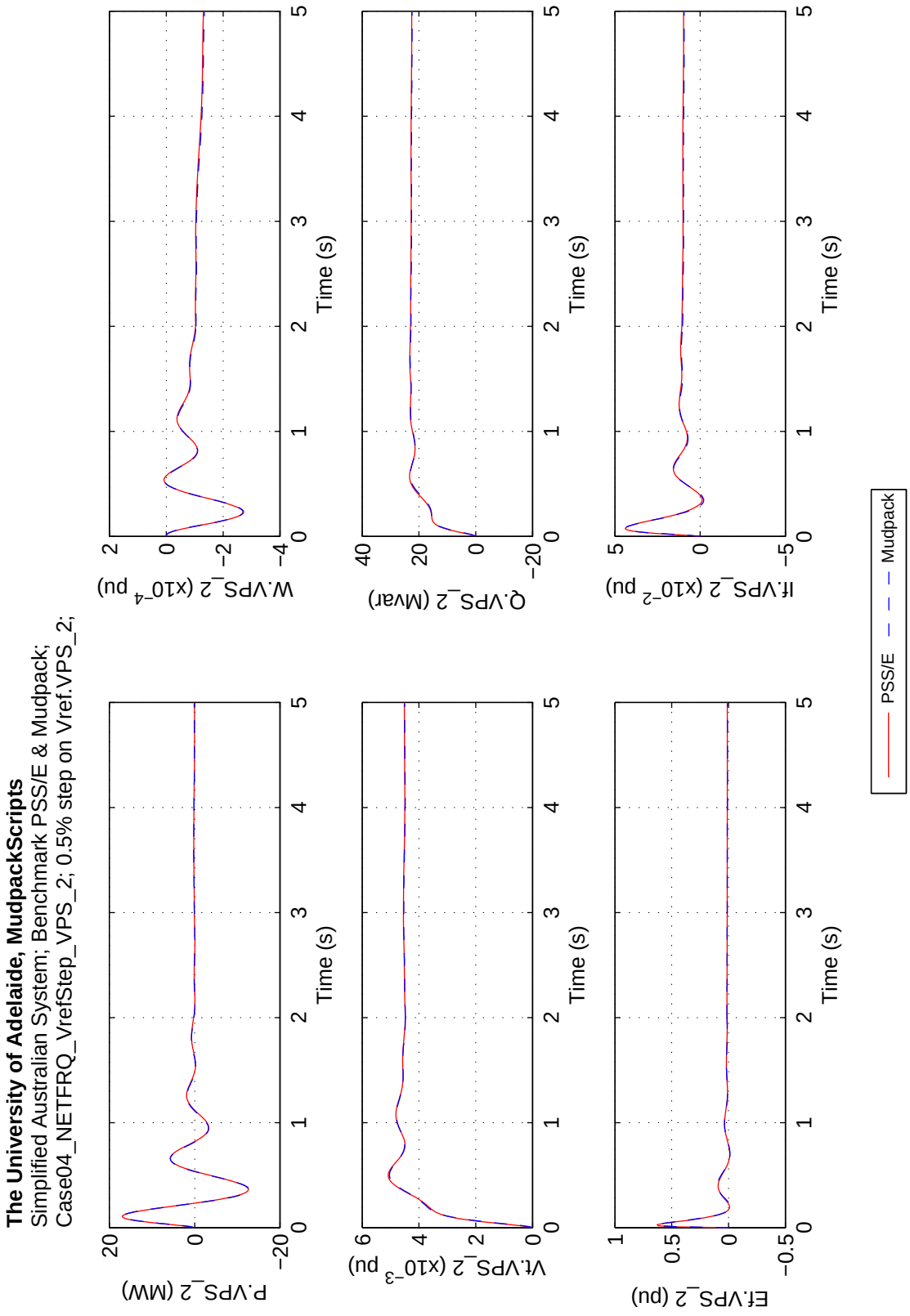

Figure 31 As for Figure 28 but for Case 4 and generator VPS_2.

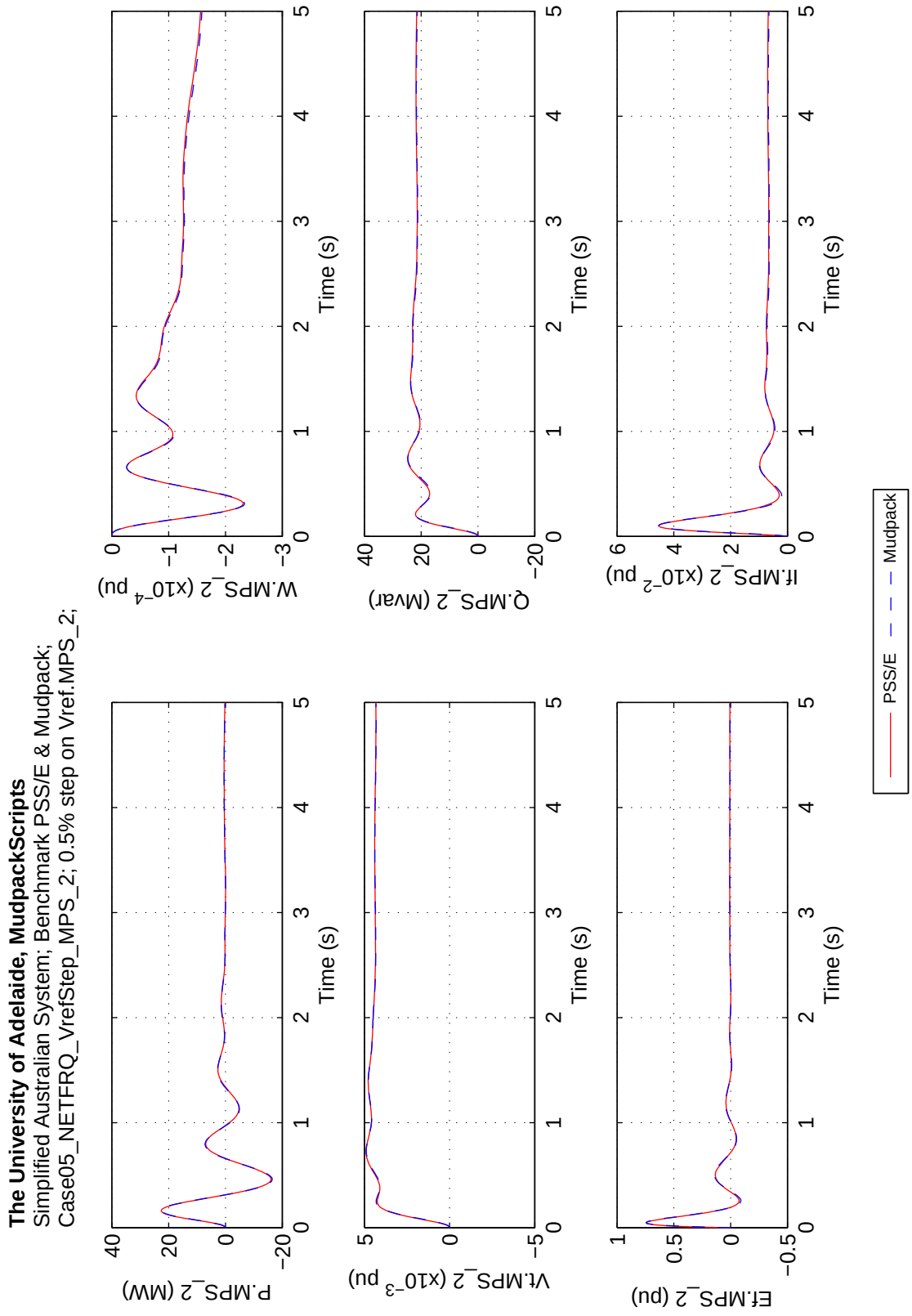

Figure 32 As for Figure 28 but for Case 5 and generator MPS_2.

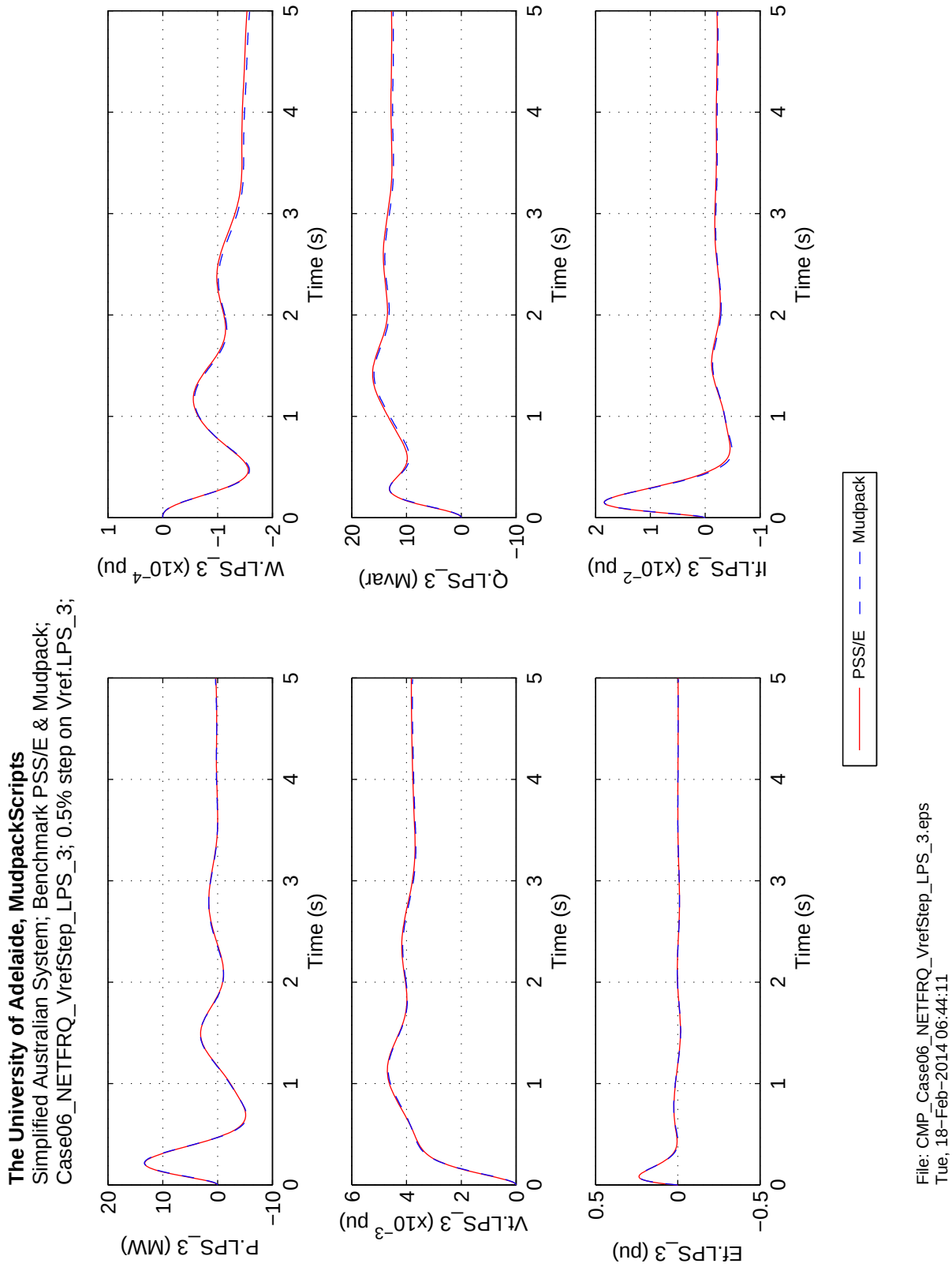

Figure 33 As for Figure 28 but for Case 6 and generator LPS_3.

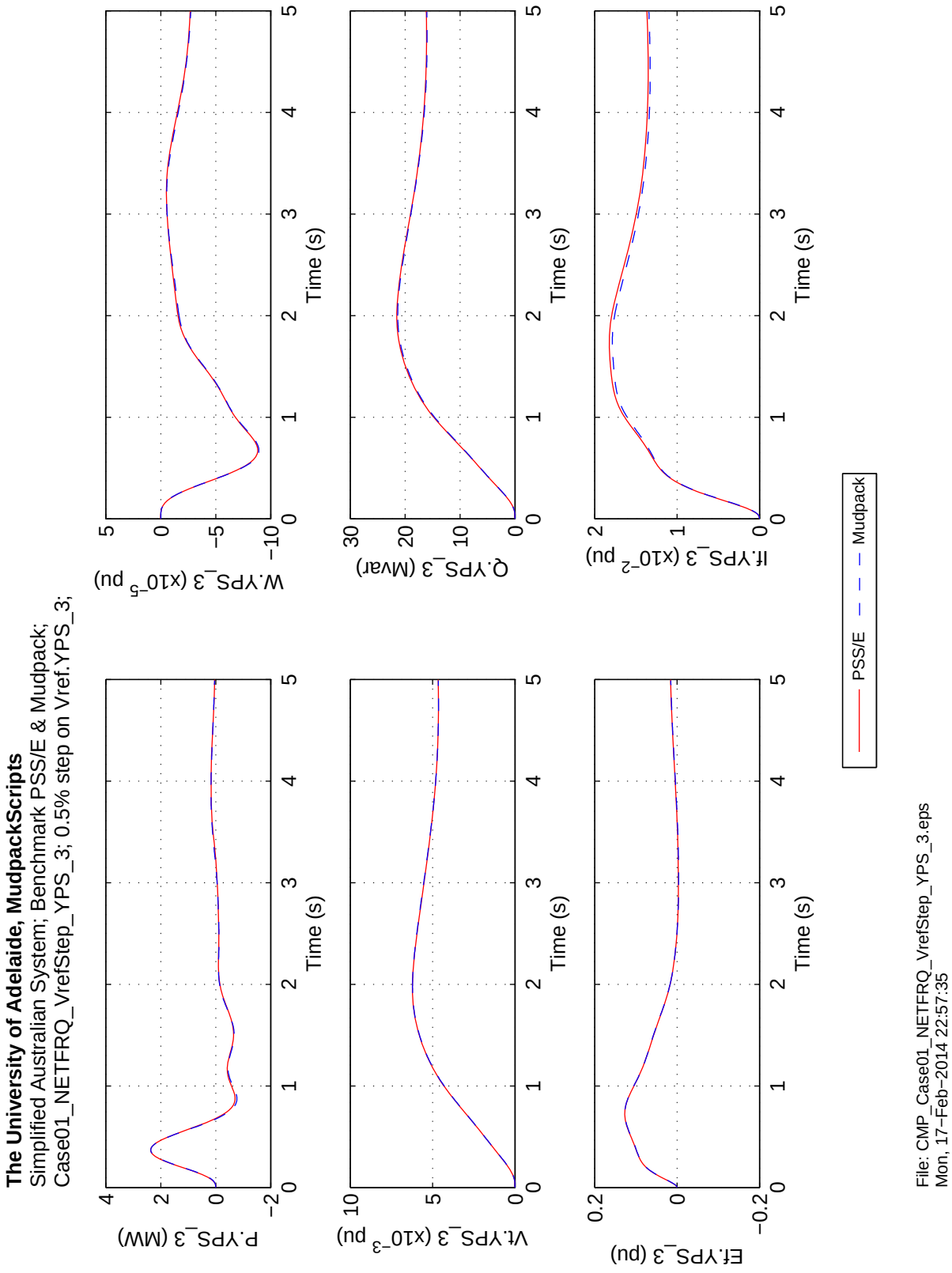

Figure 34 As for Figure 28 but for Case 1 and generator YPS_3.

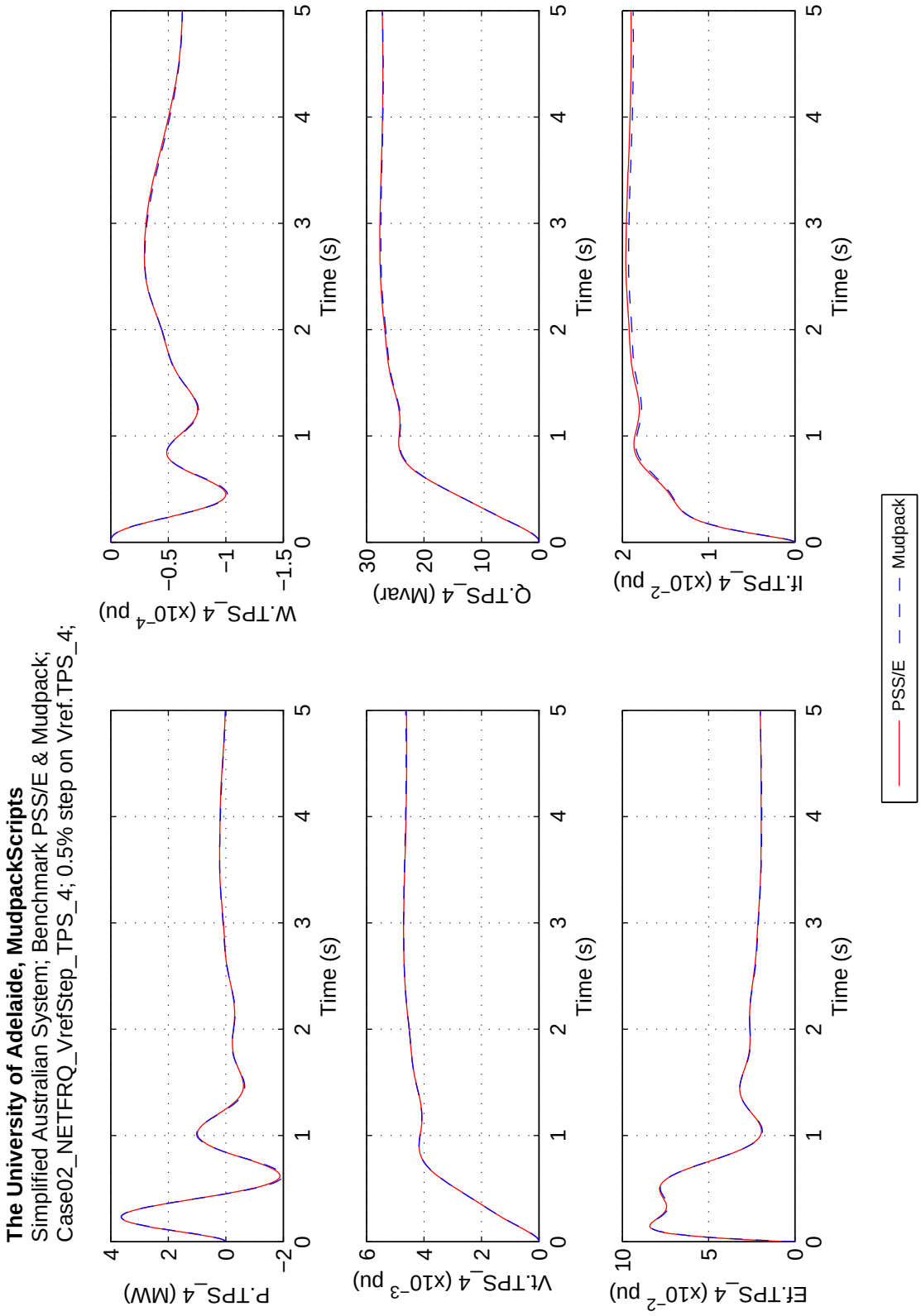

Figure 35 As for Figure 28 but for Case 2 and generator TPS_4.

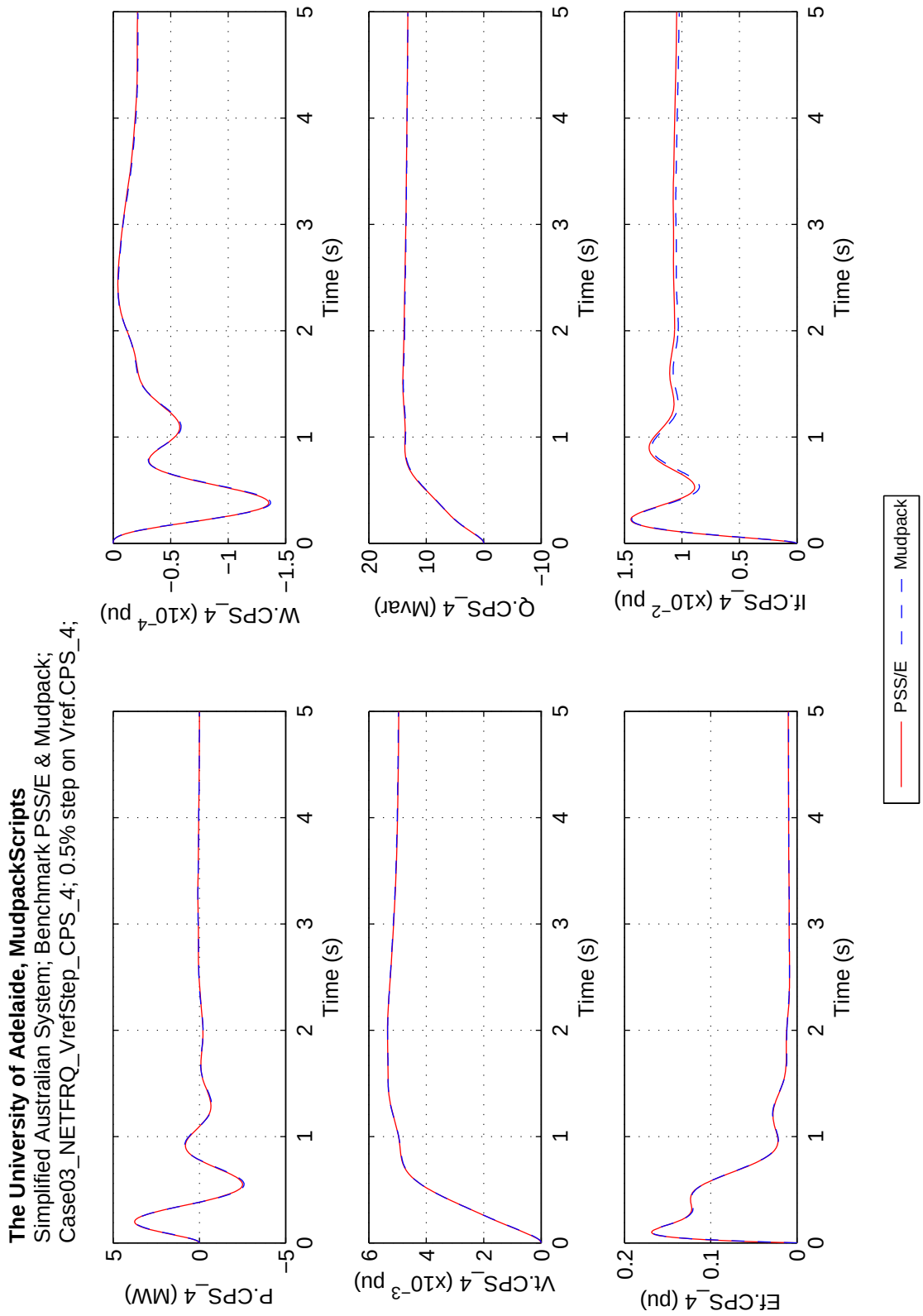

Figure 36 As for Figure 28 but for Case 3 and generator CPS_4.

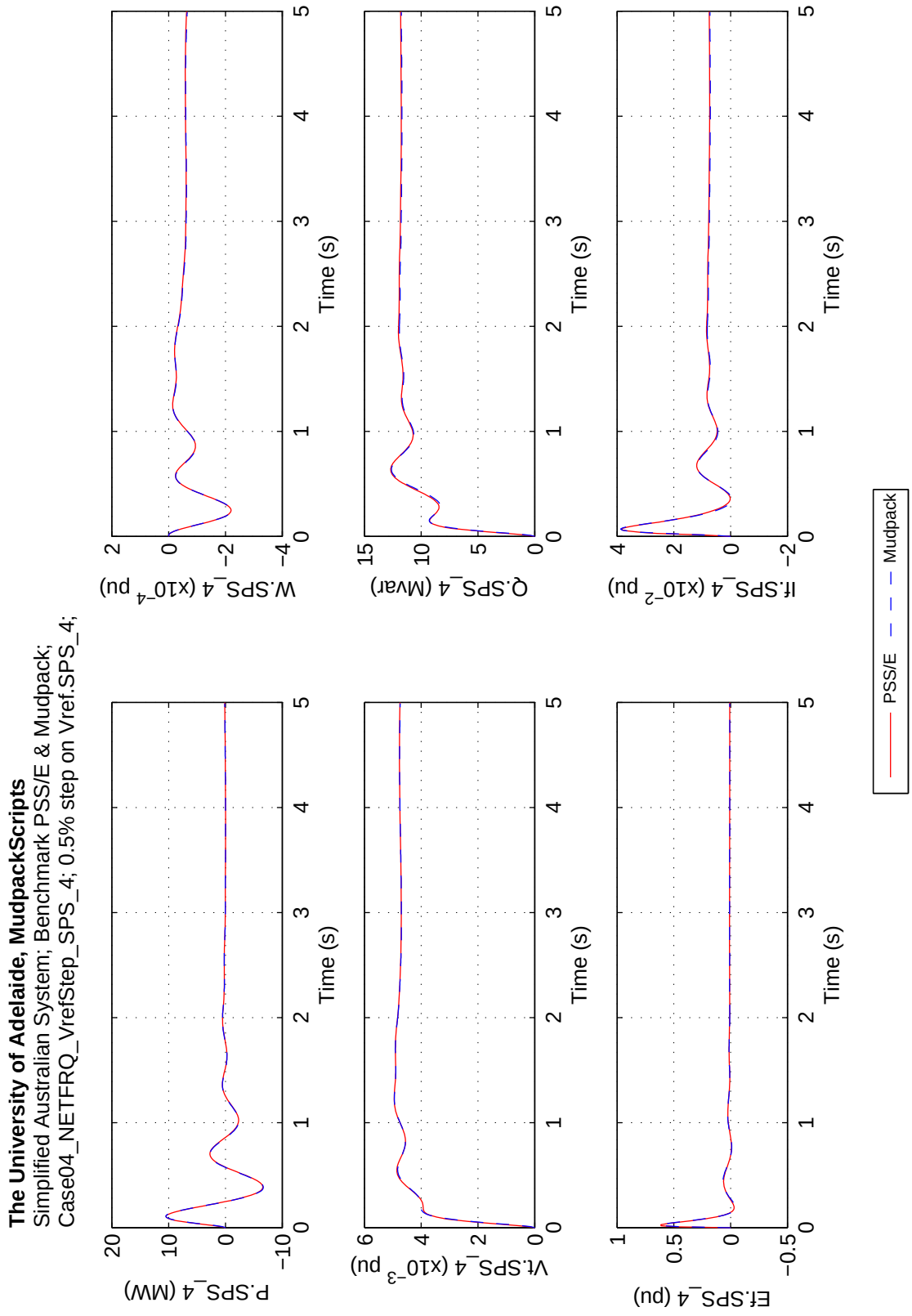

Figure 37 As for Figure 28 but for Case 4 and generator SPS_4.

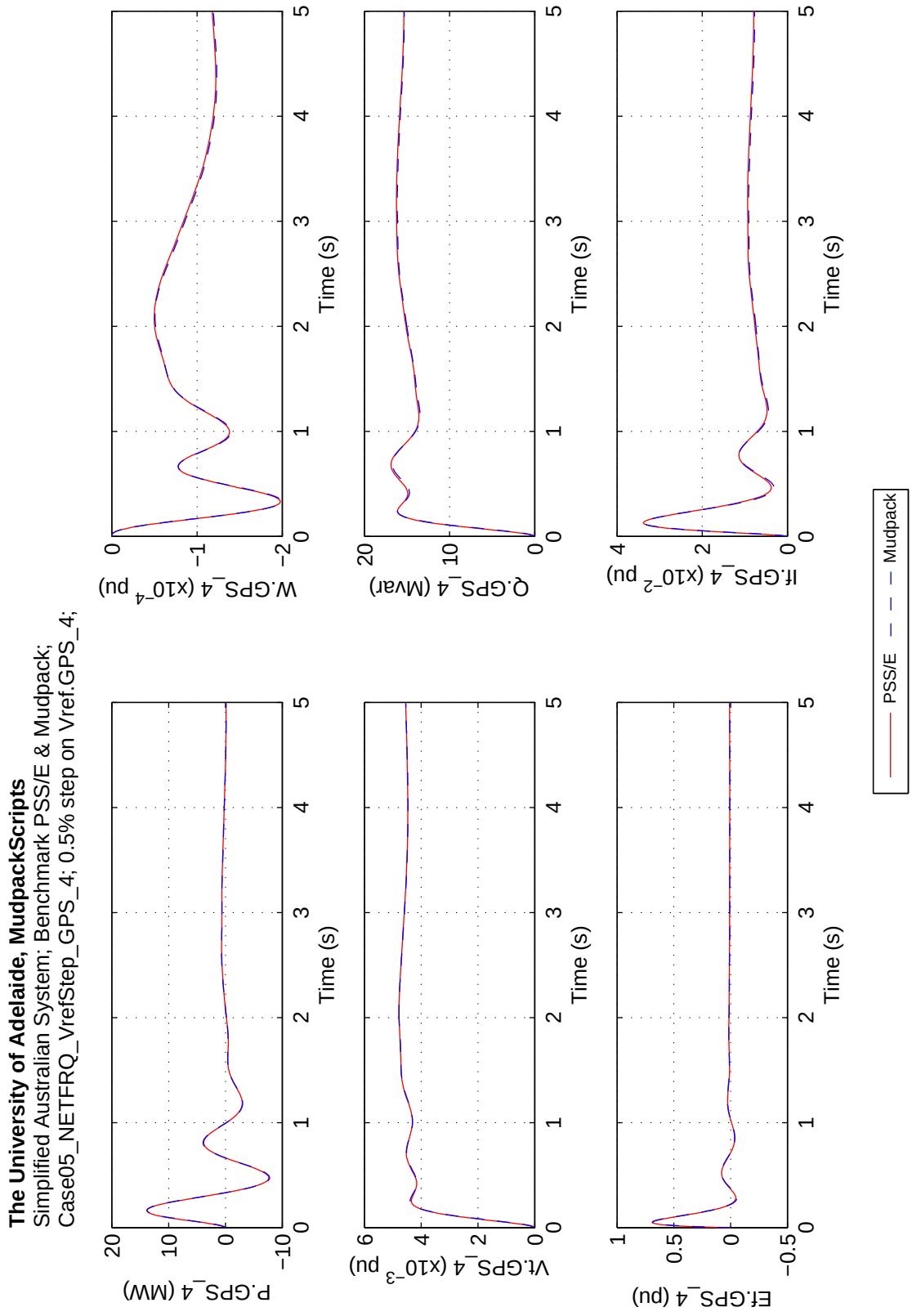

Figure 38 As for Figure 28 but for Case 5 and generator GPS_4.

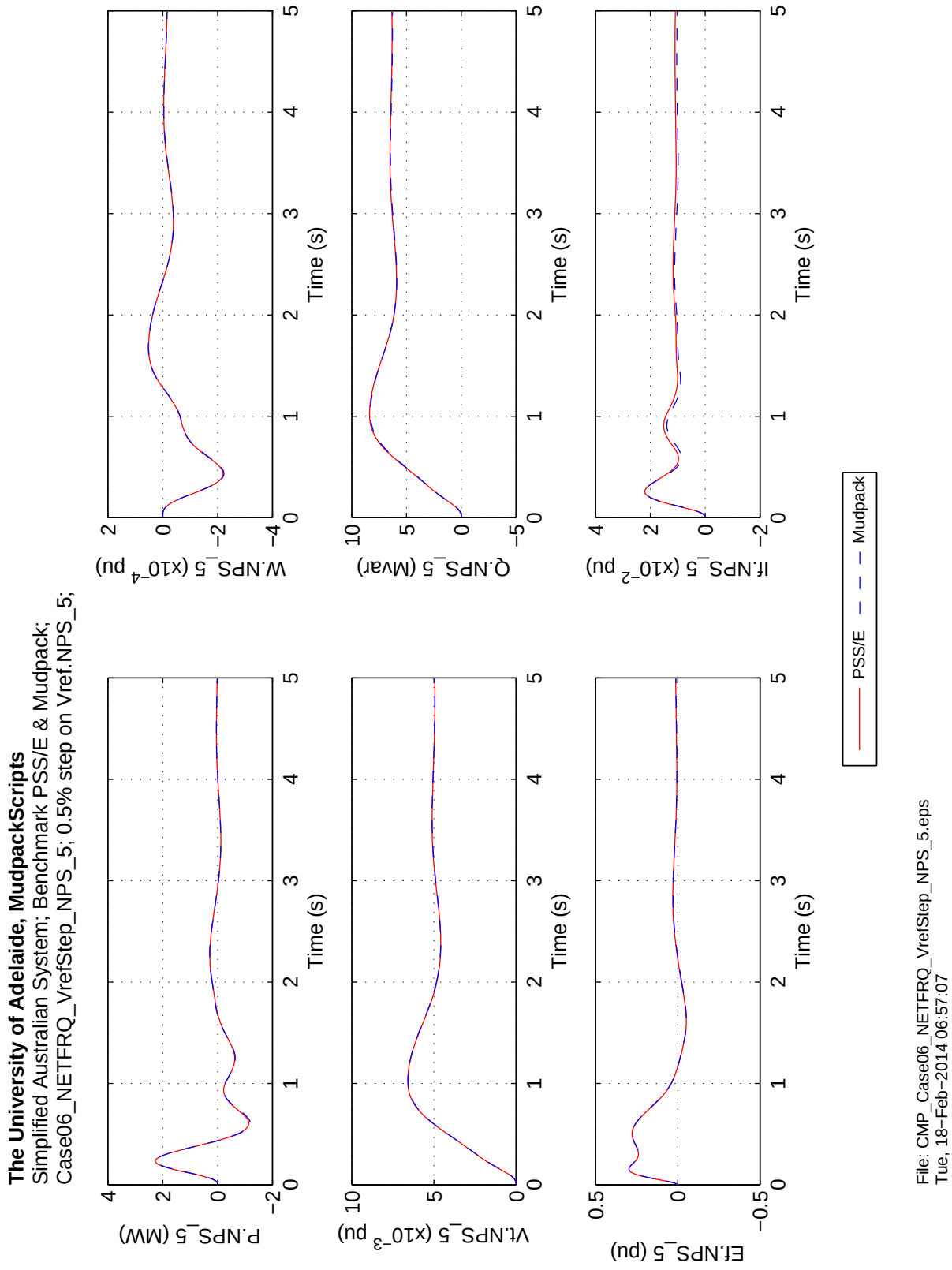

Figure 39 As for Figure 28 but for Case 6 and generator NPS_5.

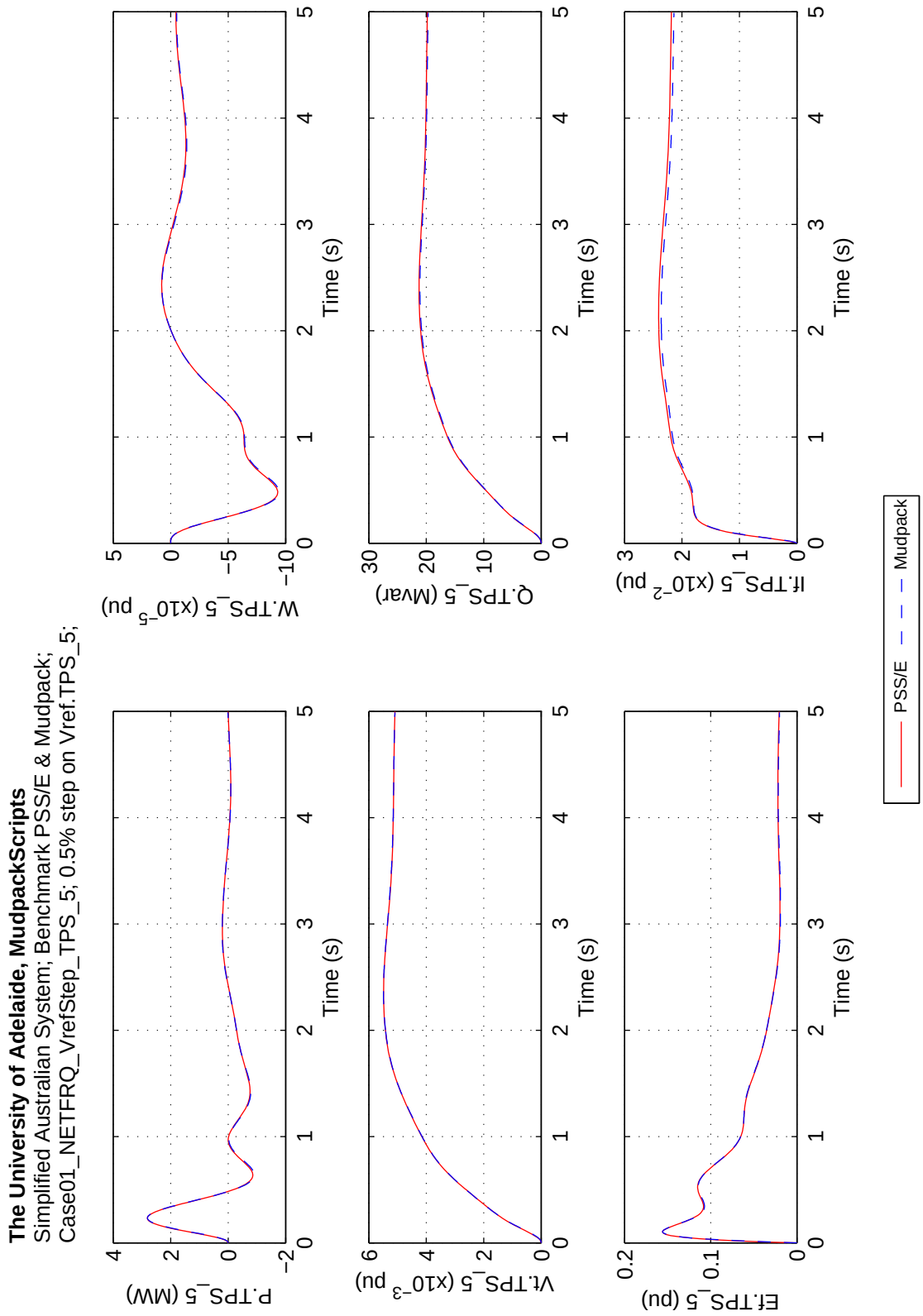

Figure 40 As for Figure 28 but for Case 1 and generator TPS_5.

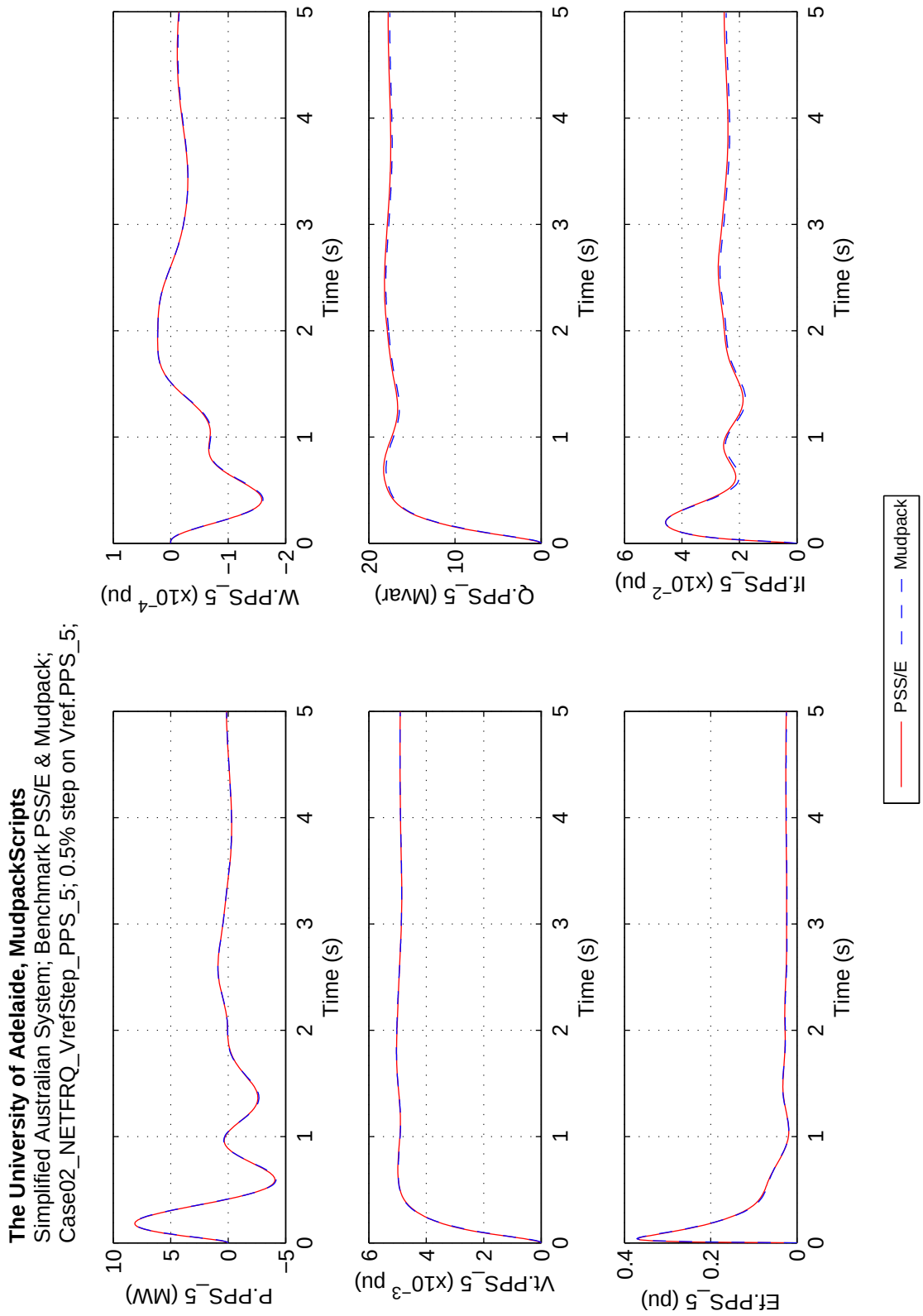

Figure 41 As for Figure 28 but for Case 2 and generator PPS_5.

III.2 Mechanical power step-responses to verify consistency of inter-area modes

For study case 1, with all PSSs in service at their design damping gain of 20.0 pu, a +10 MW step is applied to the mechanical power input of the GPS_4 machine and a compensating -10 MW step is applied to the NPS_5 machine. Since these two machines are located at either end of the system the interarea modes of oscillation are excited and the power flow in the inter-regional tie-lines contain significant inter-area modal components. Thus, the perturbations in the total line-power flow in the circuits between buses 410 & 413 (P.LN42); 217 & 102 (P.LN23); and 509 & 315 (P.LN53) are monitored. This test, which is conducted in PSS®/E and Mudpack, is intended to verify that the inter-area mode behaviour obtained with the respective simulation packages are consistent. As shown in Figure 42 the responses obtained with the two packages are practically identical (with PSS®/E NETFRQ = 1).

The results of similar tests conducted for cases 2 to 6 are shown in Figures 43 to 47 respectively and they reveal similarly very close agreement between the PSS®/E and Mudpack responses. The time-series data for these results are also provided in the DataPackage.

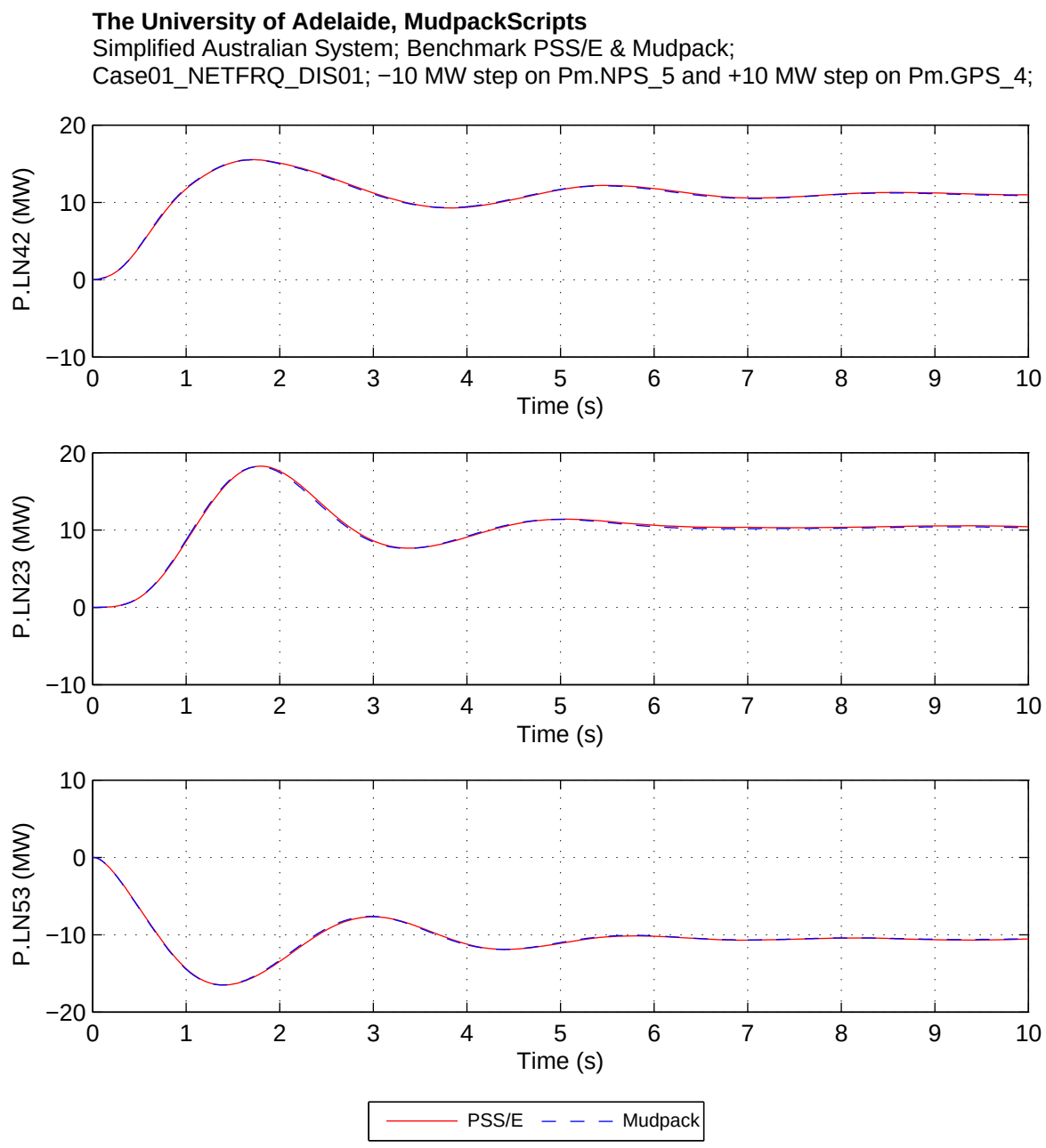

Figure 42 Case 1. Benchmark comparison between PSS®/E (with NETFRQ = 1) and Mudpack. Step change in mechanical power input of +10 MW applied to GPS_4 and a compensating change of -10 MW applied to NPS_5. Powerflow in interconnectors between areas 2 &4 (P.LN42); areas 2 & 3 (P.LN23) and areas 5 & 3 (P.LN53) are compared.

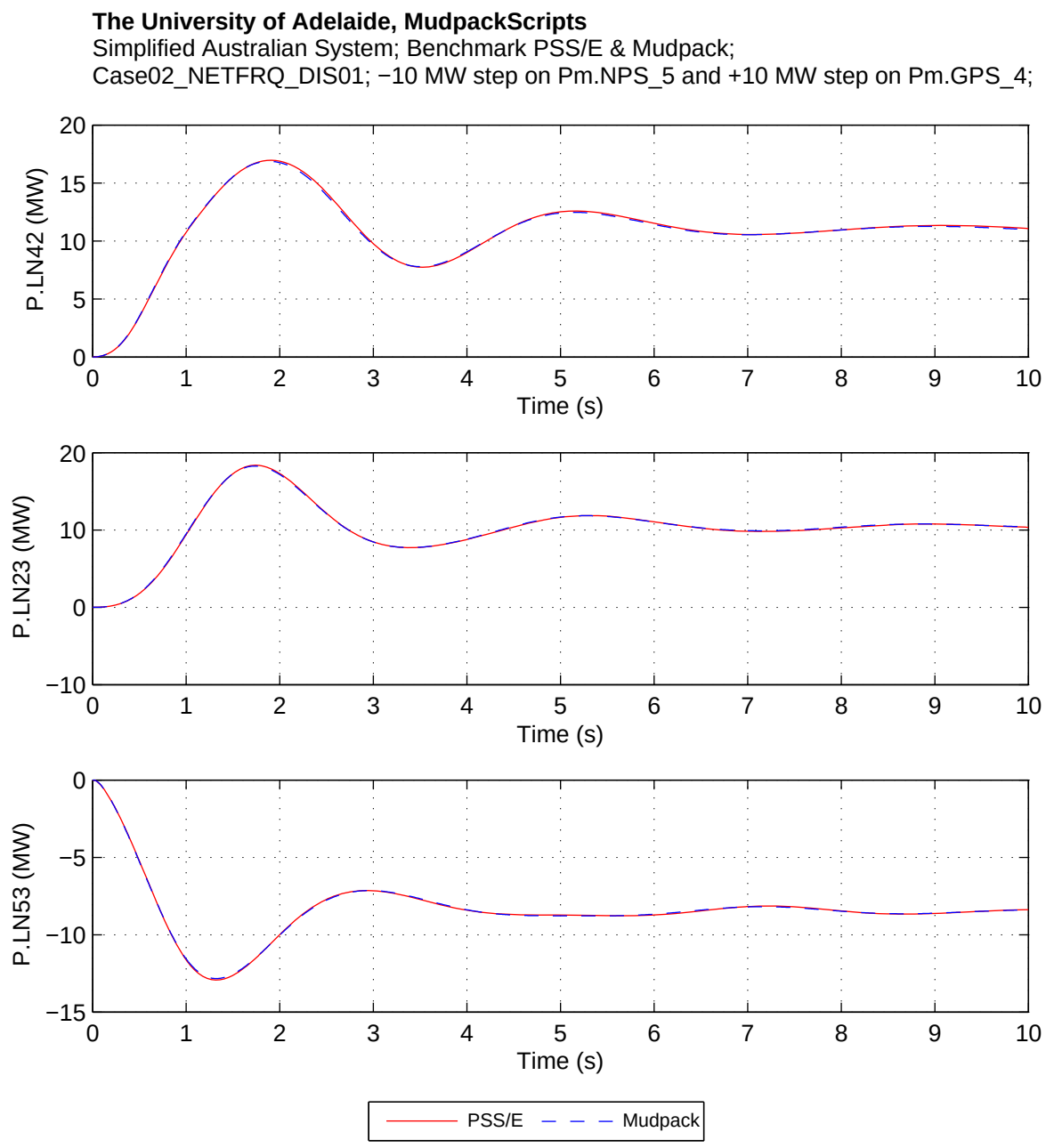

Figure 43 As for Figure 42 but for Case 2.

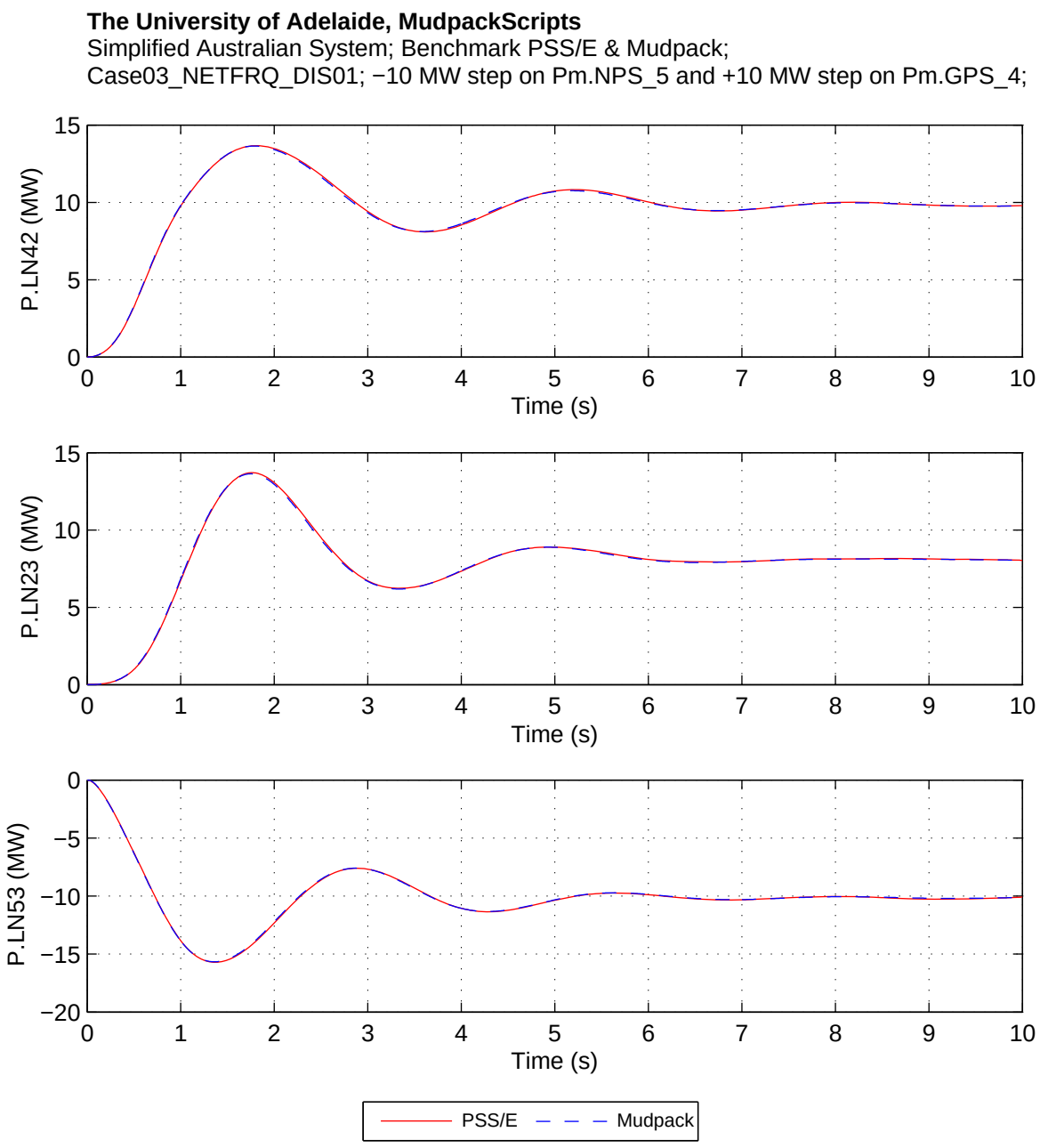

Figure 44 As for Figure 42 but for Case 3.

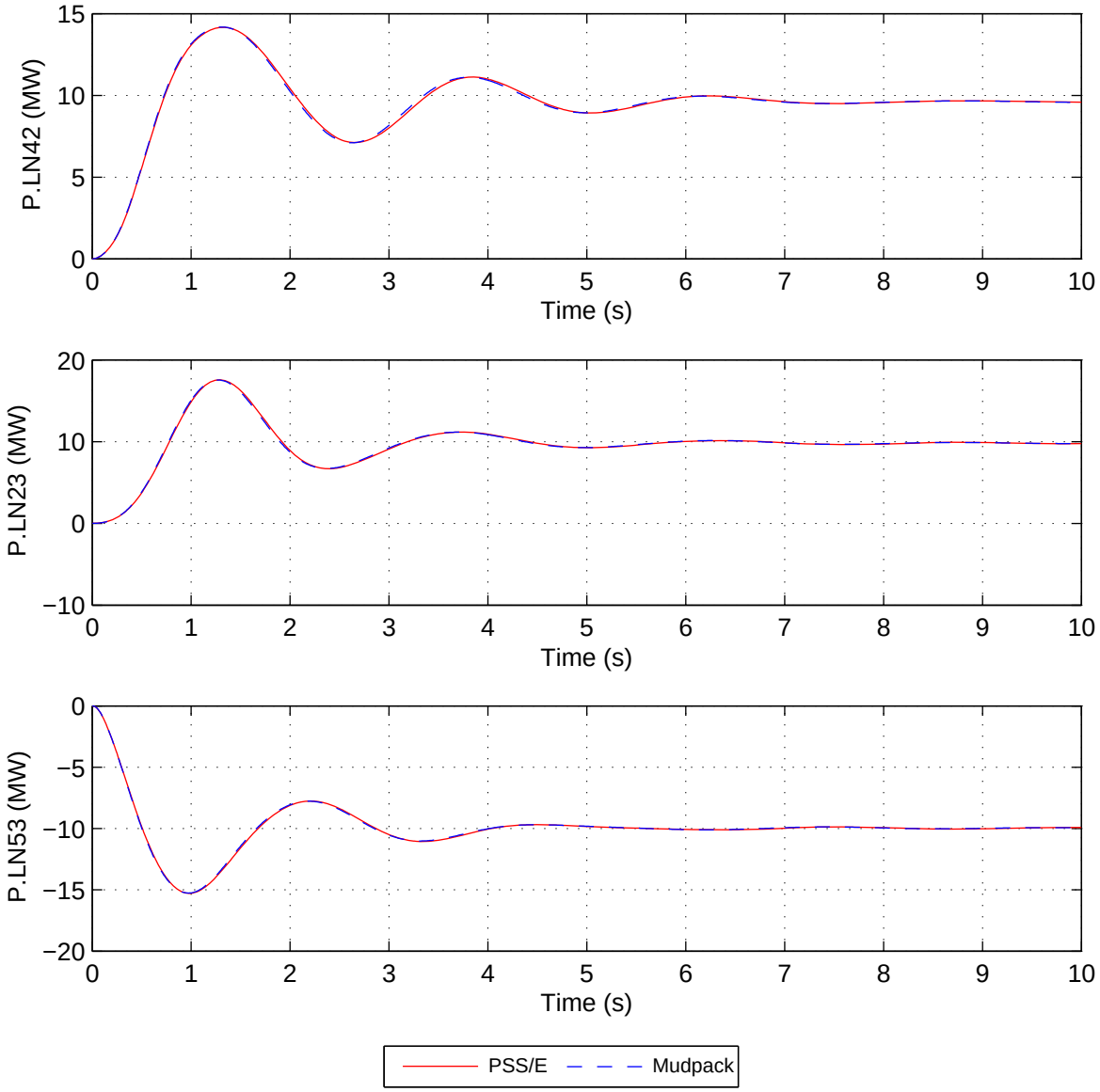

Figure 45 As for Figure 42 but for Case 4.

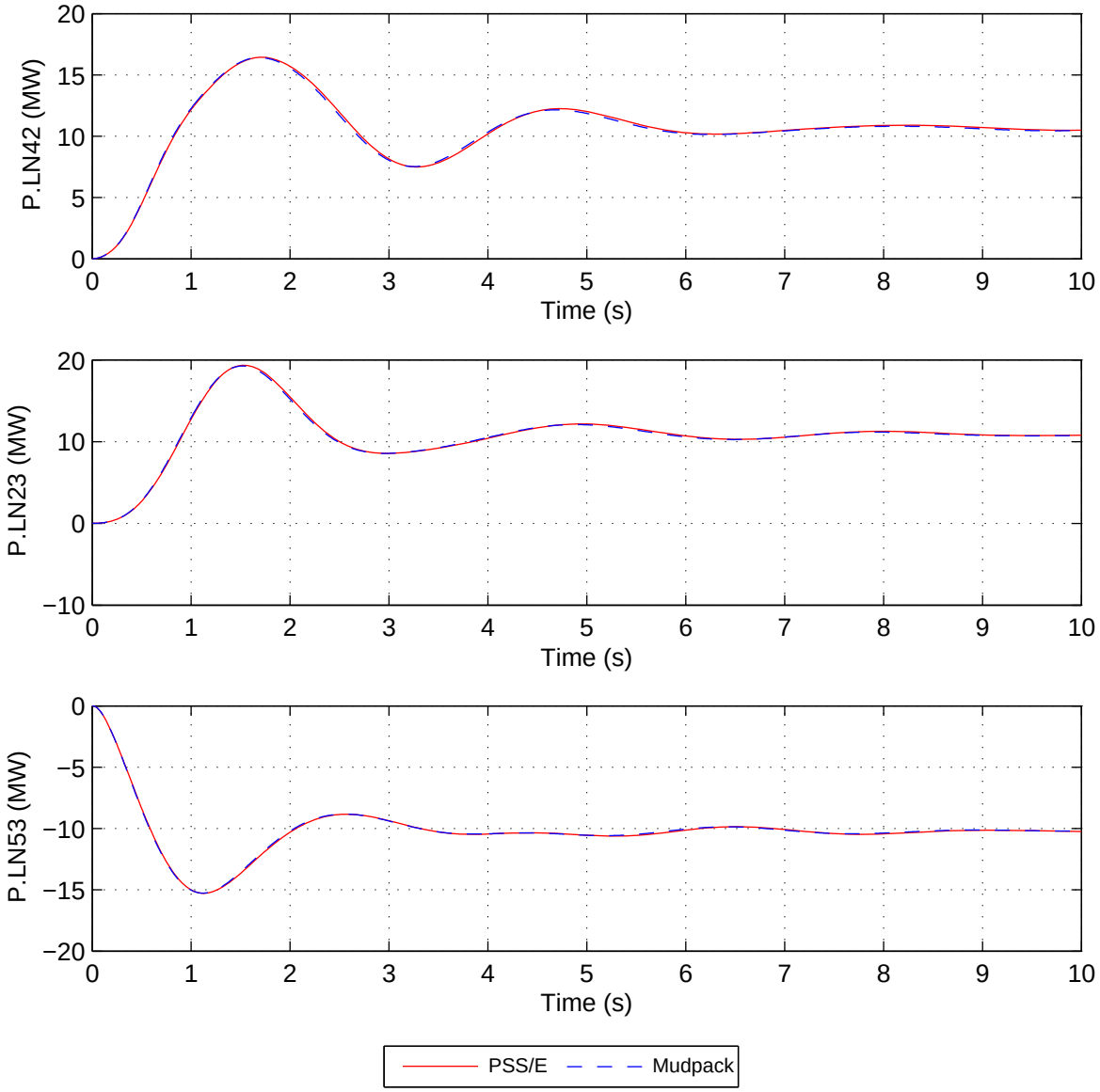

Figure 46 As for Figure 42 but for Case 5.

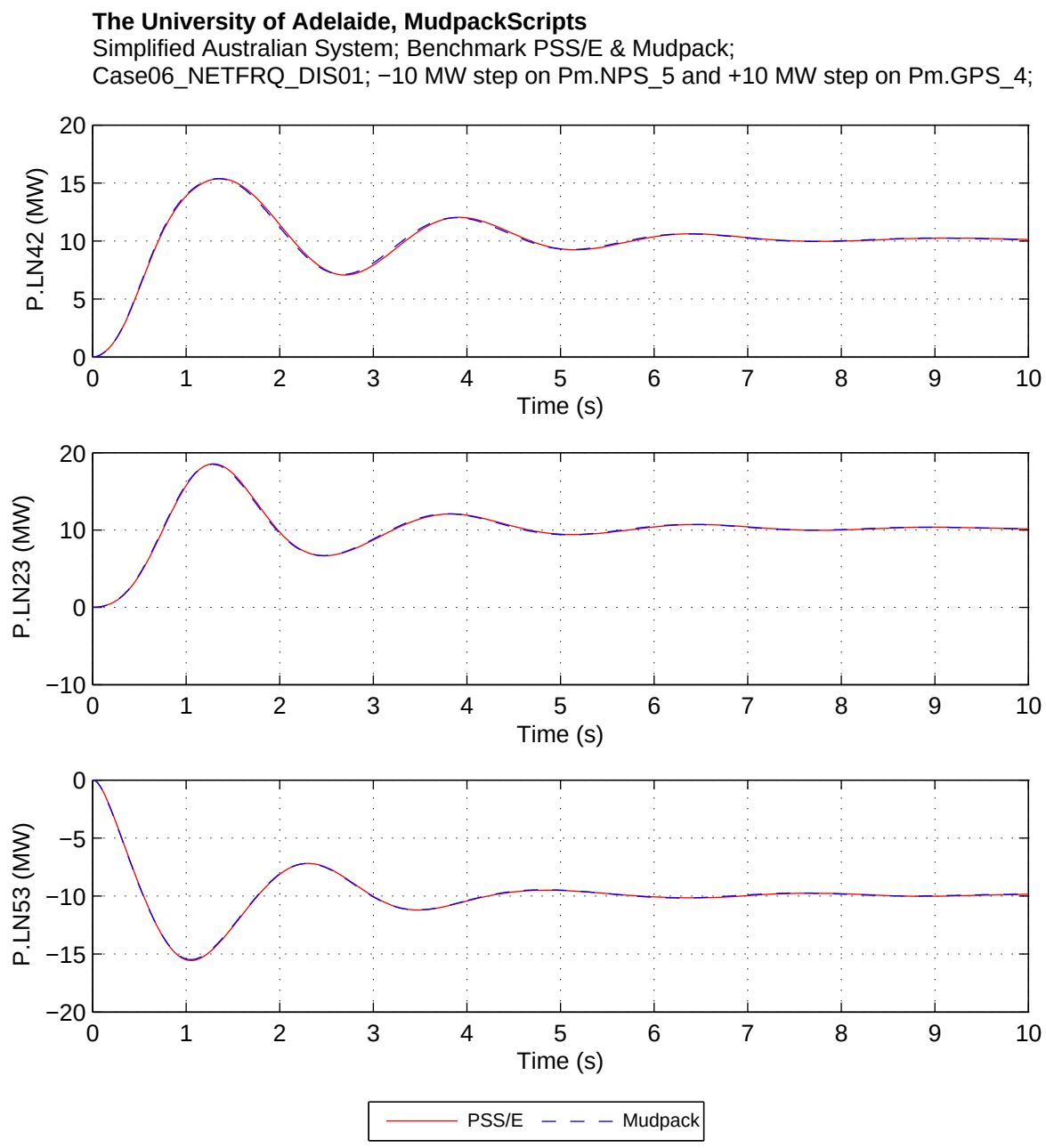

Figure 47 As for Figure 42 but for Case 6.

III.3 Benchmark comparison of the generator P-Vr characteristics computed by PSS®/E and Mudpack

The P-Vr characteristics of the fourteen generators are computed in PSS®/E for Case 2 and compared in Figures 48 to 61 with the corresponding P-Vr characteristics computed using Mudpack. There is very close agreement between the characteristics computed by the respective packages. In order to highlight any differences between the characteristics in the range of electromechanical modal frequencies the magnitude characteristics are displayed in absolute units, rather than in dB.

These results demonstrate that the implementation of the electromagnetic behaviour of the generator models and of the AVR/exciter models in the respective simulation packages are practically identical.

To the authors knowledge the PSS®/E software package does not include built-in facilities for computation of frequency-responses. A tool, AUPSSEFRTOOL, developed at Adelaide University as a PSS®/E "plug-in" has been used to compute the P-Vr characteristics within the PSS®/E program. A paper describing this tool is in preparation at time of writing. It should be mentioned at this point that the accuracy of the frequency responses computed in PSS®/E are sensitive to the integration time-step and to the amplitude of the sinusoidal perturbation applied to the voltage-reference.

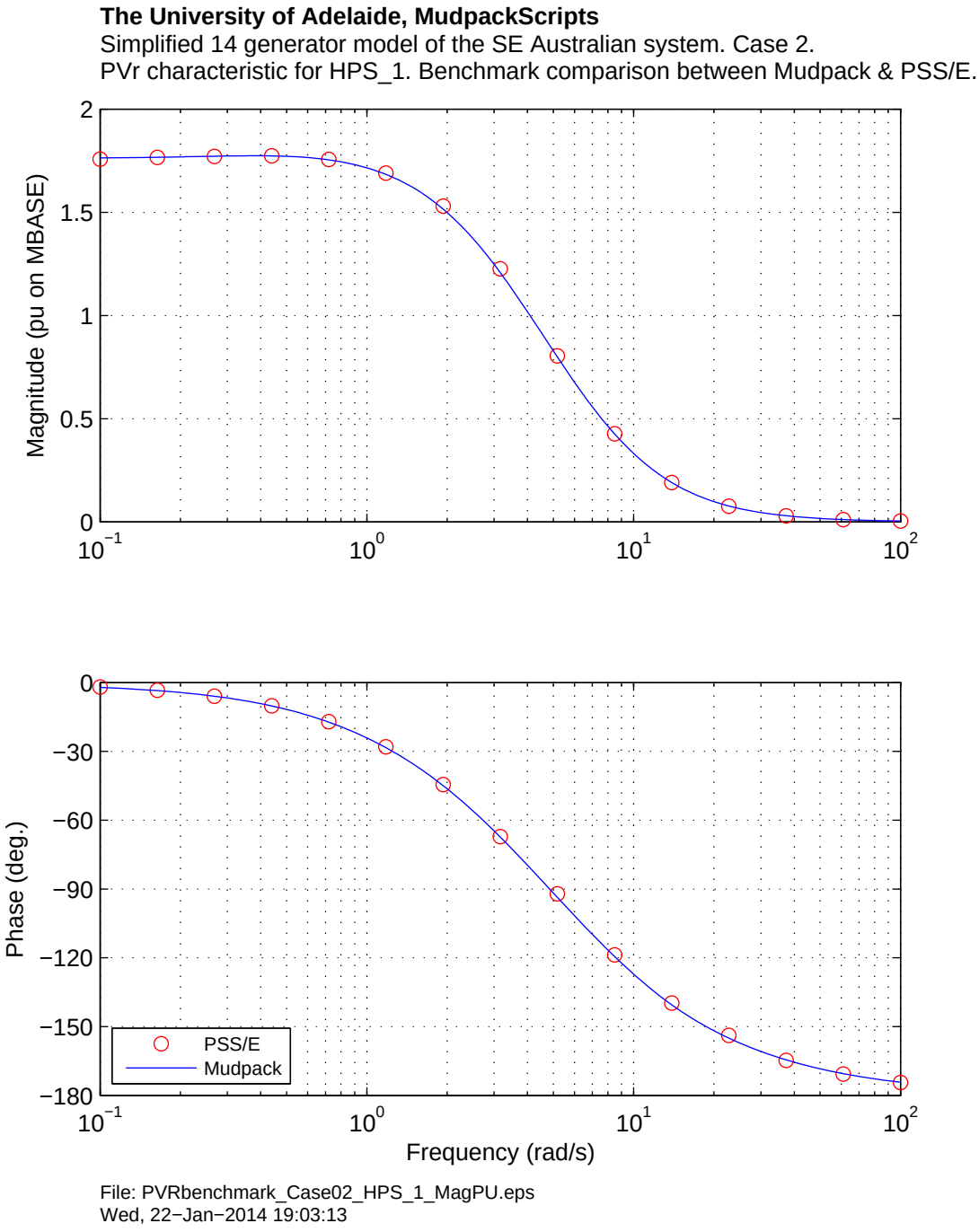

Figure 48 HPS_1 P-Vr characteristic benchmark comparison between Mudpack and PSS®/E.

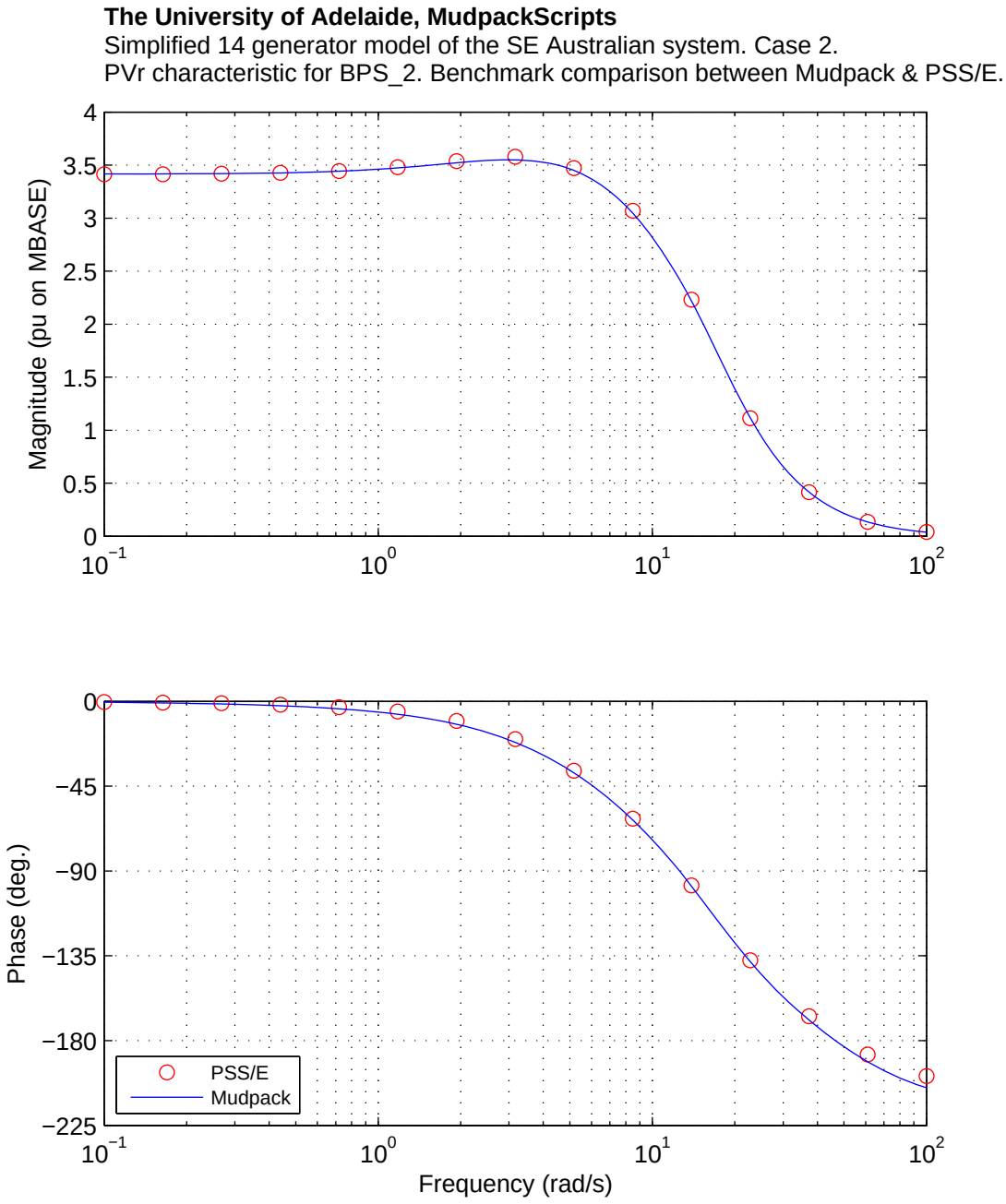

Figure 49 As for Figure 48 but for generator BPS_2.

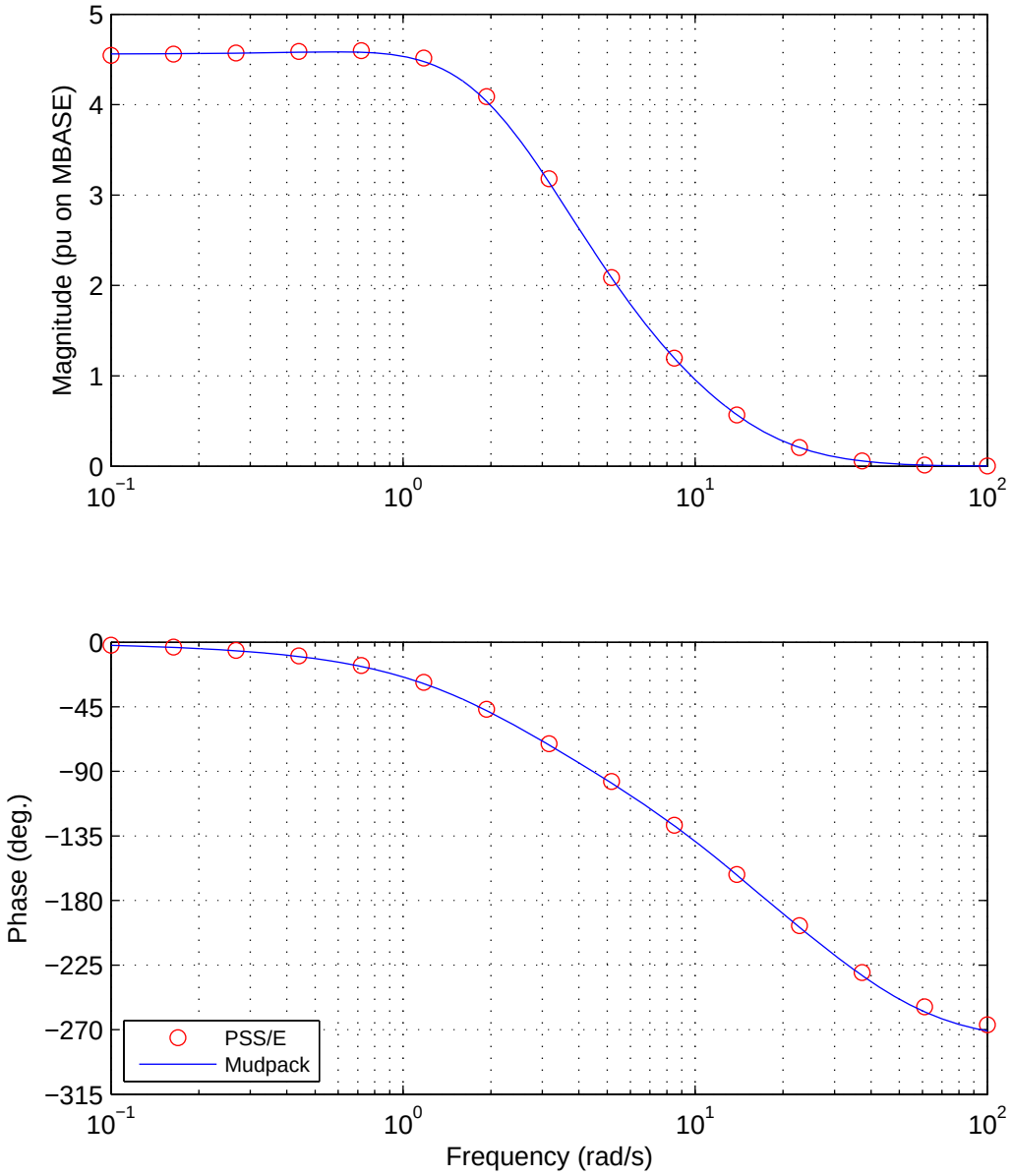

Figure 50 As for Figure 48 but for generator EPS_2.

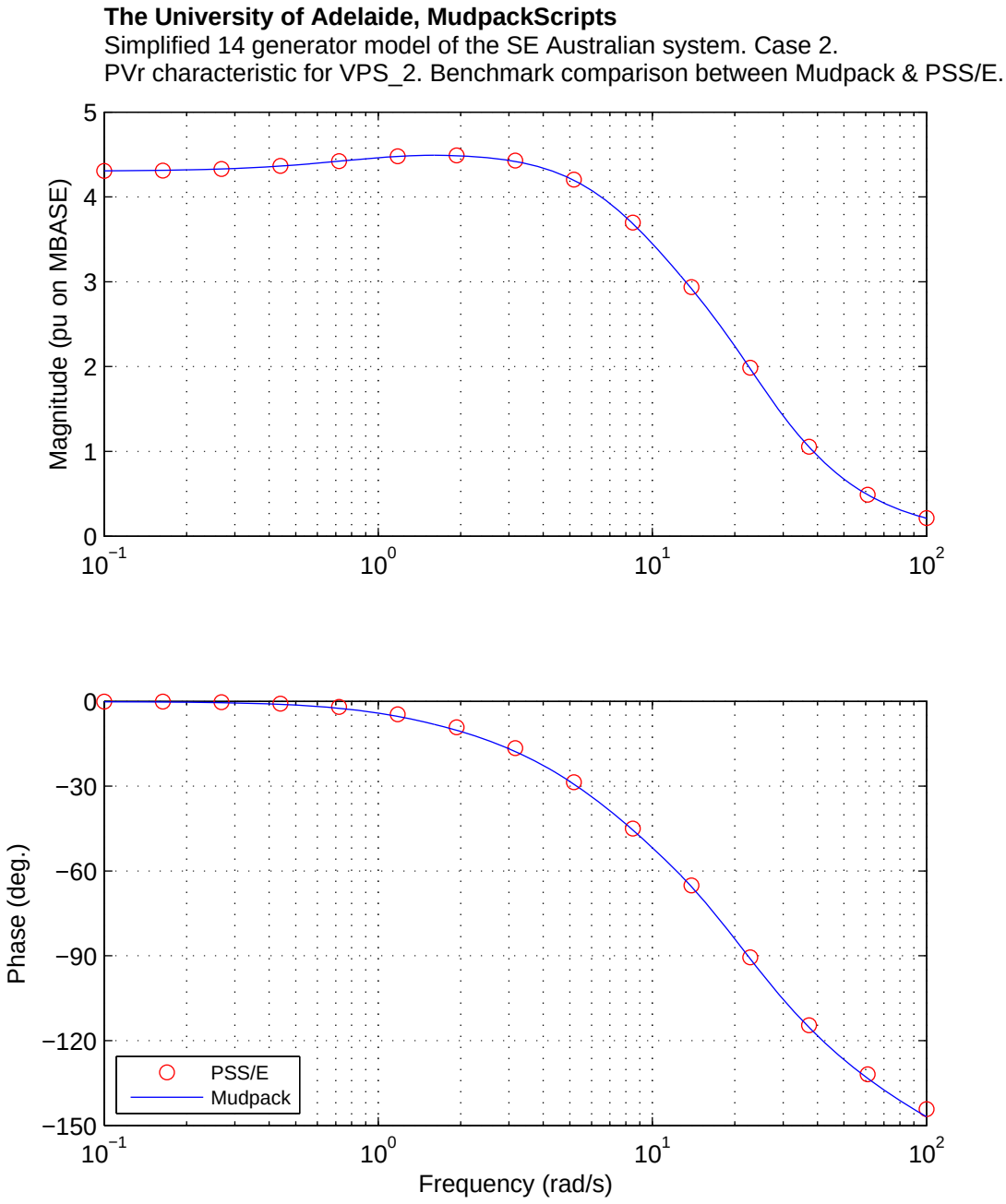

Figure 51 As for Figure 48 but for generator VPS_2.

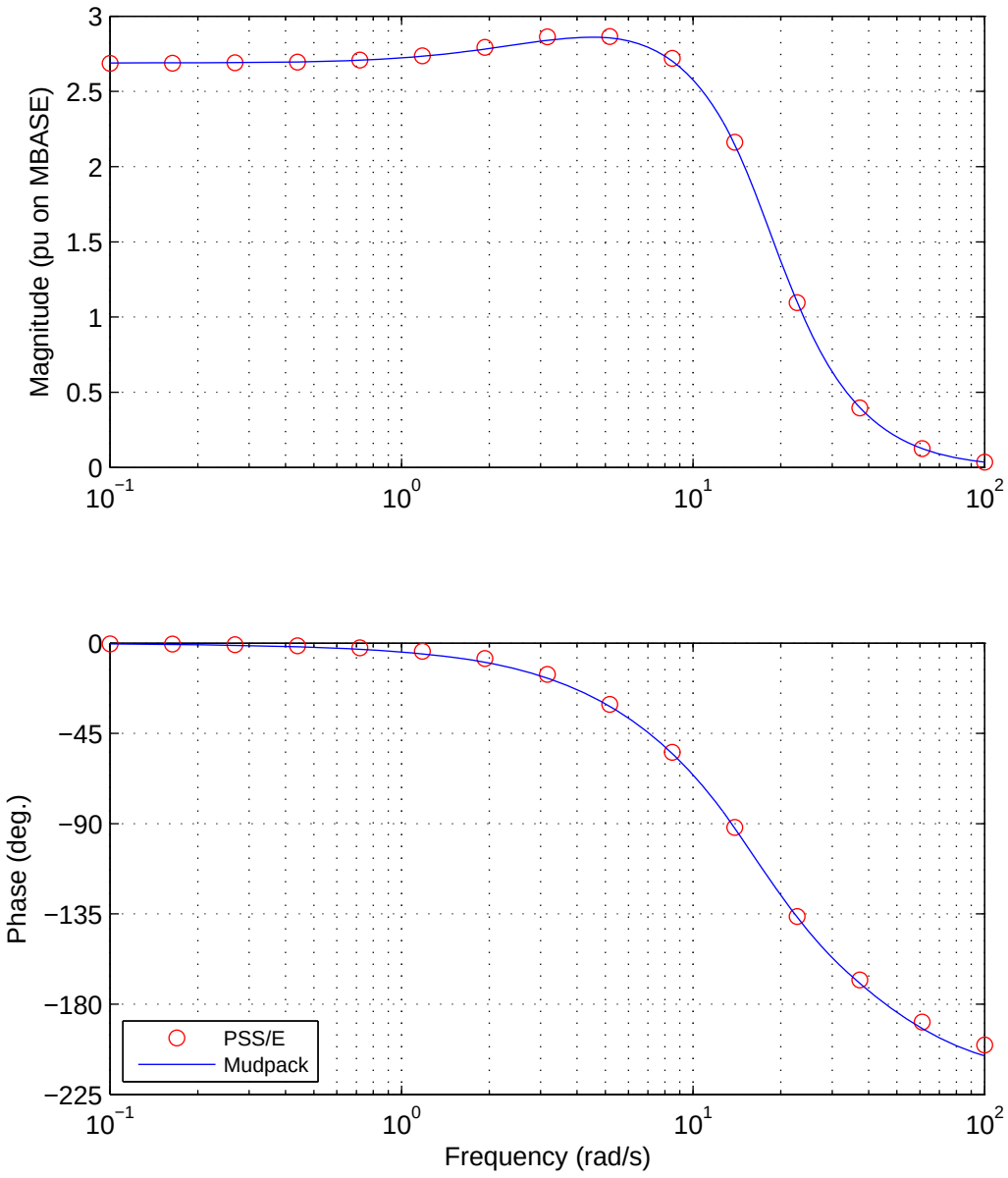

Figure 52 As for Figure 48 but for generator MPS_2.

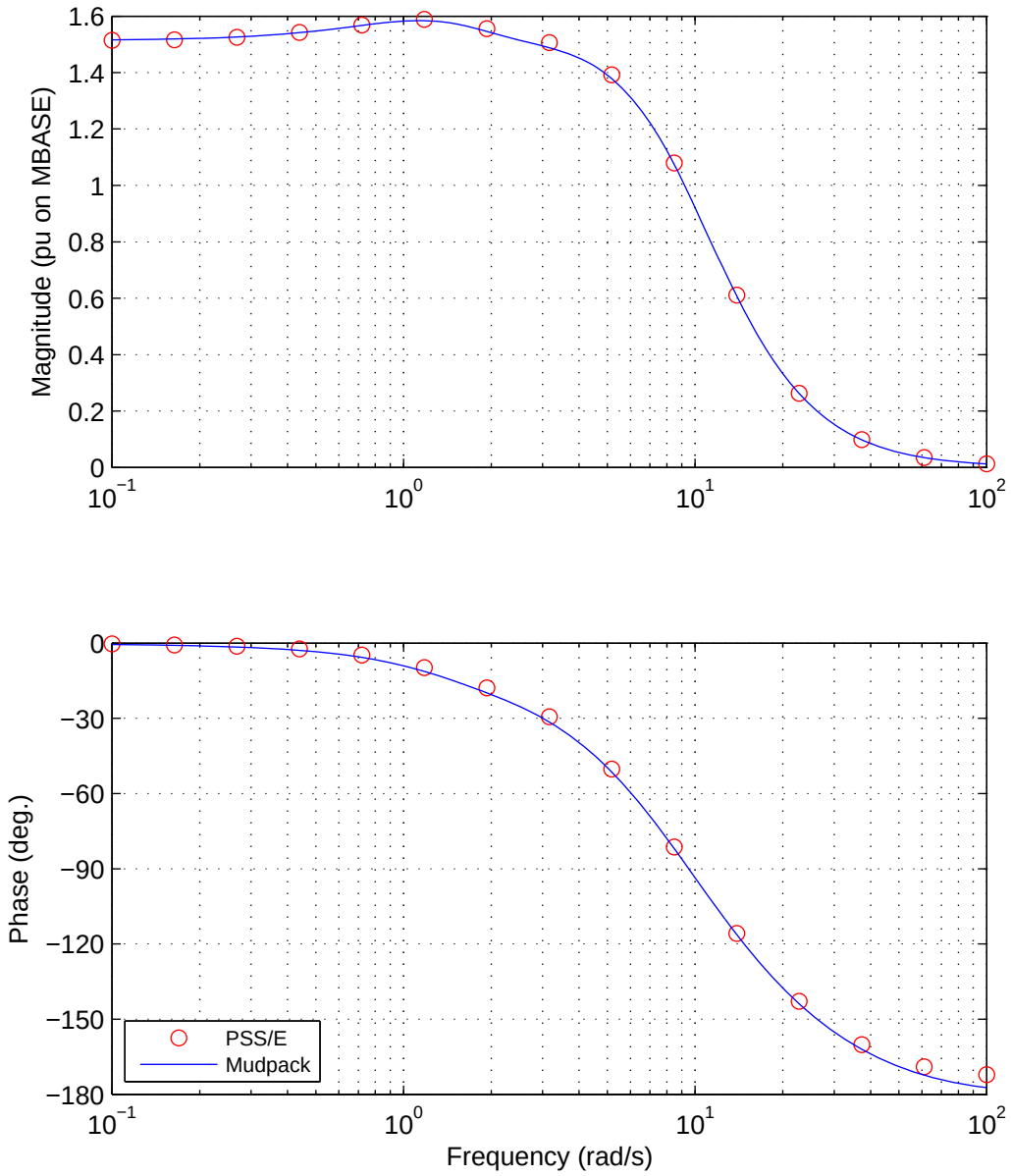

Figure 53 As for Figure 48 but for generator LPS_3.

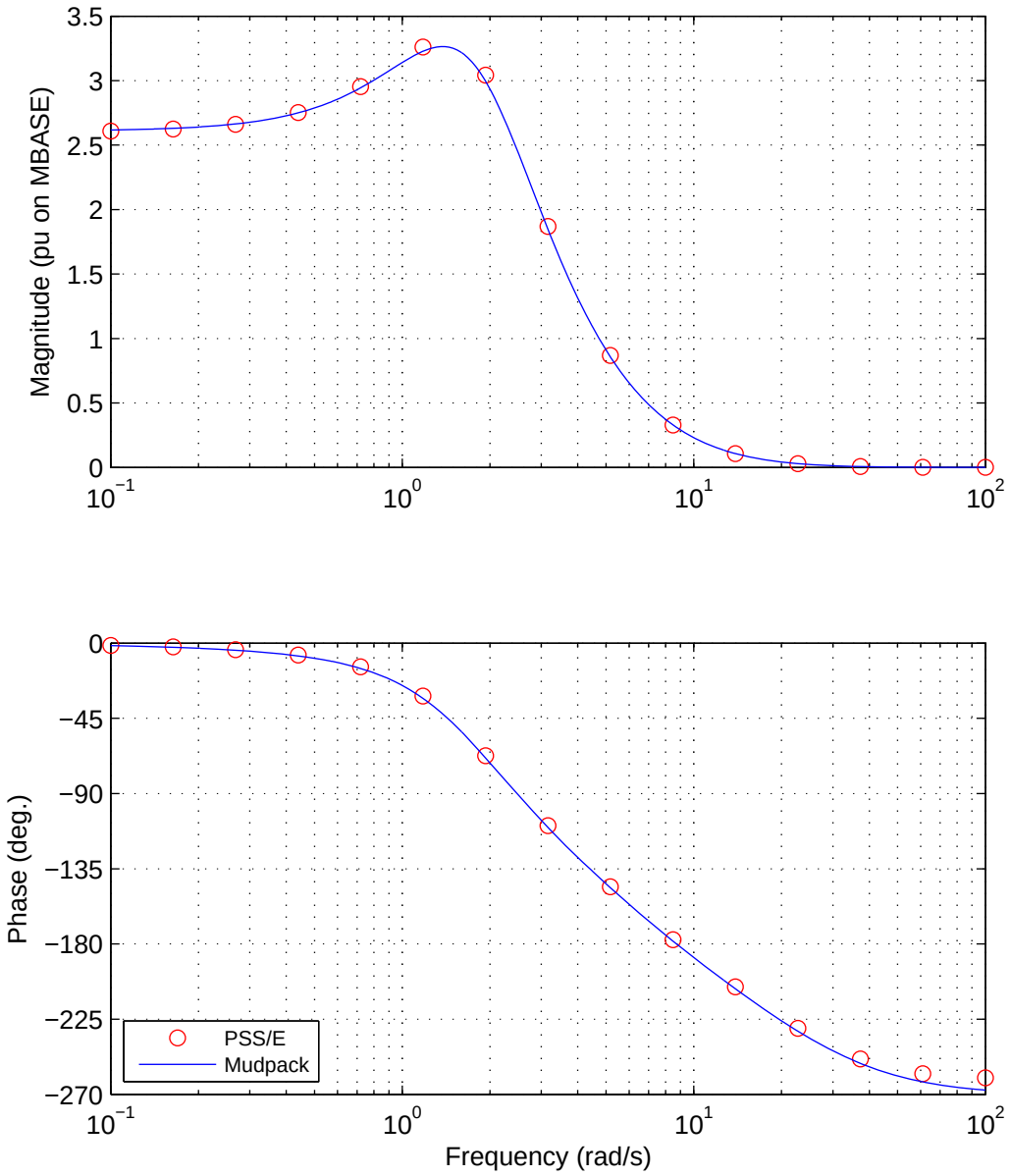

Figure 54 As for Figure 48 but for generator YPS_3.

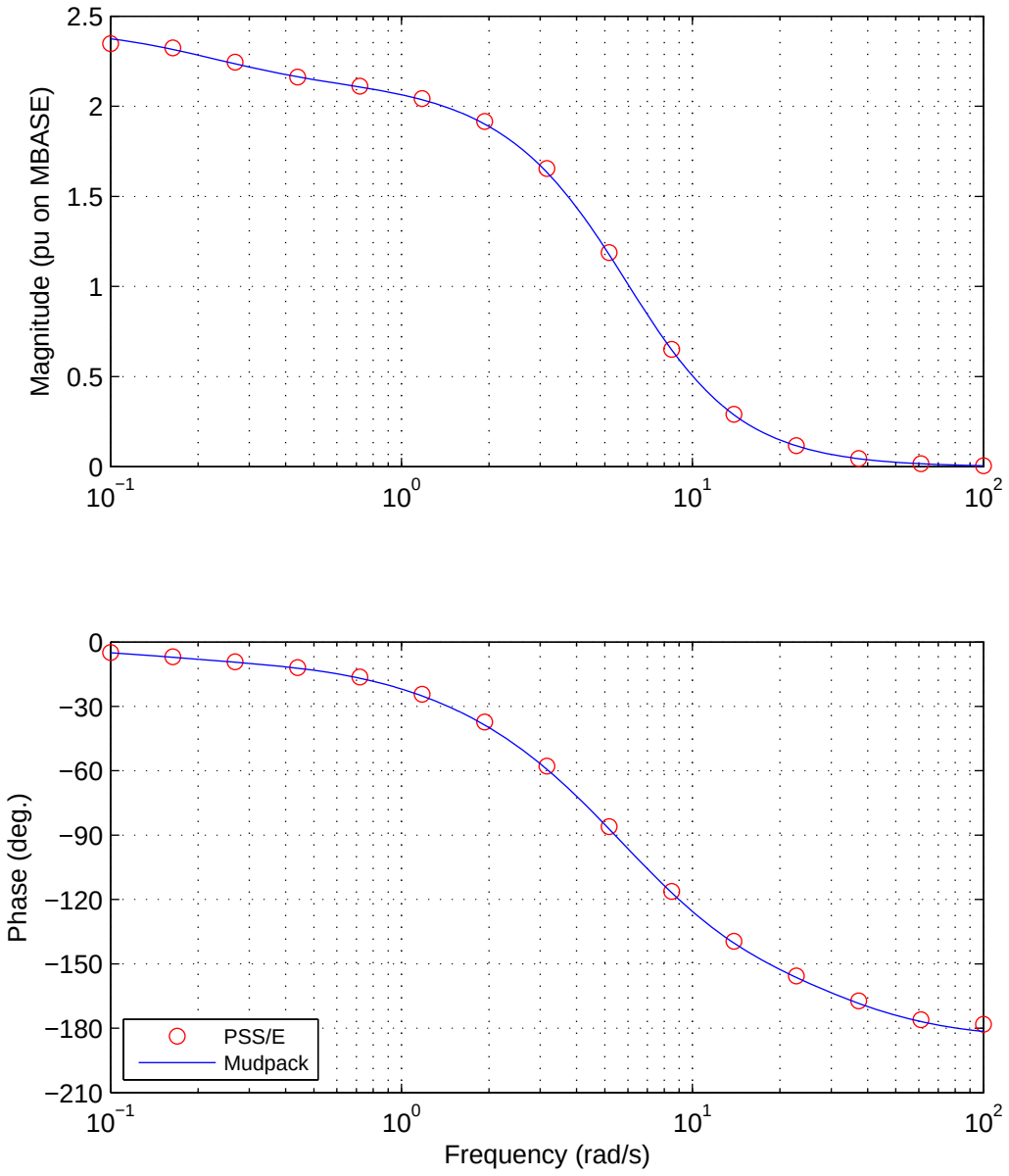

Figure 55 As for Figure 48 but for generator TPS_4.

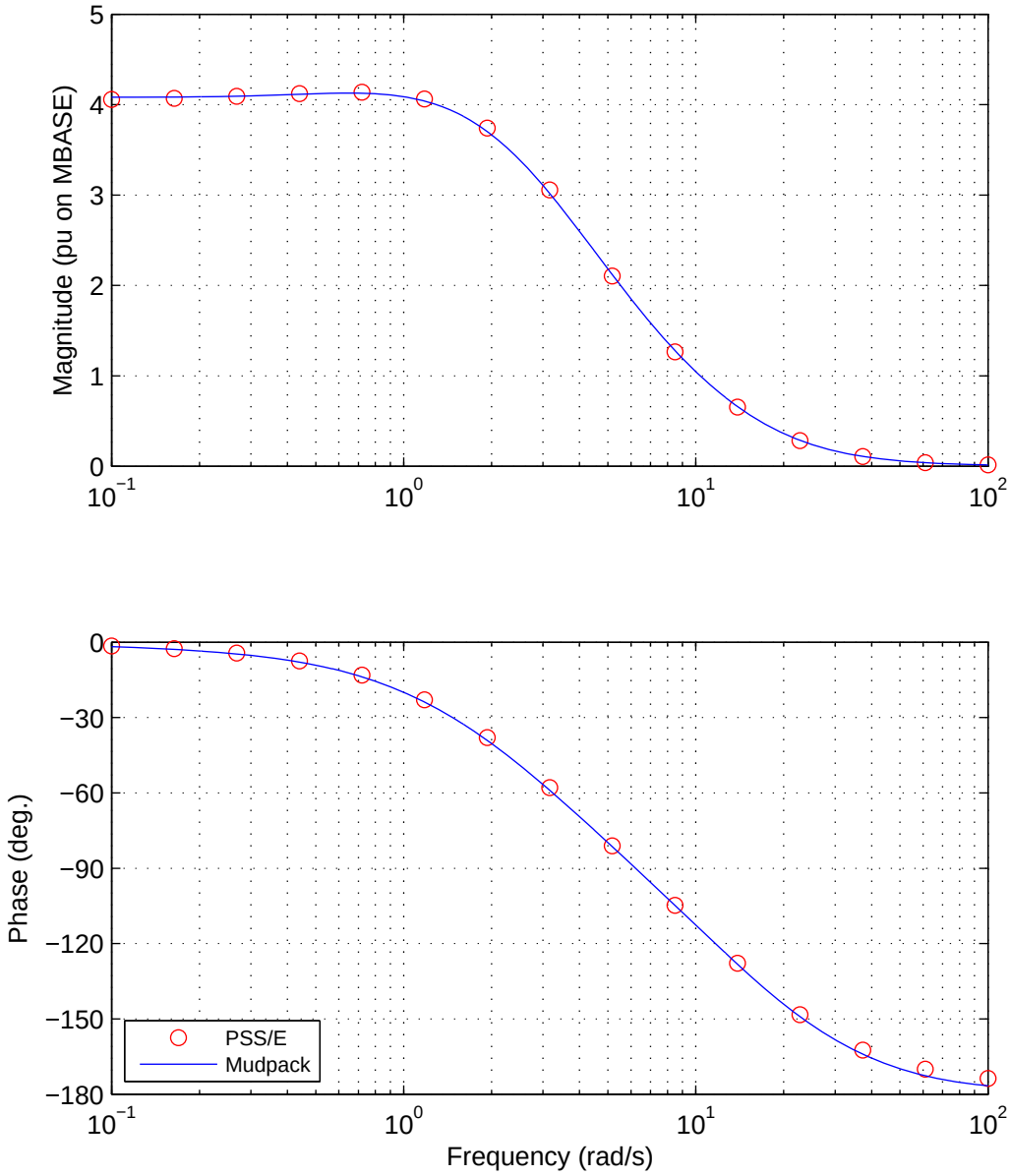

Figure 56 As for Figure 48 but for generator CPS_4.

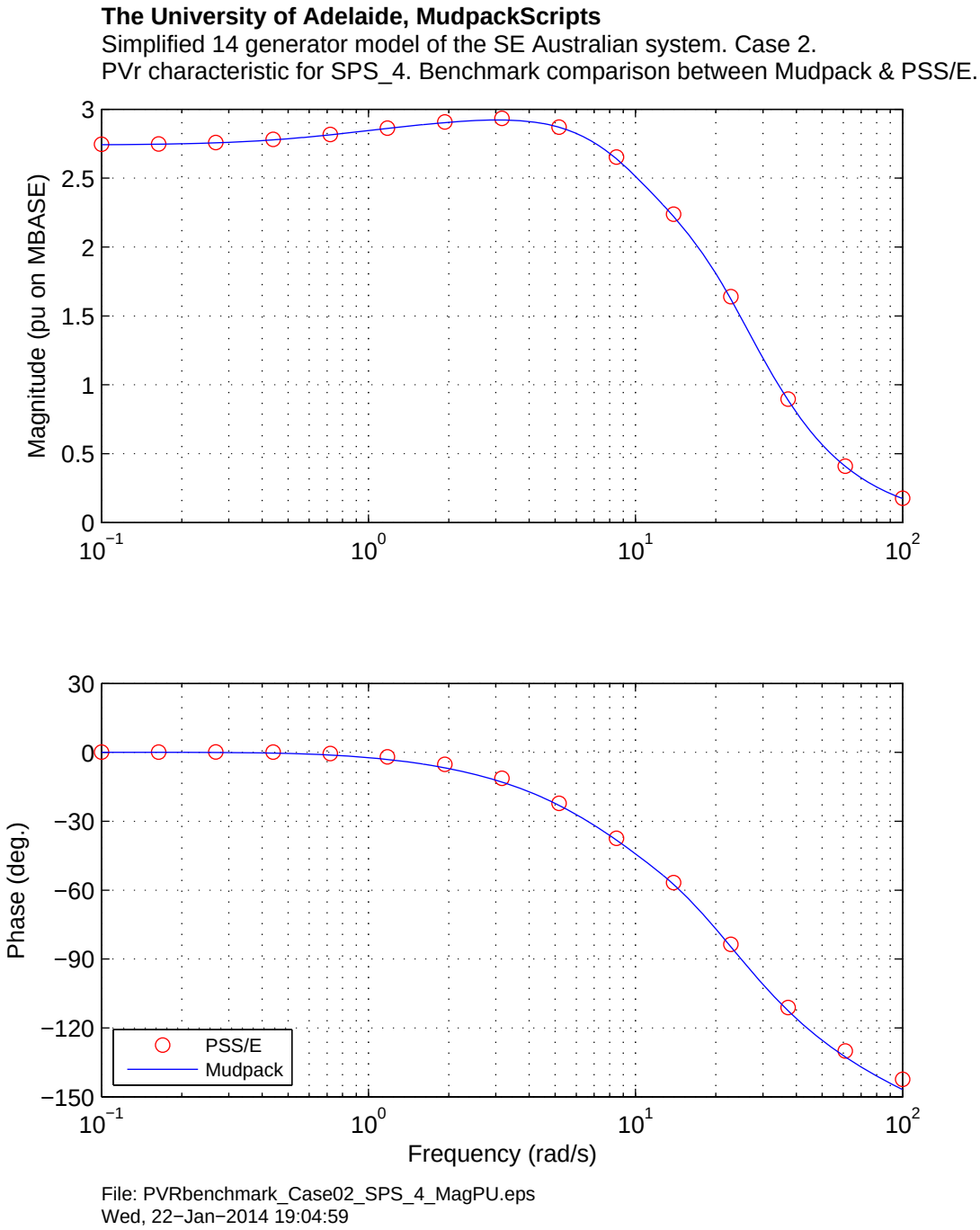

Figure 57 As for Figure 48 but for generator SPS_4.

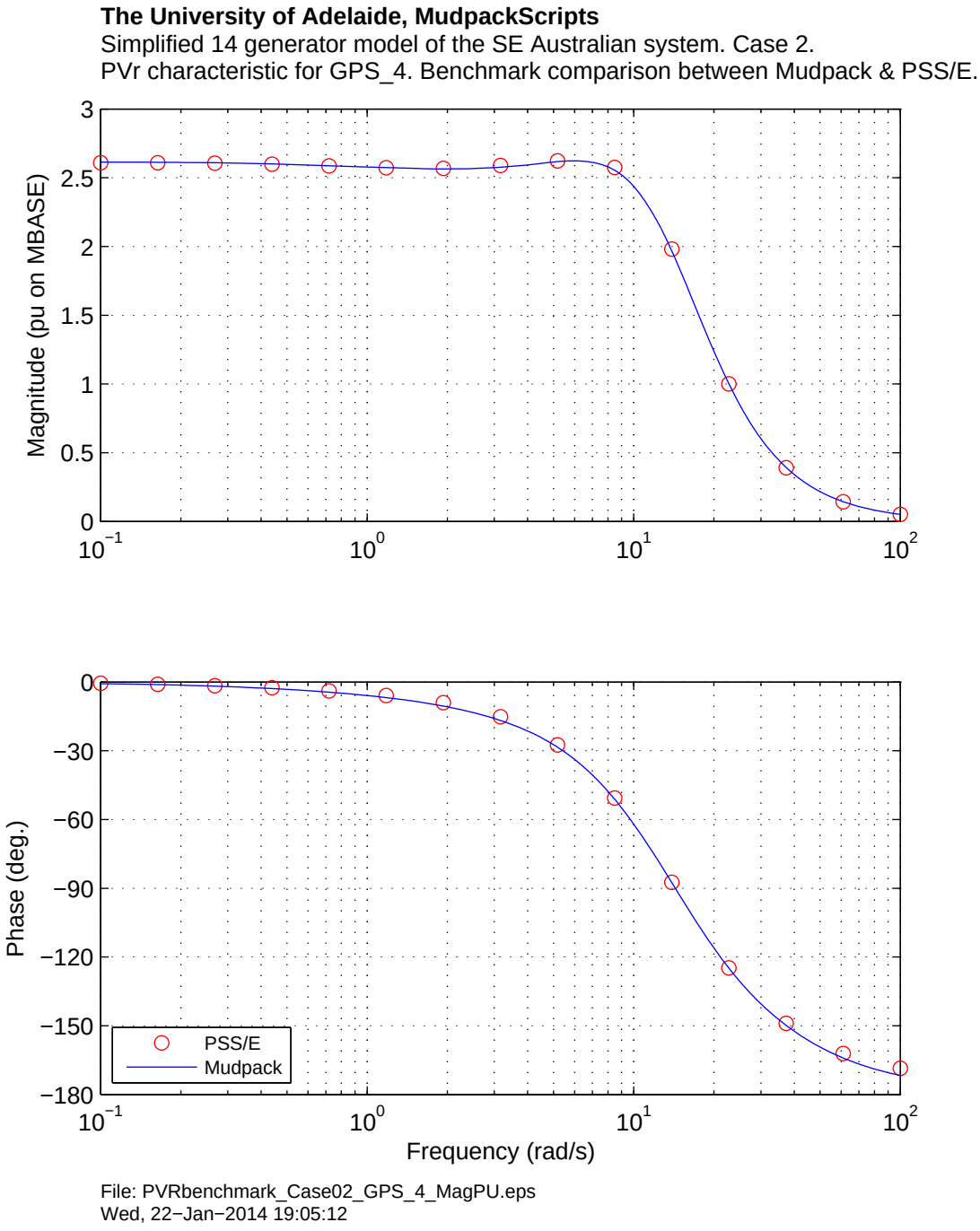

Figure 58 As for Figure 48 but for generator GPS_4.

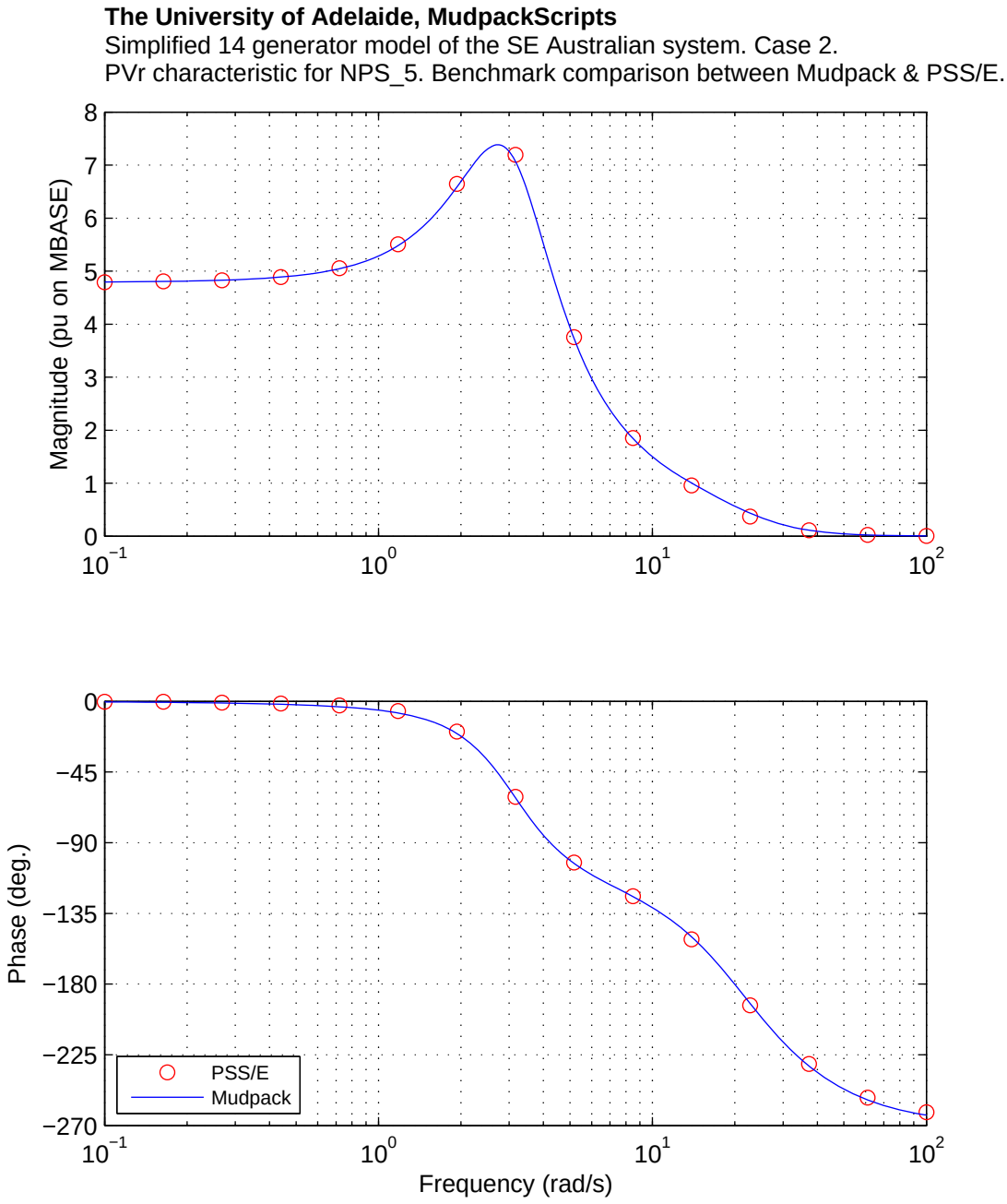

Figure 59 As for Figure 48 but for generator NPS_5.

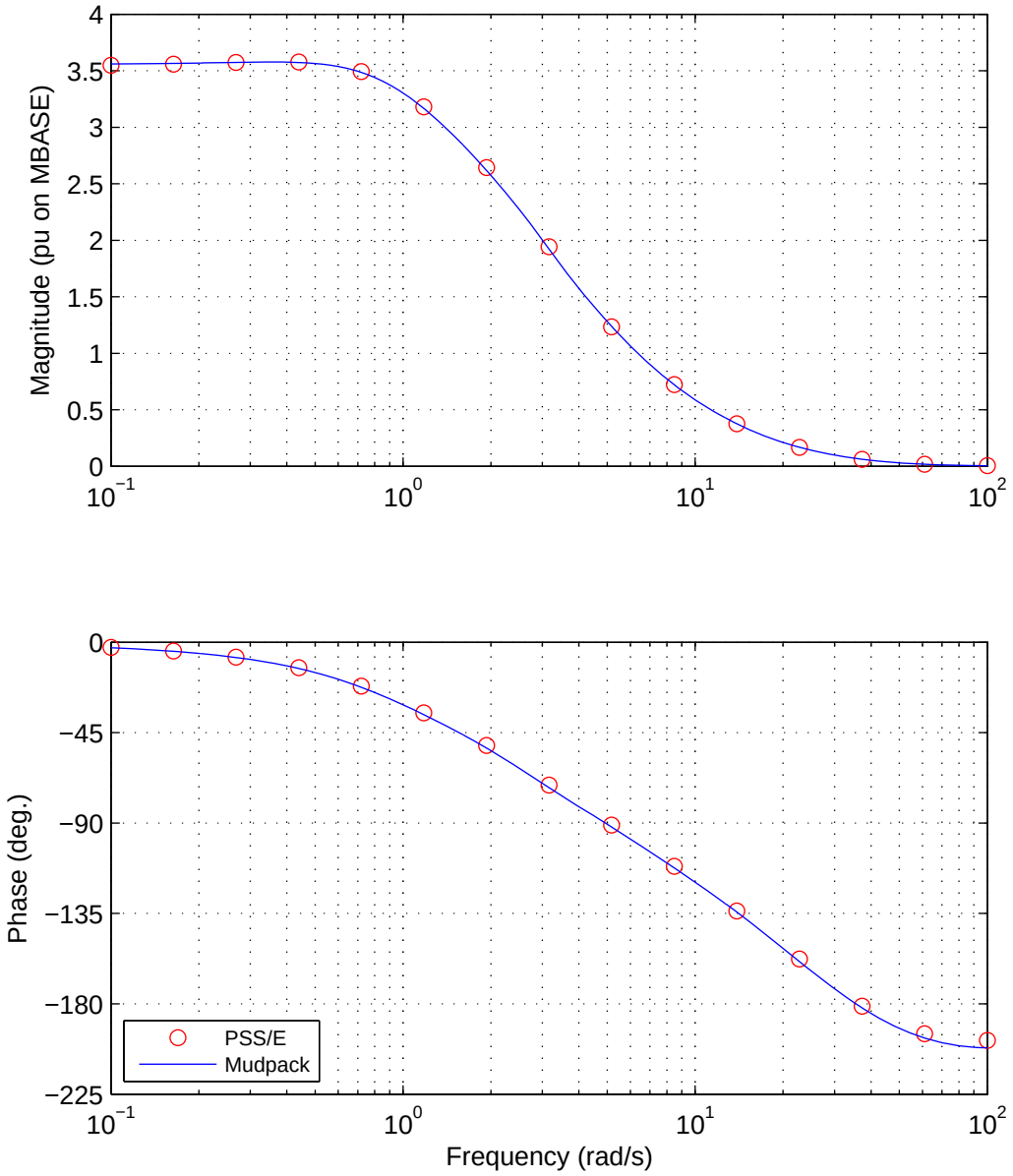

Figure 60 As for Figure 48 but for generator TPS_5.

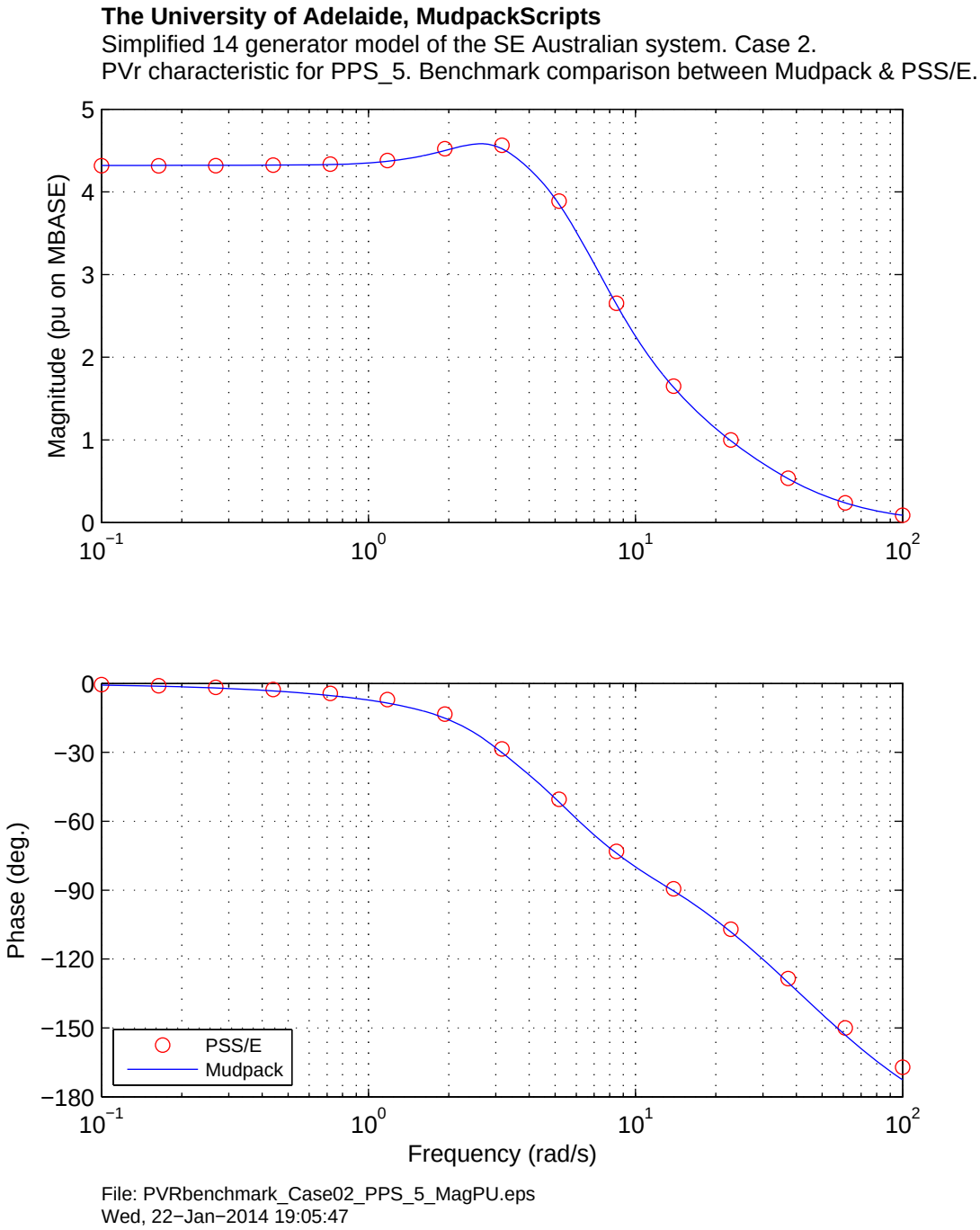

Figure 61 As for Figure 48 but for generator PPS_5.

Appendix IV PSS®/E Transient Stability Analysis

The confirmation in Appendix III of the very close agreement between the small-signal performance of the PSS®/E implementation of the simplified 14-generator model of the South East Australian system and that of the original Mudpack implementation provides a firm basis for analysing the transient stability performance of the model with the PSS®/E package. Nevertheless, it is desirable that the transient stability results presented in the following are independently validated in another transient-stability analysis package.

The transient stability studies conducted in this report are with the PSSs in-service with their design damping gains of De = 20.0 pu on the generator MVA base.

All PSS®/E studies are conducted including the frequency dependence of the network parameters (i.e. with NETFRQ = 1).

IV.1 Representation of faults in PSS®/E studies

IV.1.1 Type of fault

As mentioned earlier, in the Australian National Electricity Rules (NER) [18], a three-phase to ground fault is not generally considered to be a credible transmission system contingency event for lines operating at or above 220 kV. Rather, solid two-phase to ground faults are normally considered to be the most severe credible type of transmission system fault.

Thus, in accordance with the above practice, when assessing the transient-stability performance of the 14-generator model the response to solid two-phase to ground faults are considered.

As described in Appendix II.4 a two-phase to ground fault at node 'F' is represented by connecting an equivalent fault admittance $Y_{fe} = Y_0 + Y_2$ to node 'F' in the detailed positive-phase sequence representation of the system. The equivalent fault admittance represents the combined effect of the zero- and negative-phase sequence networks as seen from the fault location.

The equivalent fault admittances for two-phase to ground faults at each high-voltage (>= 275 kV) node in the system are listed in Table 31 for each of the six study scenarios.

IV.1.2 Fault clearance times

For faults at 275 and 330 kV nodes the fault clearance time (ΔT_c) is 100 ms; for 500 kV faults the clearance time is 80 ms. These clearance times are in accord with the primary protection clearance times specified in Clause S5.1a.8 (Fault clearance times) of the NER [18].

IV.1.3 Fault clearance

Two types of fault clearance are analysed: (i) the fault is cleared by disconnecting the equivalent fault admittance after the elapse of the applicable fault clearance time; (ii) the fault is cleared, after the elapse of the applicable fault clearance time, by simultaneously disconnecting both the equivalent fault admittance and the transmission element (line or transformer) on which the fault is deemed to have occurred.

As mentioned earlier, since the model does not include turbine/governor models events involving the disconnection of generators or loads are not and should not be considered.

IV.2 Two-phase to ground faults on the high-voltage terminals of the generator step-up transformers.

Referring to Figure 62 a two-phase to ground fault at node ‘h’ is analysed.

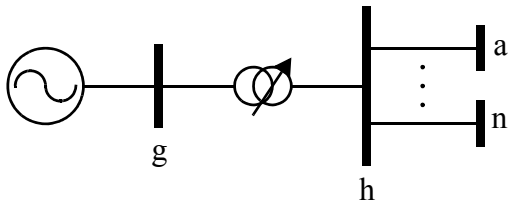

Figure 62 Network for describing faults applied to the high-voltage terminals of generator step-up transformers.

In the first study the application of the fault is represented by connecting the applicable equivalent fault admittance to ‘h’ at time T_f = 0.5 s. The fault is then simply cleared at time $T_c = T_f + \Delta T_c$ where ΔT_c is the fault clearance time in Appendix IV.1.2.

In the second study it is assumed that the fault is applied immediately adjacent to bus ‘h’ on the lowest-impedance circuit between nodes ‘h’ and ‘a’. It is cleared by disconnecting both the equivalent fault admittance and the faulted circuit at time $T_c = T_f + \Delta T_c$.

In the third and subsequent studies, faults are successively applied to the remaining circuits connected to ‘h’ with the exception of the generator step-up transformer between nodes ‘g’ and ‘h’.

For each of these faults the responses of the following variables associated with the generator connected to node ‘g’ are displayed: inertia-weighted rotor-angle (DEL), rotor speed perturbation (W), electrical power output (P), stator voltage (Vt), generator field voltage (Ef) and PSS output signal (Vs). Note that the inertia-weighted rotor-angles should not be relied on to provide modal information; rather divergence of this variable provides clear evidence of transient instability.

Inspection of the Ef and Vs responses reveals if there is prolonged limiting of the exciter and/or PSS outputs following the fault.

Such studies have been conducted for each of the fourteen generators in each of the six study cases. The results for Case 2 are displayed for each of the fourteen generators in Figures 63 to 76. The time-series data for these results and for the other five cases are provided in the Data-Package (i.e. a total of 6 x 49 = 294 studies).

It is found that the system is transiently stable for each of the faults analysed.

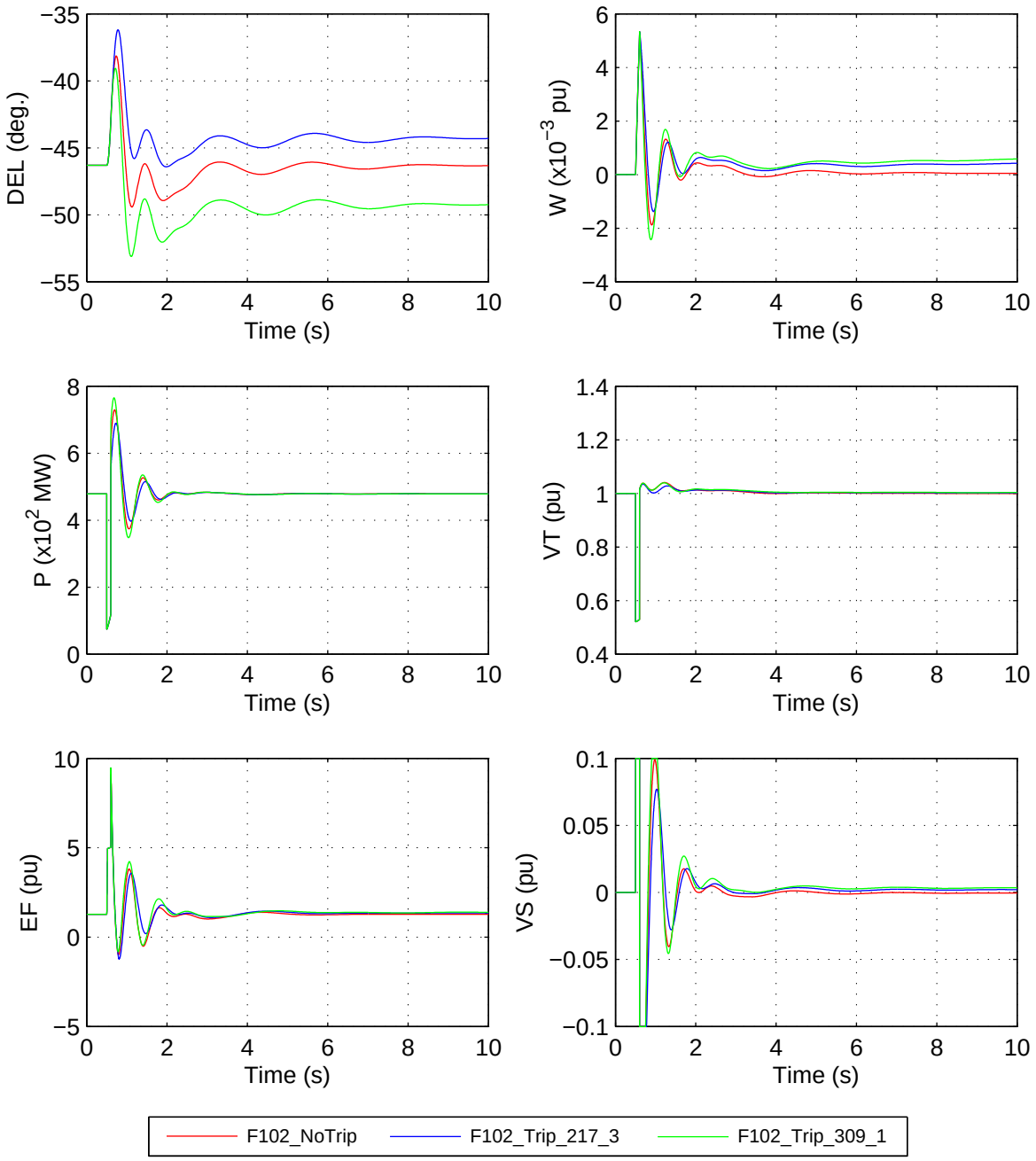

Figure 63 Case 2. Two-phase to ground fault applied to the 330 kV bus 102 on the high-voltage side of the HPS_1 generator step-up transformer at t = 0.5s. The fault is cleared 100 ms later. The responses to the following clearance scenarios are displayed: (i) fault cleared without switching any network elements; (ii) trip circuit 3 between nodes 102 and 217; (iii) trip circuit 1 between nodes 102 and 309. The responses of the following HPS_1 generator variables are displayed: inertia weighted rotor angle (DEL); rotor-speed perturbation (W); electrical power output (P); stator-voltage (Vt); generator field voltage (Ef); PSS output signal (Vs).

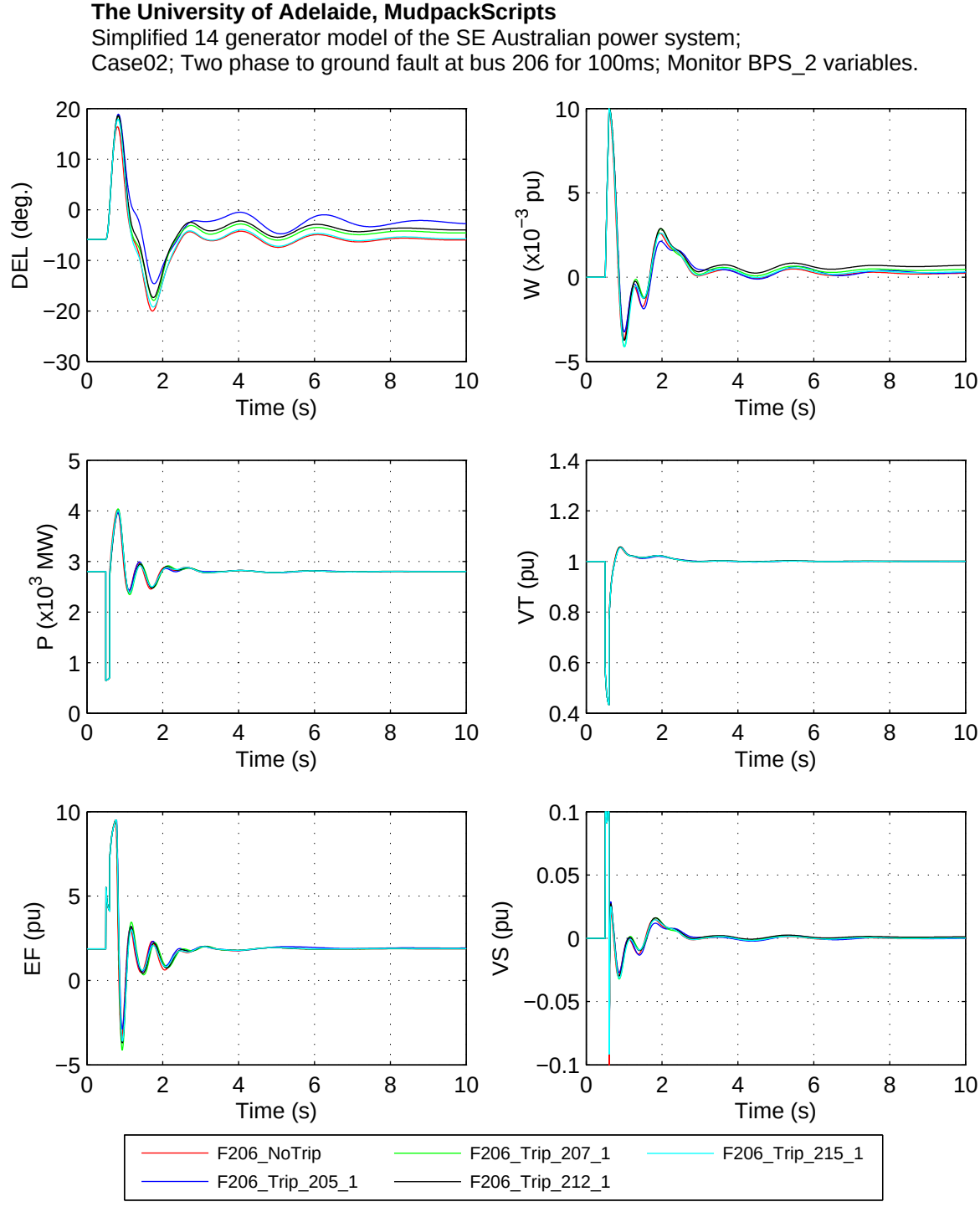

Figure 64 Case 2. Similar to Figure 63 but for generator BPS_2 and a fault applied to bus 206.

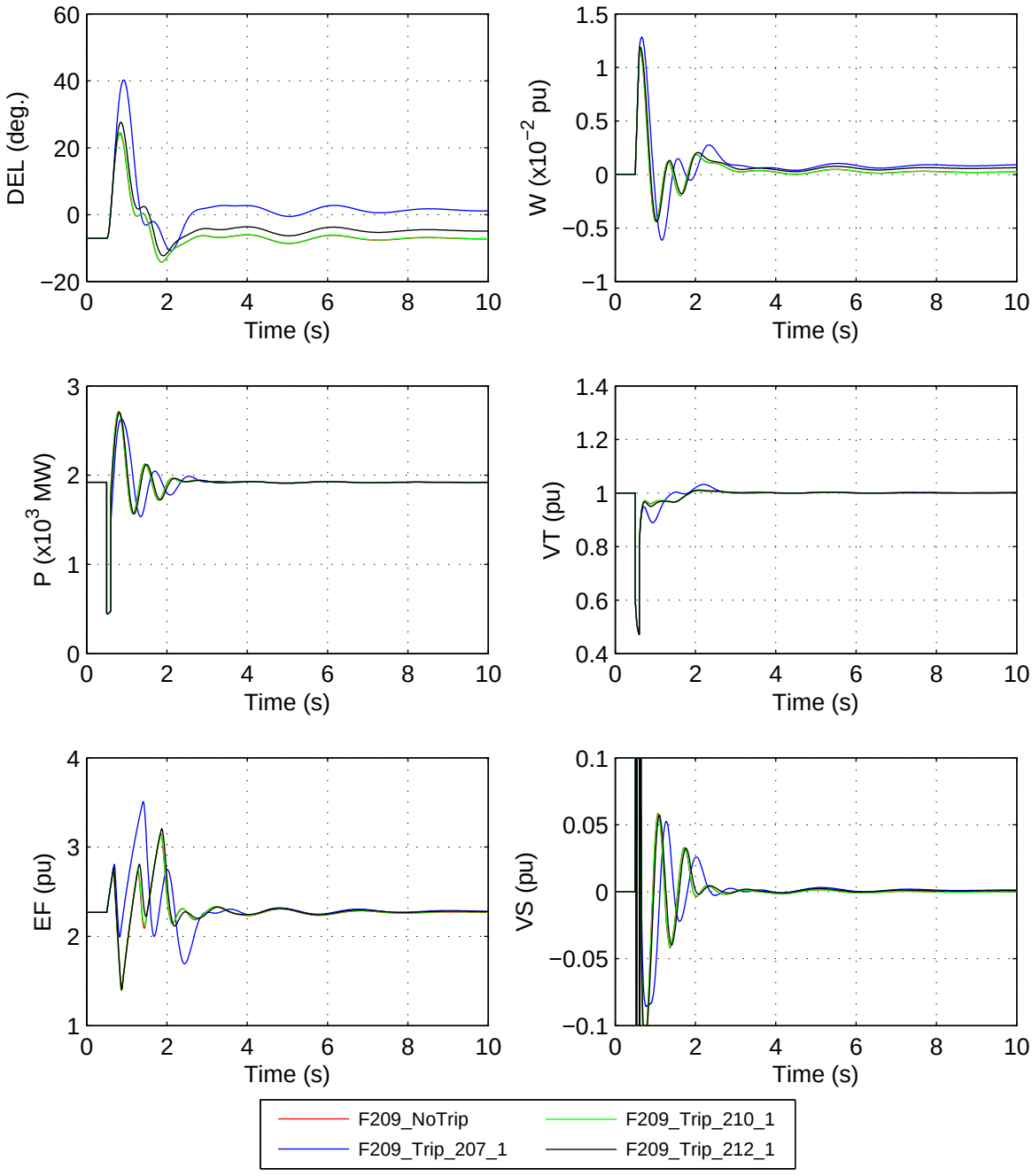

Figure 65 Case 2. Similar to Figure 63 but for generator EPS_2 and a fault applied to bus 209.

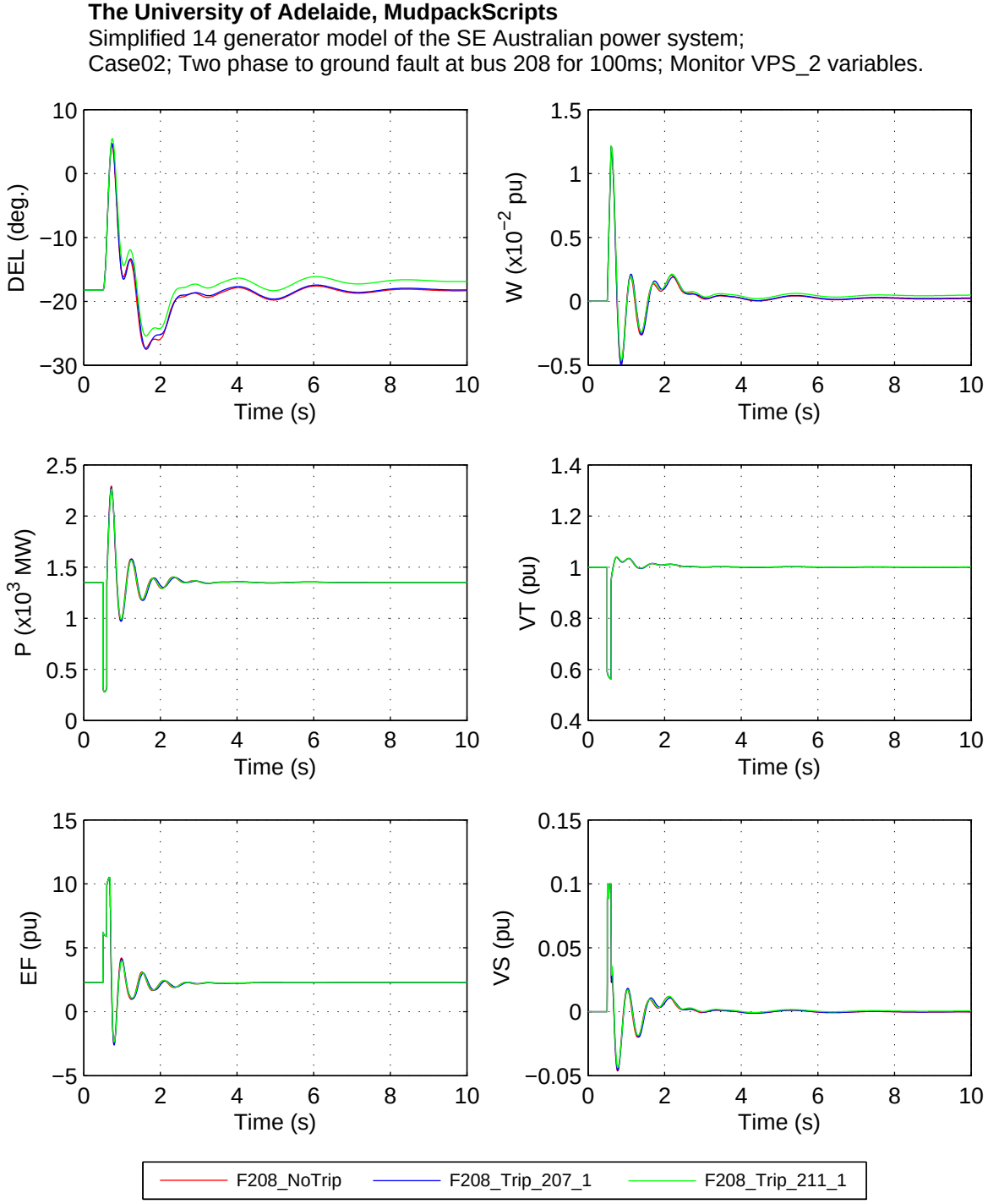

Figure 66 Case 2. Similar to Figure 63 but for generator VPS_2 and a fault applied to bus 208.

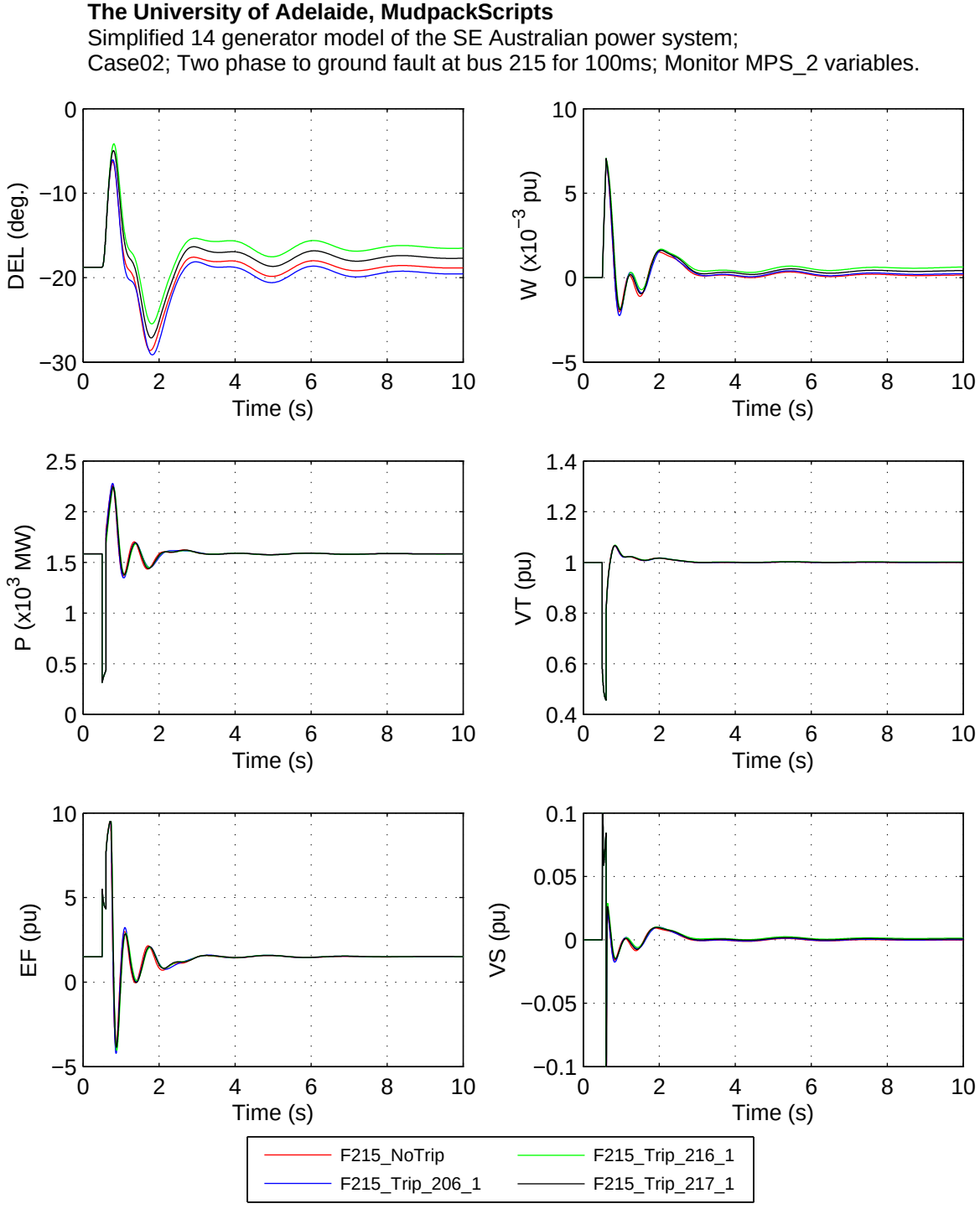

Figure 67 Case 2. Similar to Figure 63 but for generator MPS_2 and fault applied to bus 215.

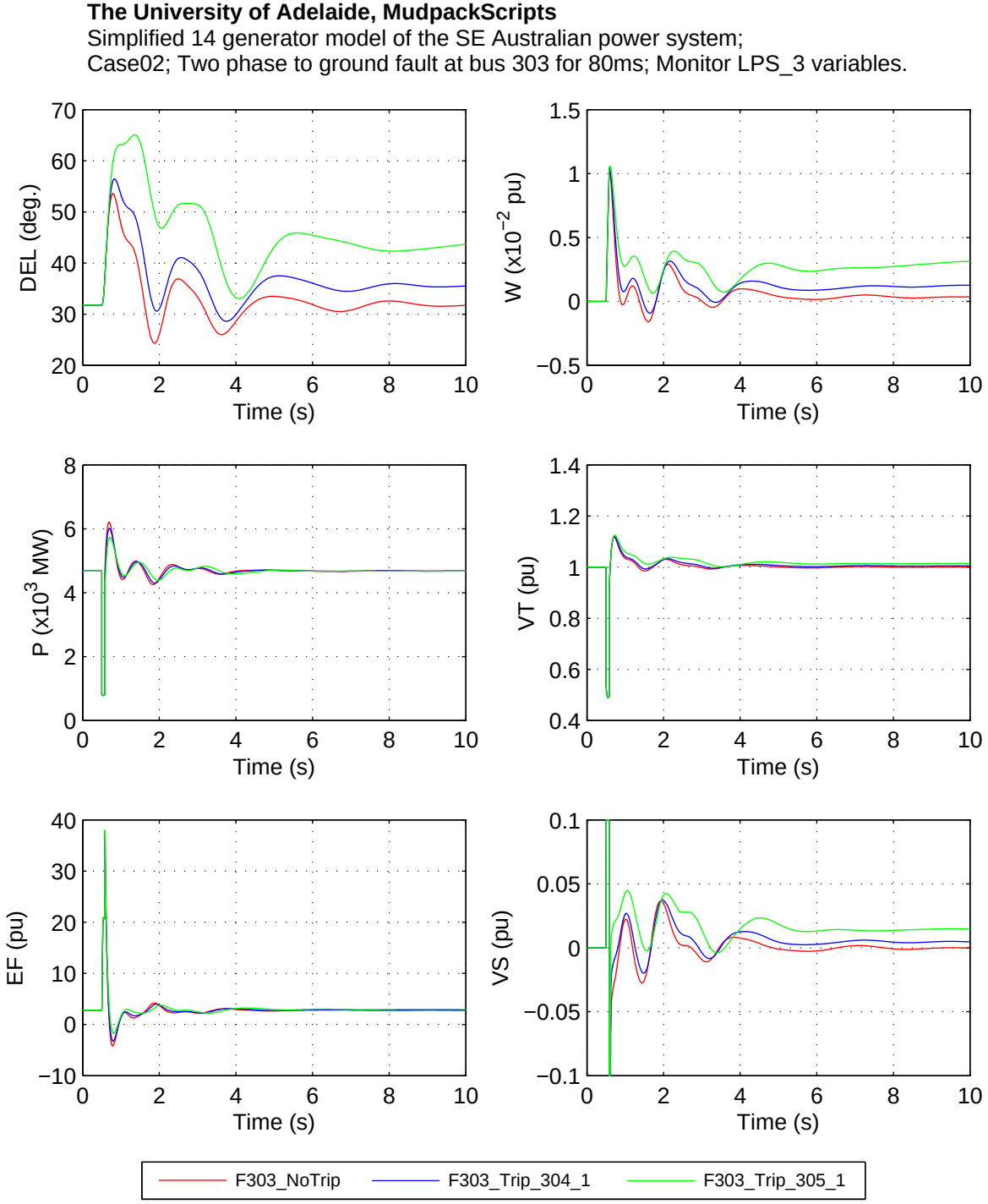

Figure 68 Case 2. Similar to Figure 63 but for generator LPS_3 and a fault applied to bus 303.

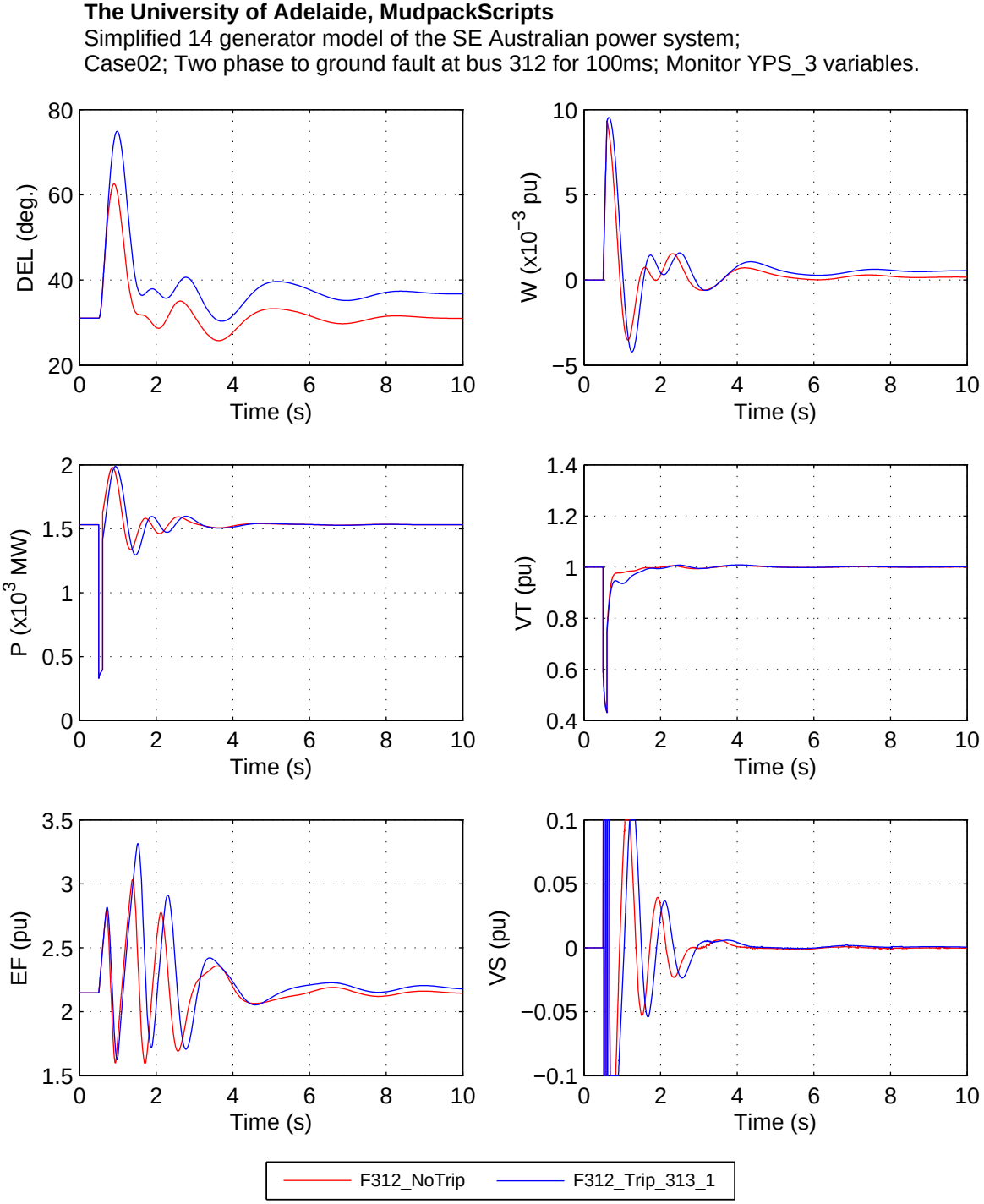

Figure 69 Case 2. Similar to Figure 63 but for generator YPS_3 and a fault applied to bus 312.

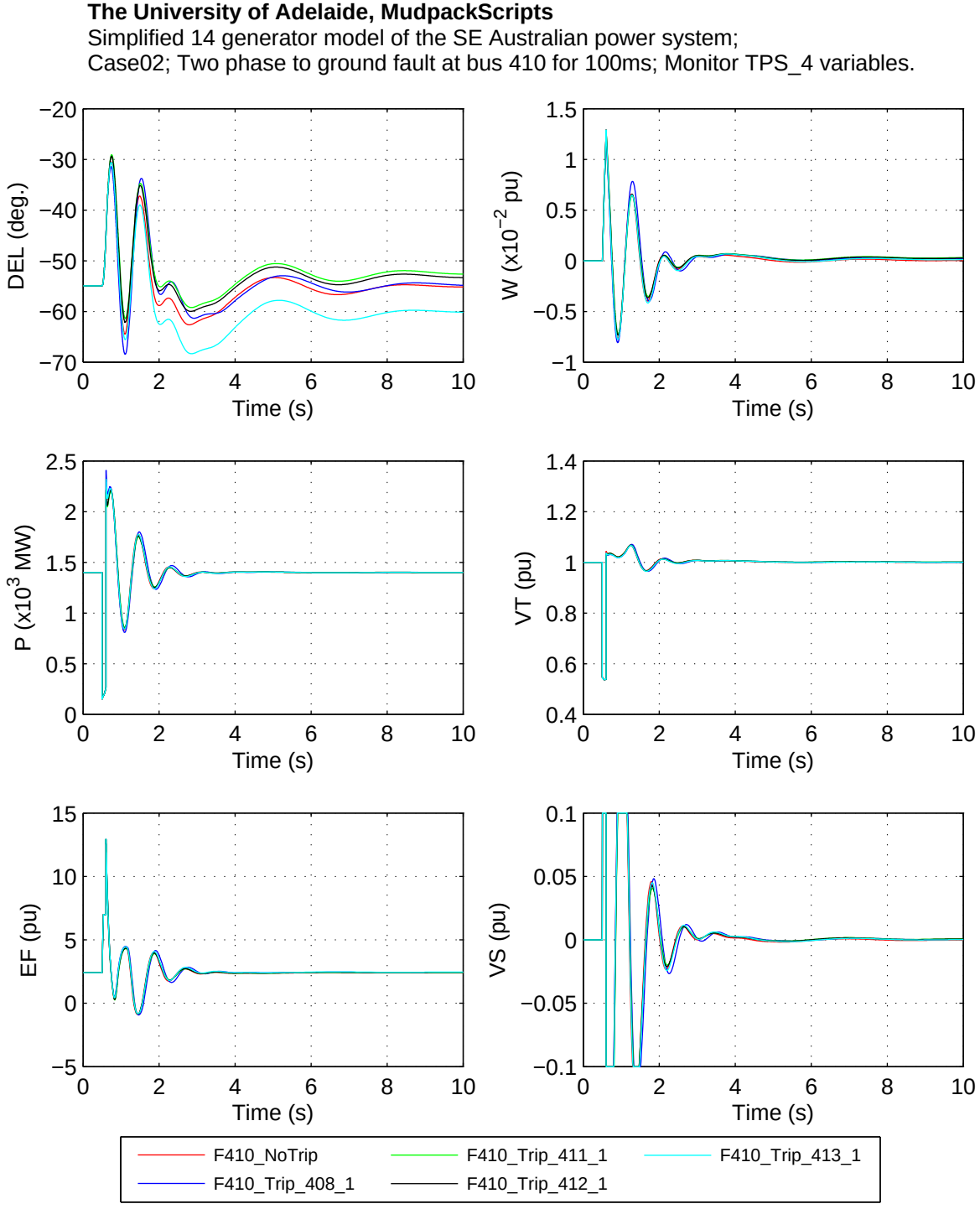

Figure 70 Case 2. Similar to Figure 63 but for generator TPS_4 and a fault applied to bus 410.

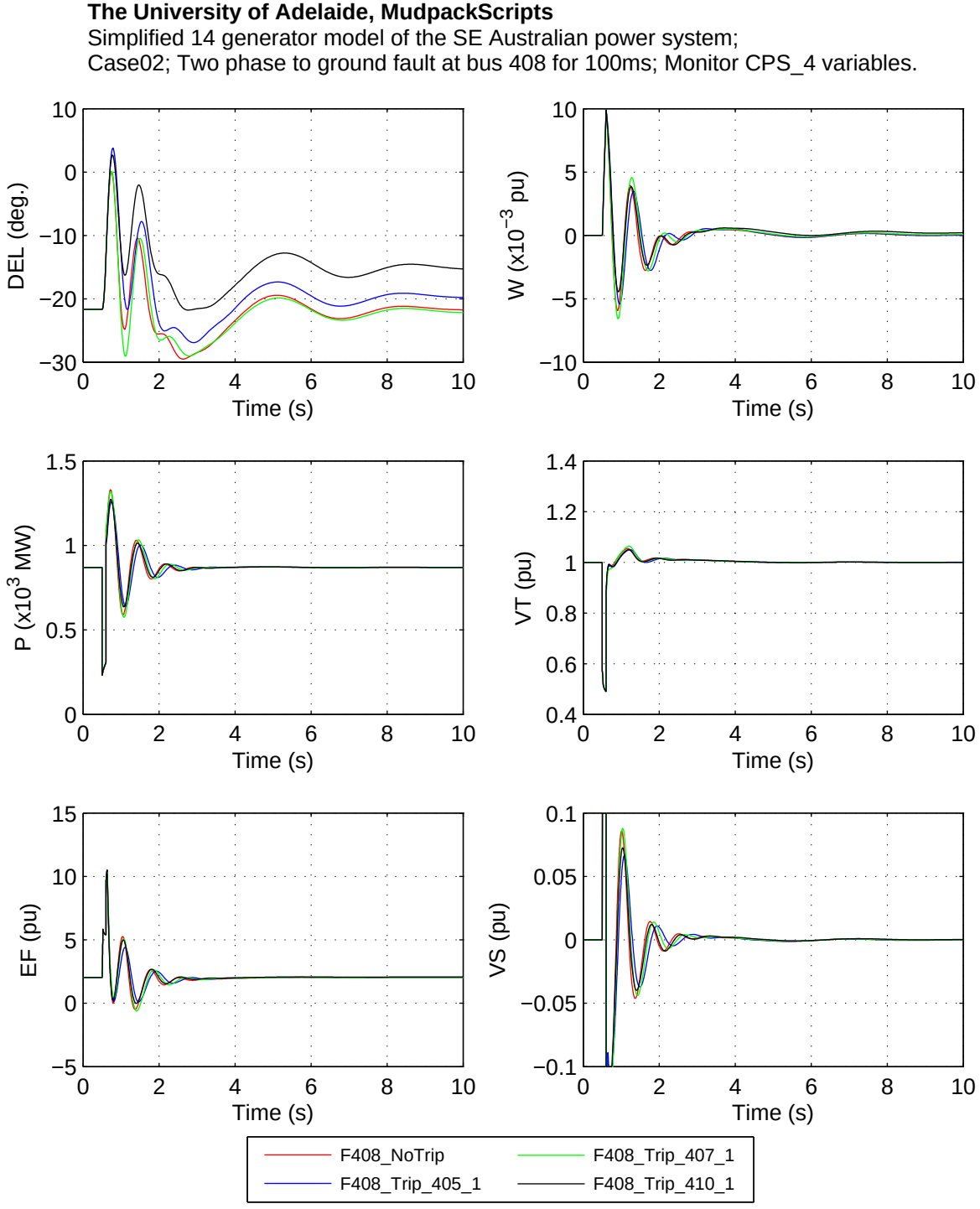

Figure 71 Case 2. Similar to Figure 63 but for generator CPS_4 and a fault applied to bus 408.

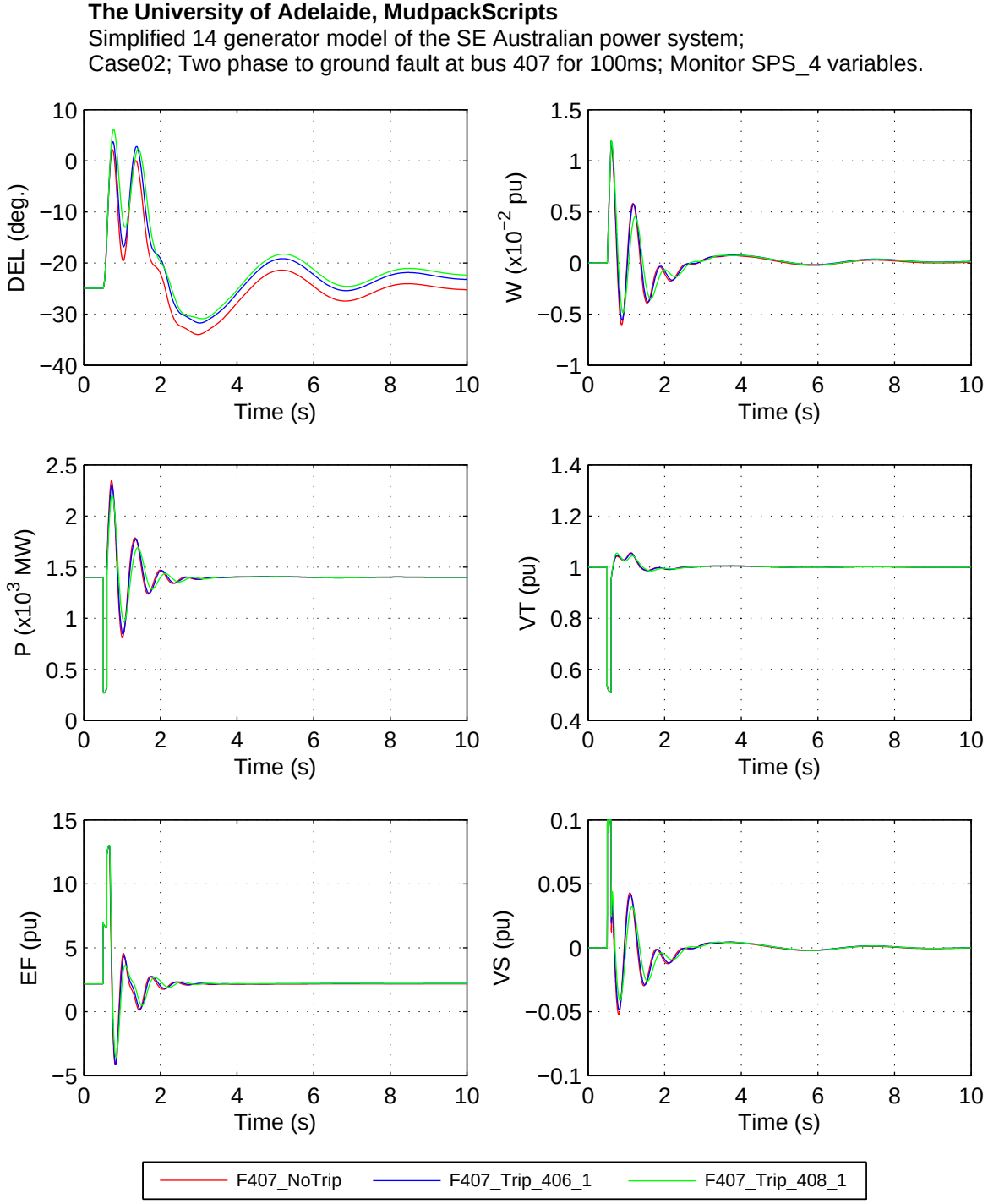

Figure 72 Case 2. Similar to Figure 63 but for generator SPS_4 and a fault applied to bus 407.

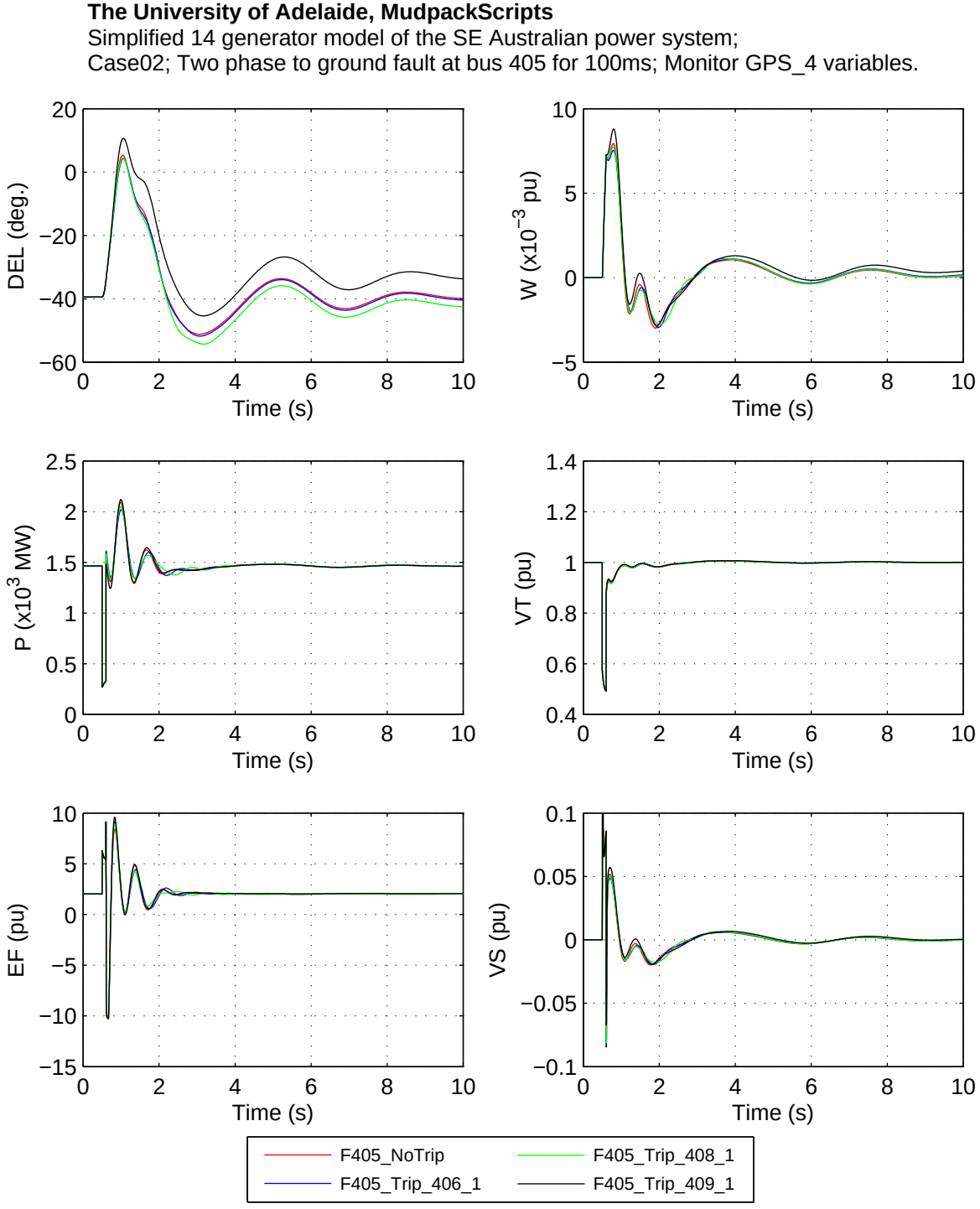

Figure 73 Case 2. Similar to Figure 63 but for generator GPS_4 and a fault applied to bus 405.

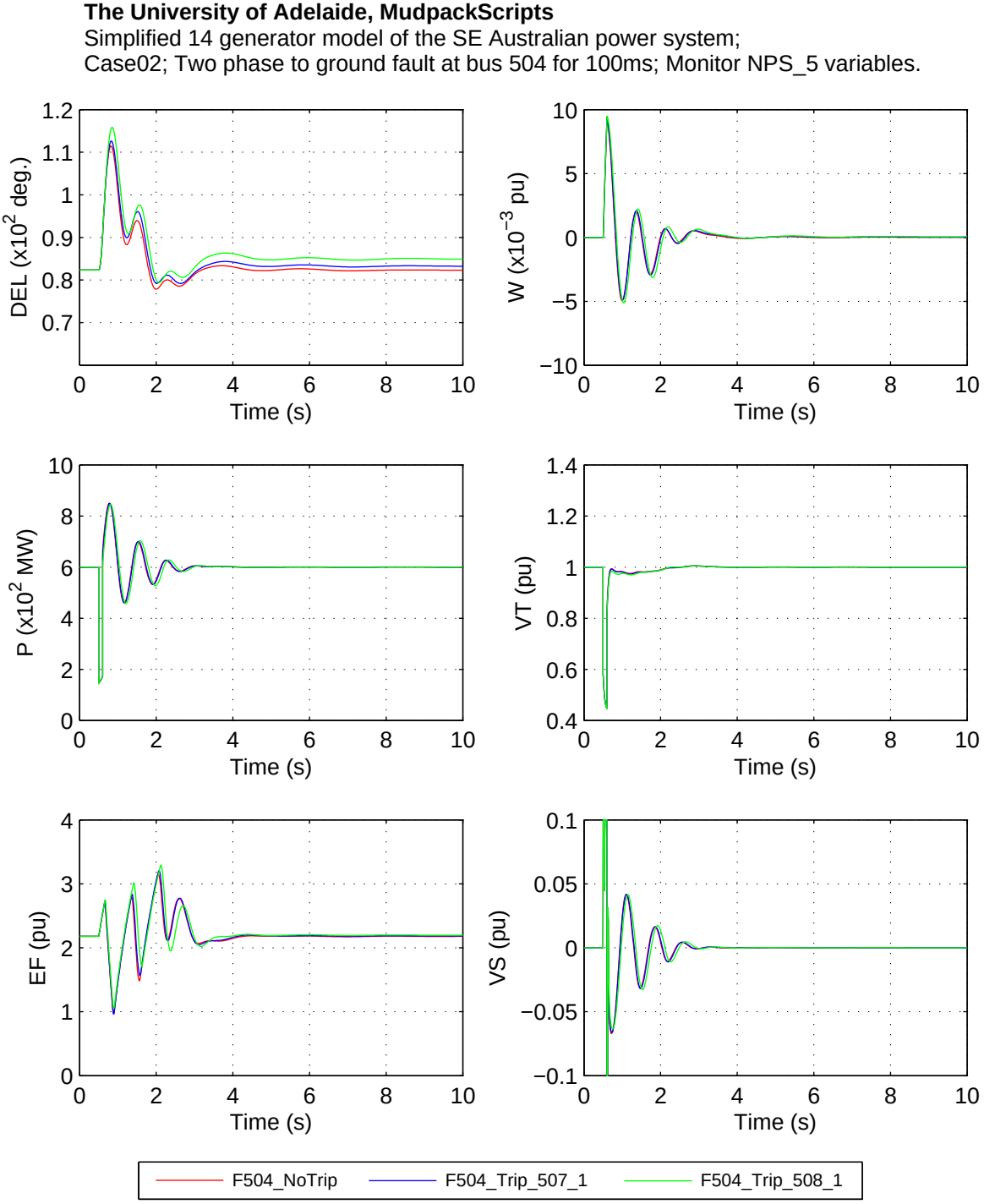

Figure 74 Case 2. Similar to Figure 63 but for generator NPS_5 and a fault applied to bus 504.

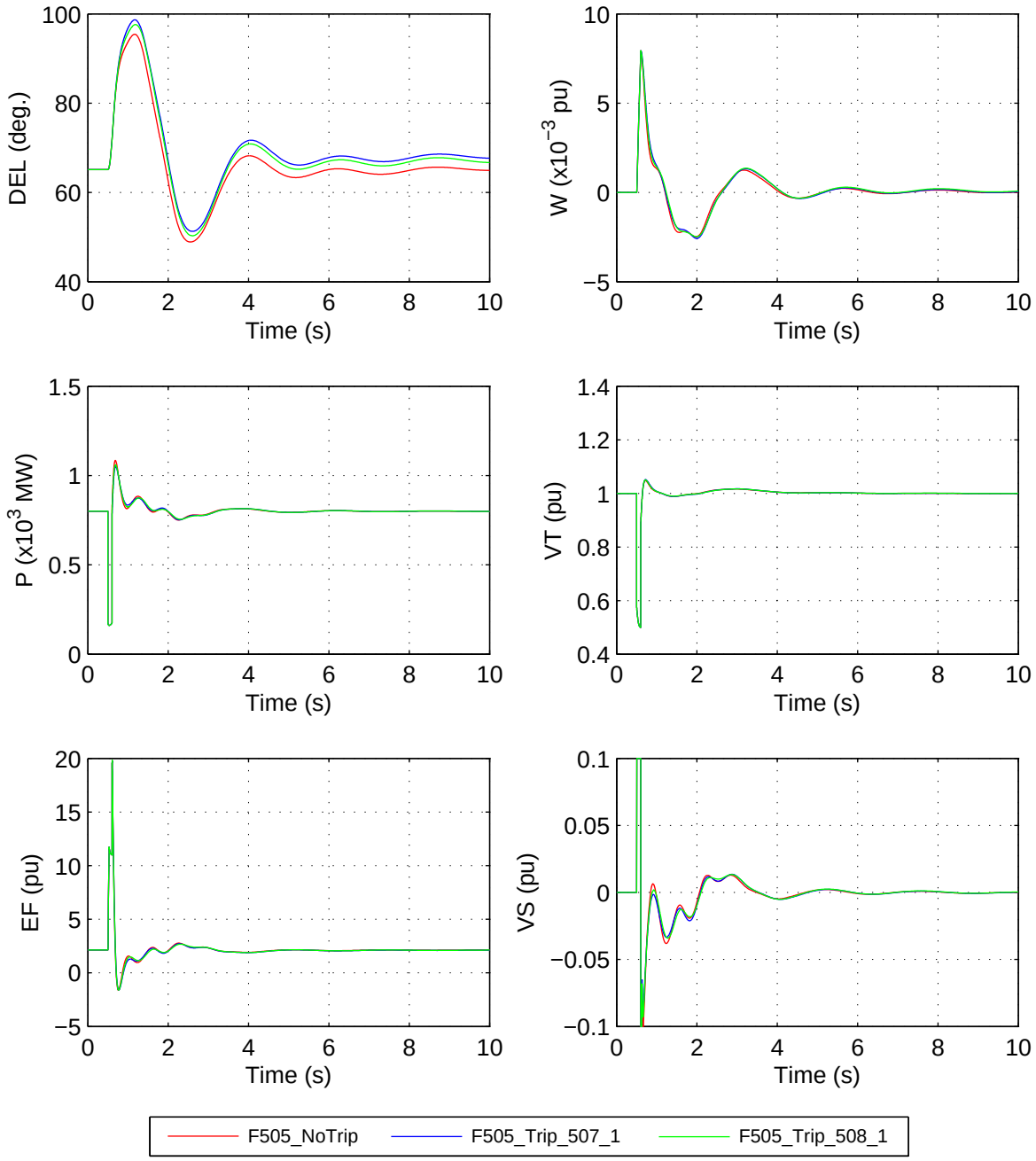

Figure 75 Case 2. Similar to Figure 63 but for generator TPS_5 and a fault applied to bus 505.

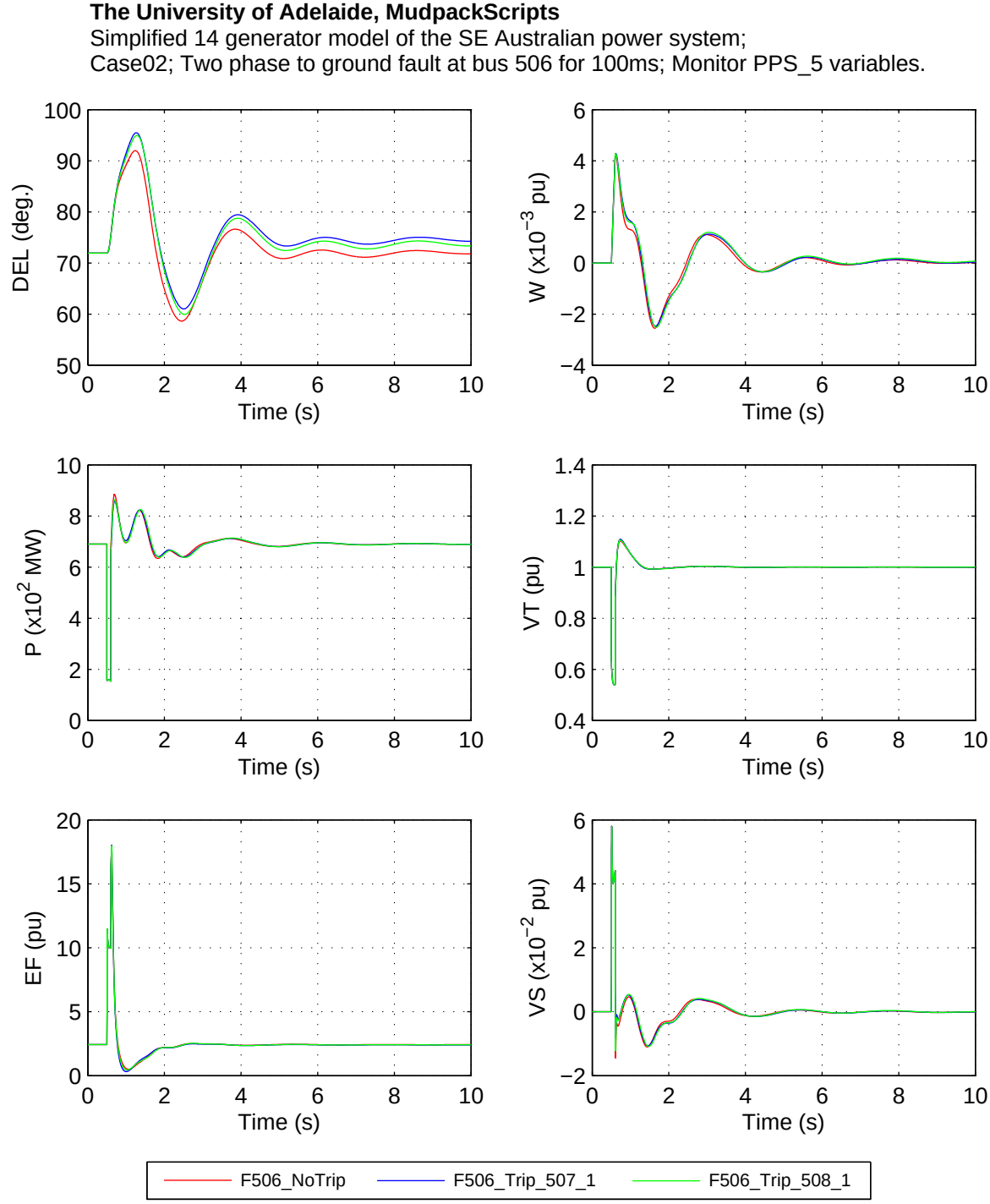

Figure 76 Case 2. Similar to Figure 63 but for generator PPS_5 and a fault applied to bus 506.

IV.3 Two-phase to ground faults at other transmission system buses

Apart from the faults applied at the high-voltage terminals of the generator step-up transformers, two-phase to ground faults are similarly analysed at the other 31 nodes in the high-voltage transmission network. The only difference is in the presentation of the results. For each fault at other transmission buses the inertia-weighted rotor-angles (DEL), rotor-speed perturbations

(W) and stator-voltages (Vt) of each of the fourteen generators are displayed. Note that the inertia-weighted rotor-angles should not be relied on to provide modal information; rather divergence of this variable provides clear evidence of transient instability. For each case, studies are conducted for a total of 115 fault scenarios – 31 are bus faults which are cleared without switching a network element; and 84 are faults in which a circuit element (transmission line or transformer) is disconnected to clear the fault.

Results are presented for the following two fault scenarios in Case 2:

1. A two-phase to ground fault applied to the 275 kV #1 circuit between buses 507 and 509 immediately adjacent to bus 507 at time t = 0.5 s. The fault is cleared 100 ms later by tripping the circuit. The generator variables are displayed in Figure 77. In addition, the terminal voltage, susceptance and reactive power outputs of all five SVCs are displayed in Figure 78. In Figure 79 the powerflow on the interconnectors from area 2 to 4 (P.LN_413_410); from area 3 to 2 (P.LN_102_217); and from area 5 to 3 (P.LN_509_315) are displayed. The system is transiently stable.
2. A two-phase to ground fault is applied to the 275 kV #1 circuit between buses 410 and 413 immediately adjacent to bus 413 at time t = 0.5 s. The fault is cleared 100 ms later by tripping the circuit. Results, in the same format as above, are displayed for this fault in Figures 80 to 82. The system is transiently stable.

It is found that the system is transiently stable for each of the 6 x 115 = 690 faults analysed.

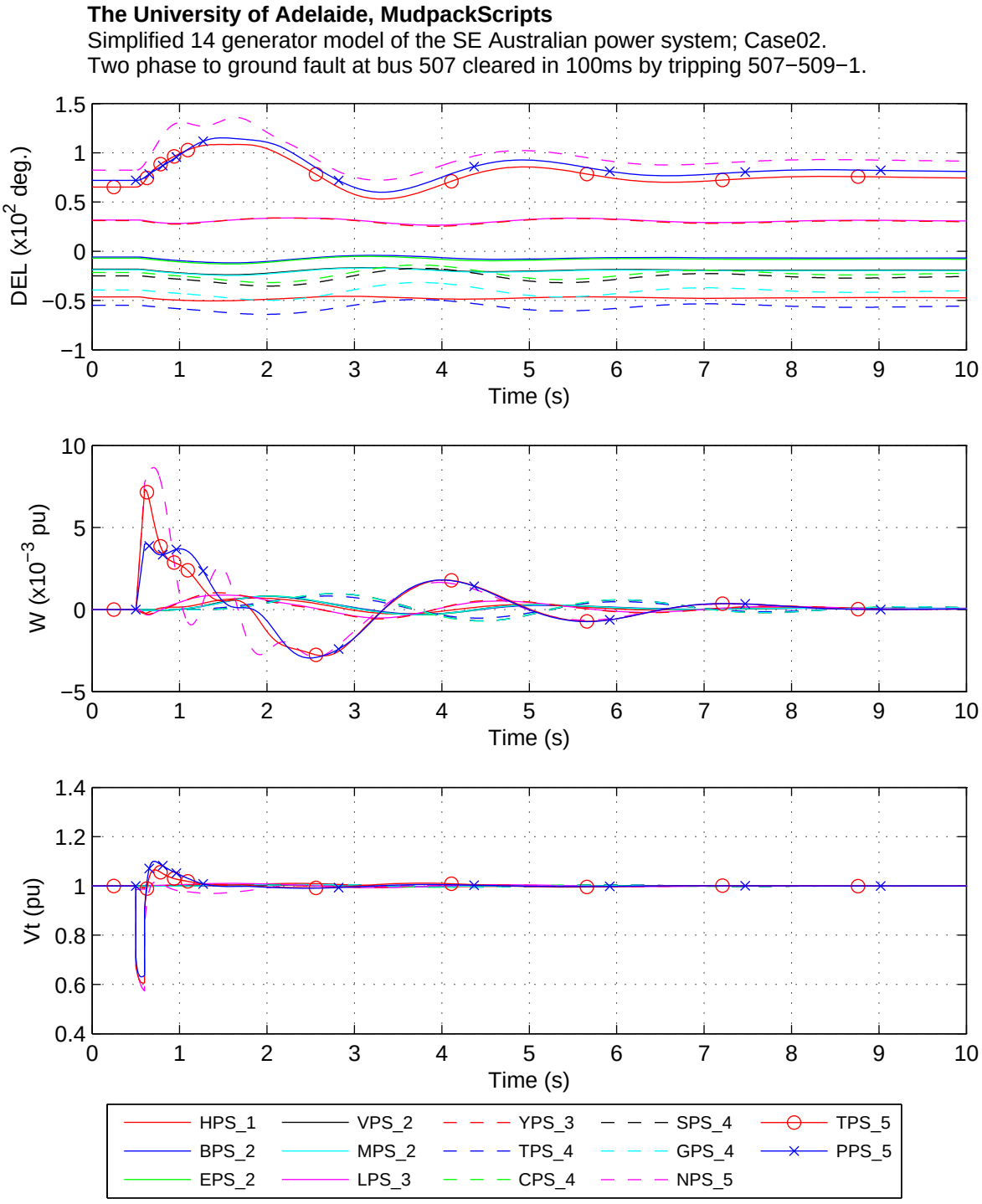

Figure 77 Case 2. Two-phase to ground fault applied to the 275 kV #1 circuit between buses 507 and 509 immediately adjacent to bus 507 at time t = 0.5 s. The fault is cleared 100 ms later by tripping the circuit. The inertia-weighted rotor-angles (DEL), rotor-speed perturbations (W) and stator-voltages (Vt) of all 14 generators are displayed.

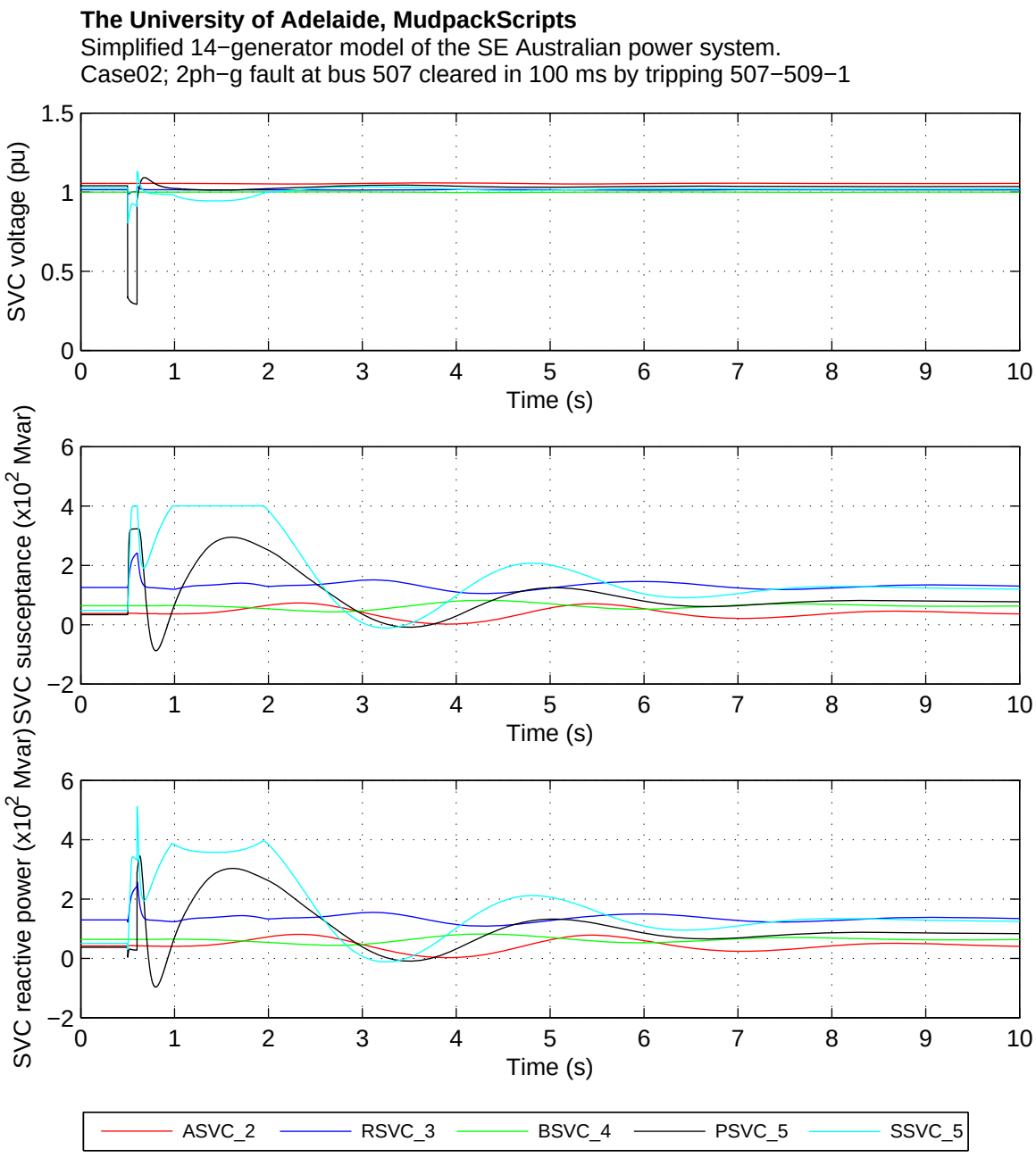

Figure 78 [Continuation of Figure 77] Case 2. Two-phase to ground fault applied to the 275 kV #1 circuit between buses 507 and 509 immediately adjacent to bus 507 at time t = 0.5 s. The fault is cleared 100 ms later by tripping the circuit. The terminal voltage, susceptance and reactive power output of all five SVCs are displayed.

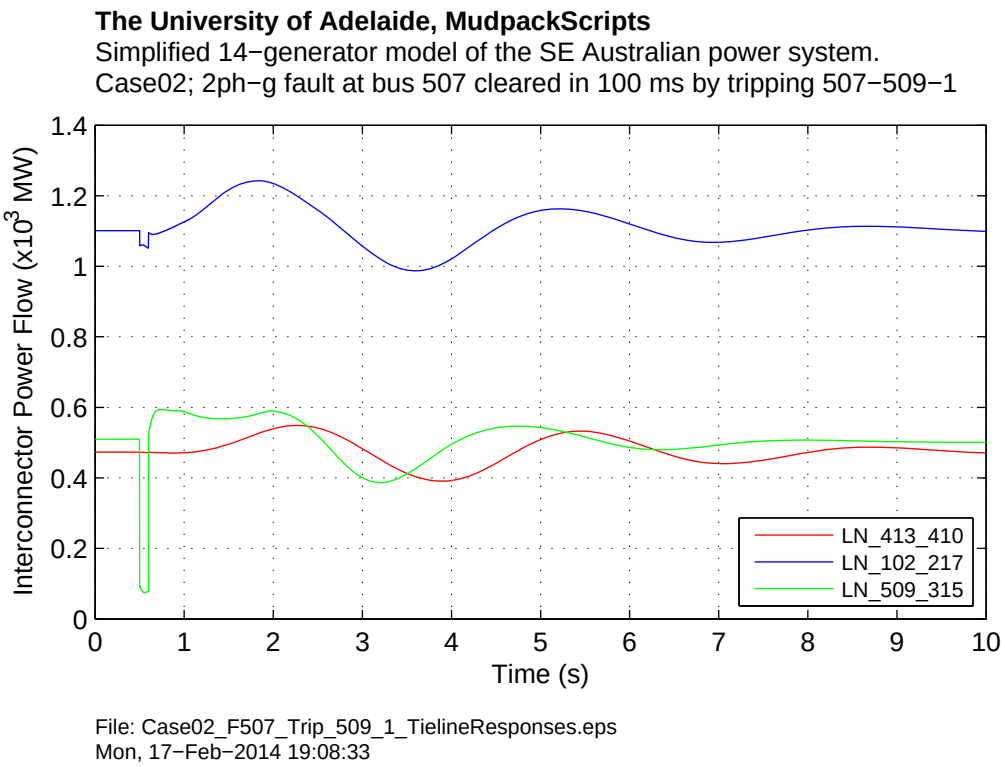

Figure 79 Continuation of Figure 77] Case 2. Two-phase to ground fault applied to the 275 kV #1 circuit between buses 507 and 509 immediately adjacent to bus 507 at time t = 0.5 s. The fault is cleared 100 ms later by tripping the circuit. The interconnector power flows are displayed.

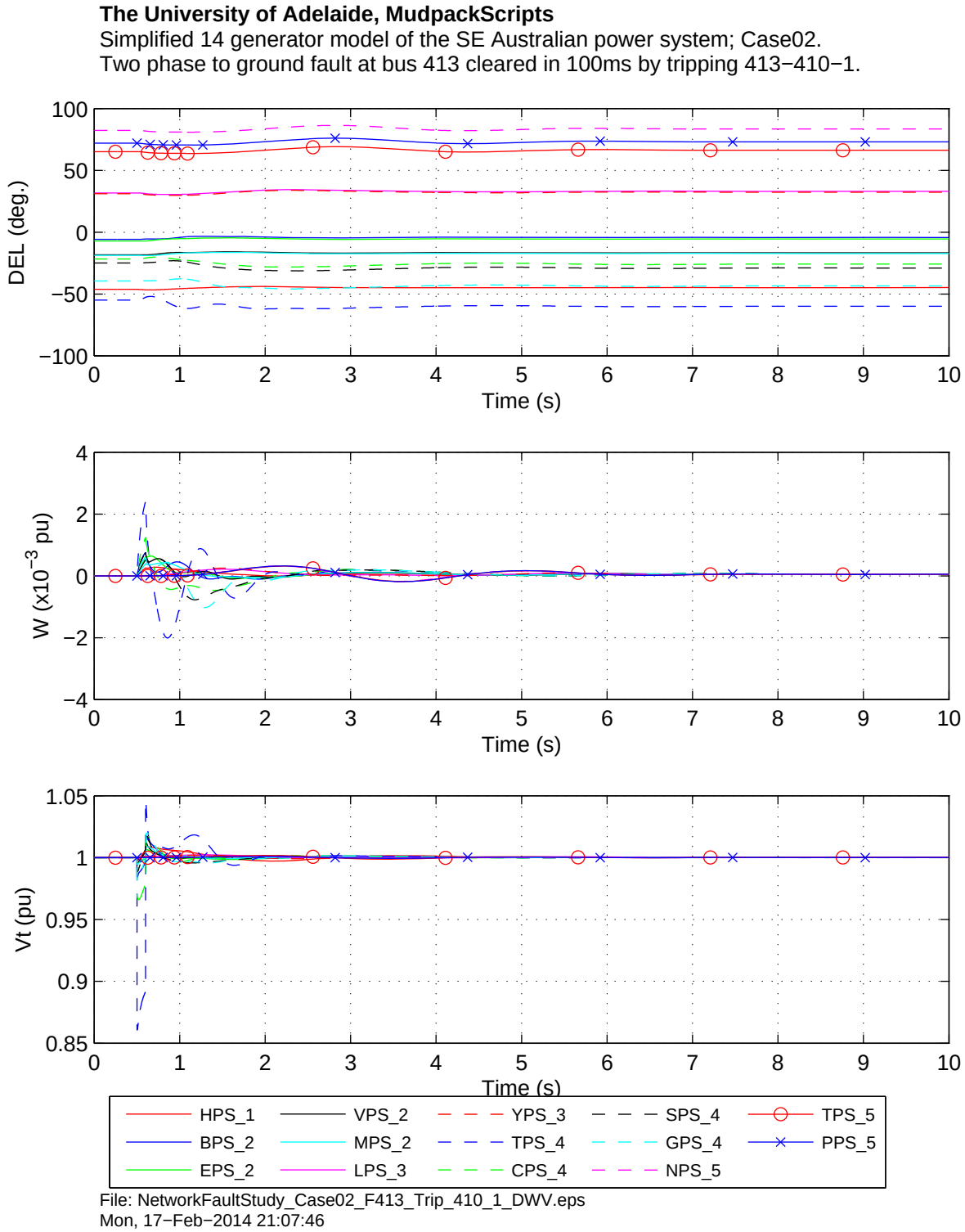

Figure 80 Case 2. Two-phase to ground fault applied to the 275 kV #1 circuit between buses 410 and 413 immediately adjacent to bus 413 at time t = 0.5 s. The fault is cleared 100 ms later by tripping the circuit. The inertia weighted rotor angles (DEL), rotor-speed perturbations (W) and stator-voltages (Vt) of all 14 generators are displayed.

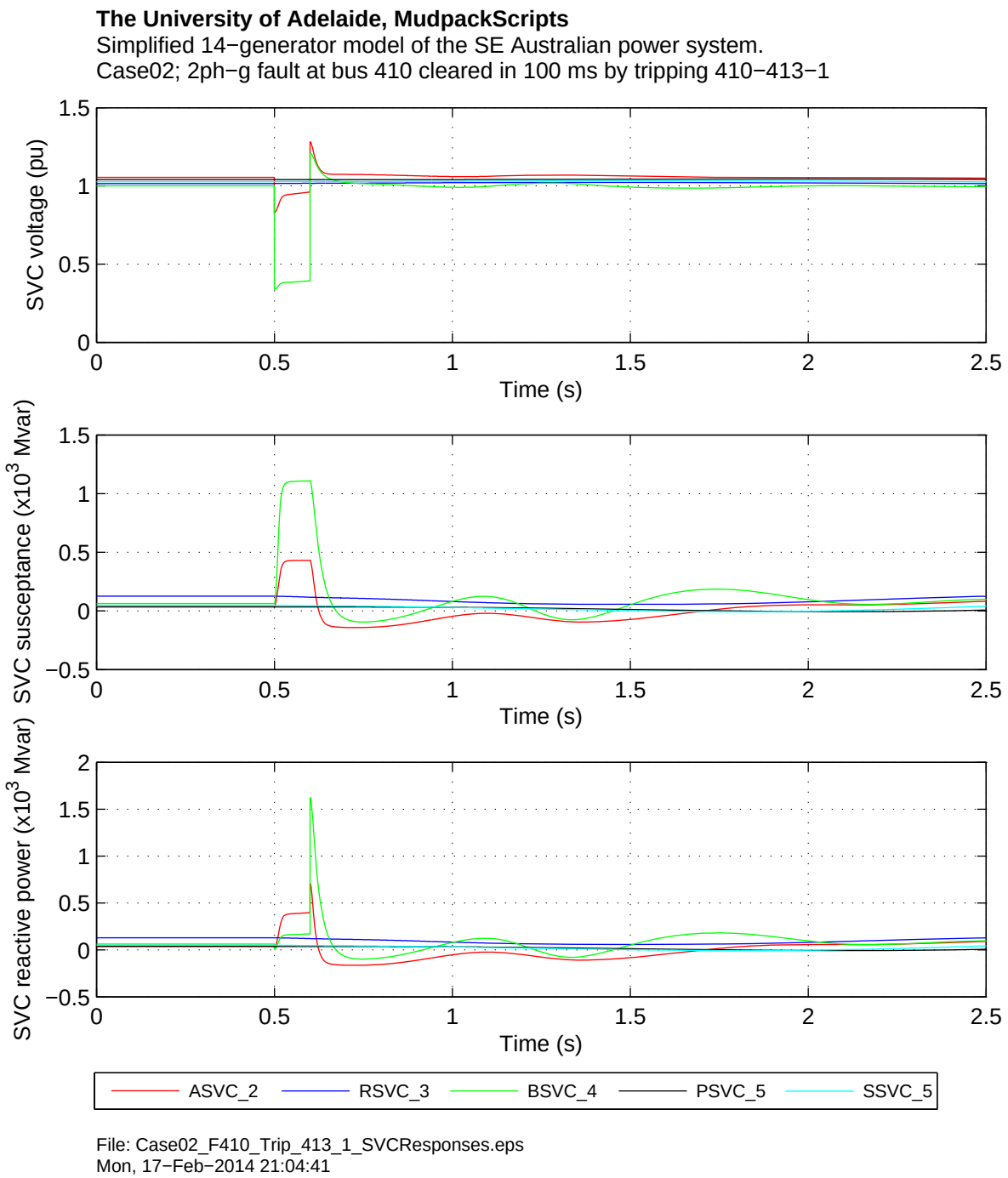

Figure 81 [Continuation of Figure 80] Case 2. Two-phase to ground fault applied to the 275 kV #1 circuit between buses 410 and 413 immediately adjacent to bus 413 at time t = 0.5 s. The fault is cleared 100 ms later by tripping the circuit. The terminal voltage, susceptance and reactive power output of all five SVCs are displayed.

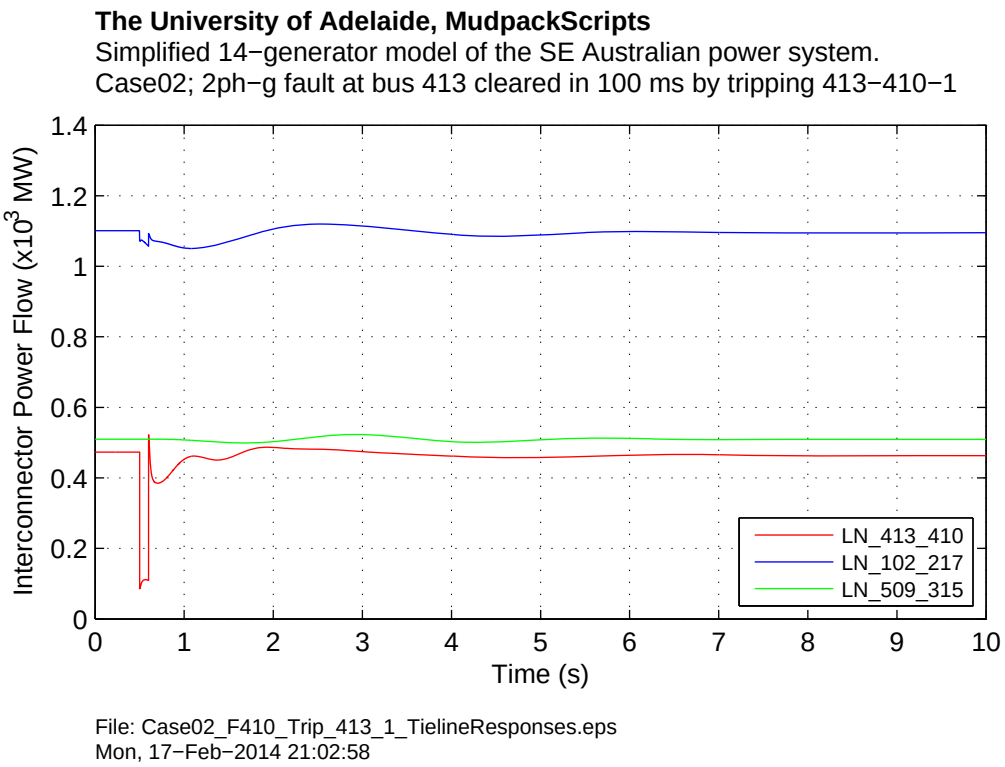

Figure 82 Continuation of Figure 80] Case 2. Two-phase to ground fault applied to the 275 kV #1 circuit between buses 410 and 413 immediately adjacent to bus 413 at time t = 0.5 s. The fault is cleared 100 ms later by tripping the circuit. The interconnector power flows are displayed.

Appendix V Model data and results package

V.1 Online sources of data and results

The data and results listed below are available from the following web-sites:

1. http://www.eleceng.adelaide.edu.au/groups/PCON/PowerSystems/IEEE/AU14G/Ver04
2. <DJV: IEEE website??>

If you have any problems downloading the data please contact David.Vowles@adelaide.edu.au.

V.2 Model data

The archive file AU14GenModelData_Ver04.zip is available for download from the websites listed in Appendix V.1. It contains the loadflow data for the six study cases in PSS®/E loadflow raw data format (version 29); the dynamics model data in PSS®/E and Mudpack formats; and the network sequence data in PSS®/E compatible format and loadflow solution reports. Refer to the file AU14GenModelData_Ver04_Contents.pdf in the archive for further information on its contents.

V.3 State-space models and eigenanalysis results in Matlab format

The archive file AU14GenModel_StateSpaceAndEigen_Matlab_Ver04.zip is available for download from the websites listed in Appendix V.1. It contains the following Matlab *.mat files, generated by a small-signal analysis package [14], are provided for Cases 1 & 6, (i) with no PSSs in service, and (ii) with PSSs in service:

1. the ABCD matrices of the system are in files:
   - Case#_PSSs_Off_ABCD_Rev3_Matlab.mat; and
   - Case#_PSSs_On_ABCD_Rev3_Matlab.mat;
2. the eigenvalues, the eigenvectors and participation factors are in:
   - Case#_PSSs_Off_Eigs_Rev3_Matlab.mat; and
   - Case#_PSSs_On_Eigs_Rev3_Matlab.mat,

where # is the case number, 1 or 6.

Refer to AU14GenModel_StateSpaceAndEigen_Matlab_Ver04_Contents.pdf in the archive for further information on its contents.

V.4 Small-signal time-response results

The archive file AU14GenModel_SmallSignal_TimeResponse_Results_Ver04.zip is available for download from the websites listed in Appendix V.1. It contains in Matlab and CSV format time-series data from the Mudpack and PSS®/E step-response tests reported in Appendices III.1 and III.2. It also contains PDF files displaying the results of the step-response tests. A Matlab mfile is also provided to assist the user to graphically display time series data. Refer to the file AU14GenModel_SmallSignal_TimeResponse_Results_Ver04_Contents.pdf in the archive for further information on its contents.

V.5 PSS®/E transient stability analysis results

The archive file AU14GenModel_TransientStabilityResults_Ver04.zip is available for download from the websites listed in Appendix V.1. It contains in Matlab and CSV format time-series data from the PSS®/E transient-stability tests reported in Appendix IV. It also contains PDF files displaying the results of the transient-stability studies. A Matlab mfile is also provided to assist the user to graphically display time series data. Refer to the file AU14GenModel_TransientStabilityResults_Ver04_Contents.pdf in the archive for further information on its contents.